Studi e Ricerche

Scienze e Tecnologie

Synthesis and biological evaluation of 1,5-diphenylpyrrole derivatives as COX-2 selective inhibitors and NO-releasing agents and development of a novel BRD9 chemical probe

Sara Consalvi

University Press

Sapienza Università Editrice

Collana Studi e Ricerche 87

Scienze e Tecnologie

Synthesis and biological evaluation of 1,5-diphenylpyrrole derivatives as COX-2 selective inhibitors and NO-releasing agents and development of a novel BRD9 chemical probe

Sara Consalvi

SAPIENZA
UNIVERSITÀ EDITRICE
2020

Sapienza Università Editrice
Piazzale Aldo Moro 5 – 00185 Roma

www.editricesapienza.it
editrice.sapienza@uniroma1.it

Iscrizione Registro Operatori Comunicazione n. 11420

ISBN 978-88-9377-137-5

DOI 10.13133/9788893771375

Pubblicato a giugno 2020

Impaginazione/layout a cura di: Sara Consalvi

Cover image: photo by Chromatograph on Unsplash.

Table of Contents

1. Synthesis and biological evaluation of 1,5-diphenylpyrrole derivatives as COX-2 selective inhibitors

1.1. Introduction

Nonsteroidal Antiinflammatory Drugs (NSAIDs) are widely used for treatment of inflammatory disorders, pain and fever. Their efficacy in suppressing inflammation is related to their capability to inhibit a class of enzymes defined prostaglandin-H synthases, well known as Cyclooxygenase 1 and 2[1] (COX-1 and 2). These proteins are homodimers of 576 and 581 aminoacids, respectively. They are characterized by a high sequence homology and share more than 60% of the amino acid sequence. Each monomer of both COX-1and COX-2 is comprised of three domains: i) an N-terminal EGF (Epidermal Growth Factor) like domain; ii) a helical membrane binding domain and iii) a large catalytic domain.

In both COX-1 and COX-2 the active site is constituted by a small hydrophobic channel; despite notable similarities, the two active sites of the two proteins differ in the amino acid sequence. The main difference in the COX-2 active site is the substitution of the residue Val 523 with an Ile. As a consequence, the binding sites show different shape and size; in fact, the Val 523 substitution determines a 25% increase in COX-2 volume (394 vs 316 Å) and the presence of a second internal pocket extending off the binding site2.

Cyclooxygenases catalyze two different and consecutive reactions: a bisoxygenation, leading to the formation of prostaglandins (PGs) from arachidonic acid (AA), and a peroxidase reaction, leading to PGH_2. The latter is subsequently converted to prostaglandin D, E F and I (PGD, PGE, PGF and PGI) and to thromboxane by specific synthase[3].

These autacoids are involved in many biological functions and play

a crucial role in many physiological and pathological processes, such as inflammation reaction and resolution, gastrointestinal (GI) ulceration and cytoprotection, angiogenesis, cancer, bone metabolism, nerve growth and development, renal hemodynamic and cardiovascular diseases[4].

Although COX-1 and COX-2 share the same catalytic activities and the same substrate, they have very different biological functions and their expression is controlled by different and independent mechanisms. COX-1 is constitutively expressed and its primary function is providing an adequate level of prostanoids precursors for homeostatic regulation, such as gastric cytoprotection, regulation of renal blood flow and platelet aggregation; on the other hand, COX-2 expression is upregulated at inflammation sites as a response to pro-inflammatory stimuli (cytokines, hormones, growth factor and hypoxia) and in many neoplastic cells. Furthermore, COX-2 is also constitutively expressed in endothelial cells and some tissues such as brain, spinal cord and kidneys, suggesting that it can also play a homeostatic role under specific physiological conditions[5].

Conventional NSAIDs are widely used agents for the treatment of different pathological conditions, from small injuries, headache or fever to alleviation of severe pain, and inhibit both COX-1 and COX-2 with different selectivities (Fig. 1.1). Indeed, these drugs can be discriminated for their COX-2/COX-1 selectivity index, expressed as the ratio between IC_{50} COX-2 and COX-1.[6]

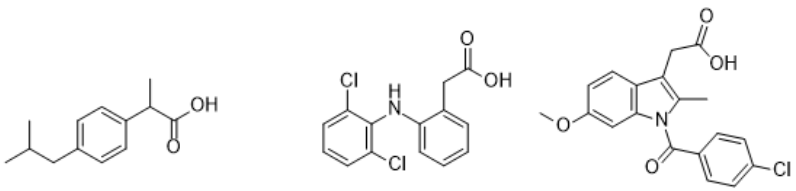

ibuprofen
SI: 15

diclofenac
SI: 0.7

indomethacin
SI: 60

Figure 1.1 Chemical structures of some conventional NSAIDs and selectivity index (SI).

The therapeutic effect is mainly attributed to the COX-2 inhibition, whereas adverse events are related to COX-1 inhibition and include gastrointestinal, renal and cardiovascular toxicity. The GI side-effects (known as NSAID-induced gastropathy) are the most relevant

problems in long-term NSAIDs administration[6-7]. In fact, since COX-1 is constitutively expressed in gastric mucosa and is responsible for production of cytoprotective prostanoids, its inhibition leads to trivial lesions or to much more serious accidents, such as bleeding, perforation or obstruction. Taking into account that anti-inflammatory properties of NSAIDs are primarily mediated by COX-2 and to circumvent GI toxicity associated with non-selective NSAIDs, a new class of anti-inflammatory agents that inhibit selectively COX-2 has been developed (coxibs) (Fig. 1.2).[6]

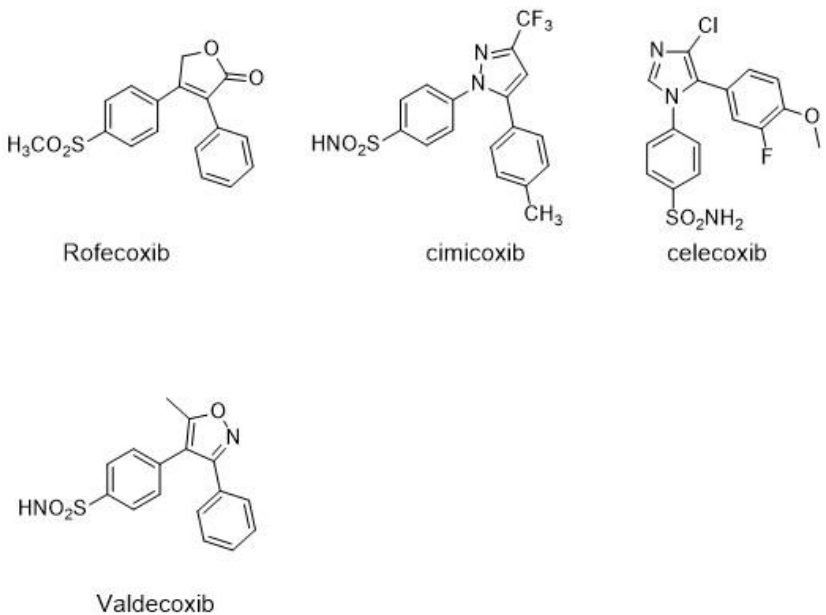

Figure 1.2 Chemical structures of some coxibs.

The differences in binding site dimensions of COX-2 account for selectivity; in fact coxib share a diarylheterocyclic structure that cannot enter the smaller COX-1 hydrophobic channel[2].

1.1.1. Pharmacological effects of COX-2 inhibition

1.1.1.1. Pain and inflammation reduction

Prostanoids are the principal mediators of the inflammatory response, and their biosynthesis is significantly increased in inflamed tissues. Through activation of specific receptors, PGE_2 and PGI_2 are

responsible for the increased vascular permeabilization and leukocyte infiltration by promoting blood flow and enhancing oedema formation. Furthermore, they reduce the threshold of nociceptor neurons to other mediators (i.e., bradykinin) by increasing neuronal activity in nociceptive nerve fibers[8,9]. COX-2 is constitutively expressed in both neurons and glia and contributes to the first phase of an inflammatory response; after a few hours it is widely upregulated in the spinal cord as a response to pro-inflammatory IL1 (interleukin 1) and can contribute to prolong central sensitization. However, there are evidences supporting that COX-1 derived prostanoids are the principal mediators implicated in the initial phase of acute inflammation and in the early response, while COX-2 pathway is mainly involved in the chronic phase of the inflammatory response, because its upregulation occurs after several hours[10].

1.1.1.2. Renal effects

COX-2 is constitutively expressed in kidney tissue and is responsible for prostanoid production in cortical and medullary structures. Since these prostanoids are involved with vasodilator and natriuretic responses, COX-2 selective inhibition can lead to an increase in blood pressure and impair response to antihypertensive drugs. Thus, renal function and blood pressure of at risk patients should be monitored during coxibs administration[5].

1.1.1.3. COX-2 and tumorigenesis

The contribution of COX-2 to tumorigenesis is supported by a large number of epidemiological and experimental studies and by the proven efficacy of coxibs in reducing the risk of colorectal adenoma recurrence[11–13].

COX-2 overexpression is found in many solid tumors, such as lung, head, neck, colorectal, breast and prostate, and it is usually associated with a very aggressive and malignant phenotype and a decreased survival among patients. COX-2 levels in tumor cells are regulated by many different mechanisms, some of which need to be elucidated[14]. Viral proteins, some environmental toxins, pathways induced by hypoxia and a positive feedback initiated by PGE_2 can stimulate its expression by activating transcription[15]. Furthermore, down regulation

of caveolin allows to maintain elevate COX-2 concentration by preventing its degradation[16]. COX-2 aberrant expression contributes to different stages of tumorigenesis, including regulation of cell proliferation, apoptosis, neovascularisation, invasion and evasion of host immune surveillance[17]. The driving force behind these oncogenic effects is the chronic inflammation that represents a risk factor for cancer initiation[17].

In the early stages of tumor initiation, COX-2 can confer resistance to apoptosis and can induce genomic instability by producing reactive oxygen and endoperoxide species. It also acts in a paracrine manner: in fact, it contributes to create a pro-inflammatory environment that promotes a transition to neoplastic cells. Among COX-2 derived prostanoids, the most relevant in cancer initiation and progression is PGE_2[14]. This mediator can activate specific receptors to stimulate cell proliferation through different signaling pathways. In addition, it promotes invasion and angiogenesis by stimulating vascular endothelial growth factor (VEGF) expression and secretion[18]. The efficacy of coxibs in colorectal cancer chemoprevention was primarily demonstrated in three clinical trials: Adenoma Prevention with Celecoxib (APC), Adenomatous Polyp Prevention on Vioxx (APPROVe)[19]and Prevention Spontaneous Adenomatous Polyps (PreSAP)[20]. However, despite its good activity, an increase in cardiovascular risk was observed in APPROVe trial, that led to rofecoxib withdrawn from the market. Currently, coxibs efficacy as antitumor is under investigation in many clinical trials against diverse solid tumors, such as lung, ovarian, colorectal, breast, prostate and biliary-pancreatic.

1.1.1.4. Coxibs and cardiovascular safety

The main prostanoids involved in the maintenance of vascular homeostasis are thromboxane A_2 (TXA_2) and prostacyclin (PGI_2). TXA_2 is produced in platelets by COX-1 and promotes aggregation and vasoconstriction. On the other hand, prostacyclin is a potent vasodilator and inhibits platelets aggregation and smooth muscle cell proliferation, modulating TXA_2 actions. Differently from TXA_2, PGI_2 is the major product of COX-2 in endothelial cells; indeed this isoenzyme is induced as a response to the hemodynamic shear and constitutes the primary source of prostacyclin *in vivo*[21].

Unlike traditional Non Steroidal Antiinflammatory Drugs

(tNSAIDs), that inhibit both isoforms, coxibs diminish PGI_2 formation without affecting TXA_2 synthesis and leads to a lack of balance in the prostacyclin/thromboxane ratio[22].

Recently, a meta-analysis of data from 639 randomized trials showed that both coxibs and conventional NSAIDs are associated with a risk of major cardiovascular events compared to placebo. However, nature and magnitude of the risks, as well as the safety of different NSAIDs regimens remain unclear. Most of the data concern four coxibs (celecoxib, rofecoxib, etoricoxib and lumiracoxib) in comparison with three high doses of conventional NSAIDS (diclofenac 150 mg, ibuprofen 2400 mg and naproxen 1000 mg). This study confirms both the gastrointestinal safety and the cardiovascular hazard associated with coxibs, but also shows that high doses of diclofenac cause similar vascular risks; furthermore, it raises the possibility that high doses of ibuprofen can exhibit a similar effect, suggesting that cardiovascular risks should be taken into account when administering every anti-inflammatory drug[23].

The double-blind, randomized trial APPROVE compared placebo to rofecoxib (Vioxx®) in a long-term use (three years) in patients with a history of colorectal adenoma. Since this trial pointed out that incidence of thrombotic events was higher for treated patients (3 per 400 patient-years for placebo and 6 per 400 patient-years for Vioxx)[24], in September 2004 Merck withdrawn Vioxx® from the market. These data shouldn't be generalized to other COX-2 inhibitors, because rofecoxib toxicity could also be related to its chemical structure[25]; as reported by Corey[26]*et al*., rofecoxib is rapidly converted to a very high reactive metabolite (maleic anhydride) that in turn can react with amino groups of many biological molecules. Maleic anhydride could also be responsible for the mechanism of atherotrombotic disease through the formation of radicals that promote lipid peroxidation. Thus, although coxibs share the same activity, significant differences exist in the same class, and their physicochemical properties should be considered. In terms of drug discovery, cardiovascular side effects can be circumvented following different strategies: i) design and development of novel agent characterized by novel scaffolds; ii) design of multitarget molecules that share two different mode of actions (i.e COX-2 inhibitors/thromboxane antagonists)[22]; iii) design of pharmacodynamic

hybrids that conjugate COX-2 inhibitors with a moiety able to mitigate adverse effect.

1.1.2. COX-inhibiting nitric oxide donors (CINODs)

Pharmacodynamic hybrids are a class of molecules that are characterized by a dual mechanism of action, by means of conjugation of two portions with different pharmacodynamic profiles. These multi-target drugs present many advantages with respect to administration of a drug-cocktail: *i)* a more predictable pharmacokinetic profile; *ii)* possibility of mitigating adverse effects; *iii)* enhancement of the pharmacodynamic profile of the native molecule and *iv)*a better patients compliance[27].

In the last years, many research groups focused their attention on molecular hybrids characterized by a nitric oxide- (NO) releasing moiety, such as beta-blocker, antimycotic and antihypertensive agents[28–30]

Endogenous NO is produced by specific synthase (NOS, NO synthases) from L-arginine in a large number of cells and plays a pivotal role in blood pressure regulation, cell proliferation, vascular homeostasis and vasorelaxant processes. In mammals, there are different isoforms of this enzyme. Neuronal NOS and endothelial NOS are constitutively expressed and are involved in cell signalling processes and vasodilatation processes, respectively. On the other hand, the iNO (inducible NO synthase) is an inducible isoform that mediates immune defense against pathogens through NO synthesis.

Due to its small size and to its instability, NO acts as a potent local modulator that rapidly diffuses through membranes to target cells and is involved in cell-to-cell communication. As extensively reported by Ignarro *et al*., it activates guanylate cyclase that in turn increases Cyclic Guanylyl Phosphate (GMPc) levels in tissues. In endothelial cells, activation of this enzyme results in a decrease of intracellular Ca^{2+} that causes smooth muscle relaxation and platelet aggregation inhibition[31].

NO plays a "bimodal role" in cancer progression and metastasis; although lower level of NO stimulates tumor progression, there is a body of evidence demonstrating that it exerts the opposite effect at higher concentration. It can act against cancer in several ways and different stages. In the early tumor stages, adequate levels of NO can cause cytotoxicity and can promote apoptosis. Furthermore, NO affects tumor cell invasion by modulating expression of matrix

metalloproteinase proteins family (MMPs) that are involved in tumor invasion[32].

Finally, in the GI tract, NO can regulate gastric blood flow and contribute to mucosal defense; furthermore, it can exert a protective effect by modulating mucus and bicarbonate secretion in gastric mucosa.

COX-inhibiting nitric oxide donors (CINODs) represent an interesting class of pharmacodynamic hybrids characterized by the conjugation of a conventional NSAID with a NO release moiety. This class of molecules has been developed with the aim of reducing GI side effects associated with conventional NSAIDs administration, taking into account the gastroprotective role of NO. Two representative members of this class are Naproxcinod (AZD3582) and NO-flurbiprofen (HTC-1026), produced by NicOx (Fig. 1.3).[33–35]

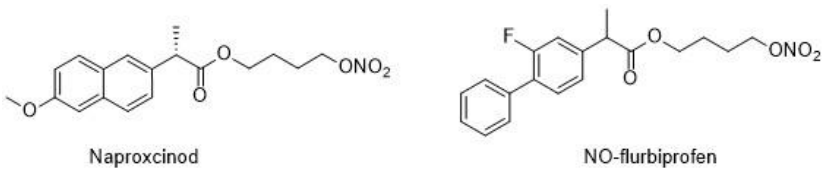

Figure 1.3. Chemical structures of Naproxcinod and NO-flurbiprofen.

Naproxcinod is in line for FDA approval. It acts as a pro-drug and after oral administration only a small amount of the parental drug was found intact in plasma. In fact, it releases *in vivo* two active metabolites, Naproxcinod and 4-nitroxybutanol, responsible for anti-inflammatory and NO-mediated effects, respectively (Fig. 1.4).

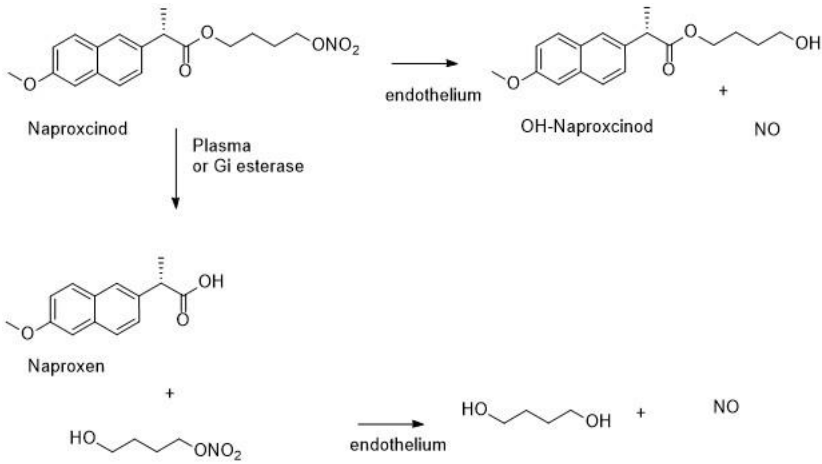

Figure 1.4. Naproxcinod metabolism *in vivo*.

When administered at the dosage of 750 mg twice daily, Naproxcinod proved to be active in reducing signals of hip or knee osteoarthritis and showed comparable effectiveness to equimolar doses of Naproxen[36]. Interestingly, although GI side-effect related to Naproxcinod seemed only slightly better than those of Naproxen, an improved cardiovascular safety appeared during these studies, also in patients with hypertension [36]. On these grounds, combination of a NO donor moiety with a coxib should provide pharmacodynamic hybrids endowed with an excellent anti-inflammatory activity, a spare GI toxicity and a reduced cardiovascular toxicity, leading to anti-inflammatory agents characterized by an increased activity and a better safety profile.

1.2. A new generation of 1,5-diphenylpyrrole derivatives as potent COX-2 selective inhibitors

1.2.1. State of the art of the project

A class of 1,5-diphenyl pyrroles endowed with anti-inflammatory properties has been developed by the group of Prof. Mariangela Biava. The research program focused on the synthesis of 1,5-diphenylpyrrole acetic ketoesters, acids, esters and ethers as potent and selective COX-2 inhibitors. These four series of derivatives were characterized by a diaryl-substituted-heterocycle scaffold, that refers to coxib family, and by a pyrrole acetic moiety that is reminiscent of indomethacin[37–43] (Fig. 1.5).

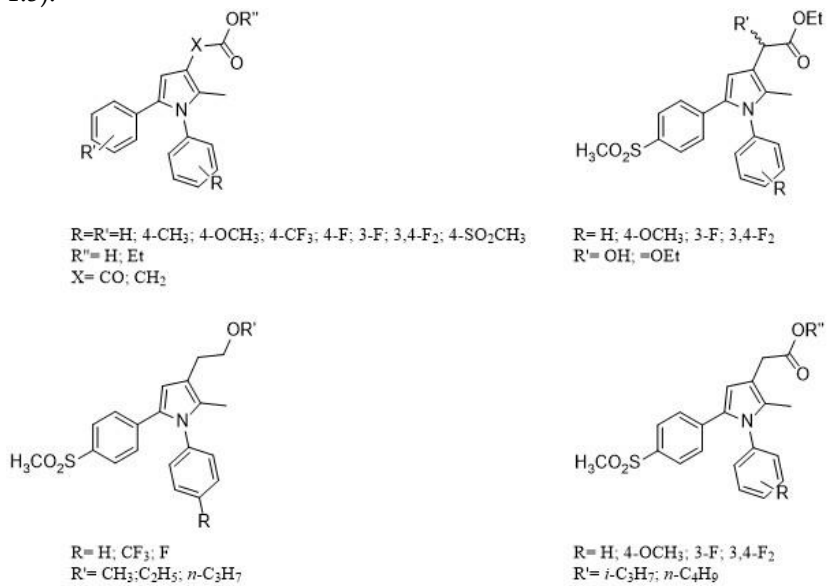

Figure 1.5. 1,5-Diphenylpyrrole acetic ketoesters, acids, esters and ethers.

1.2.1.1. First series: ketoesters, acetic ethyl esters and acids

At the very beginning, a small set of 1,5-diarylpyrrole-3-acetic and –glyoxylic acid derivatives was synthesized[37,38]. These compounds were characterized by: i) a p-methylsulfonyl substituent, alternatively placed either at C5 or N1 of the pyrrole nucleus; ii) a second phenyl group bearing diverse substituents, such as H, 3-F, 4-F, 3,4-F_2, 4-CF_3, 4-OCH_3 and 4-CH_3; iii) a ketoacid, ketoester, acetic acid and acetic ester chain at C3 (Fig. 1.6).

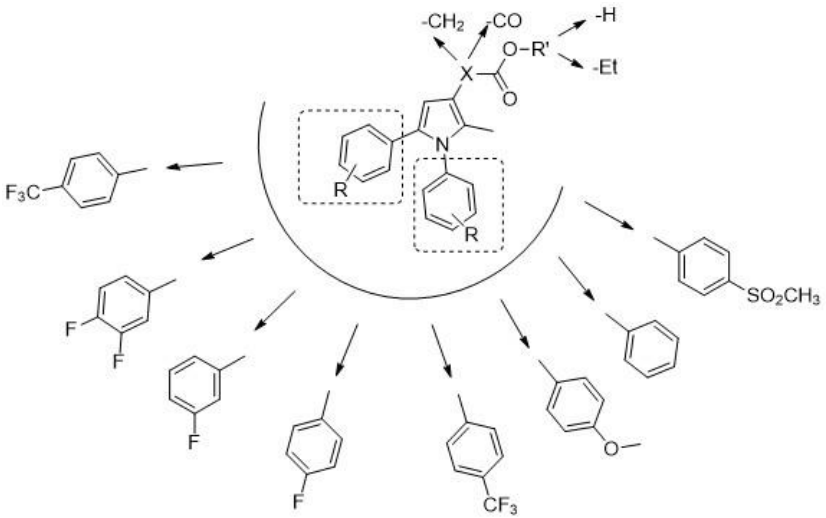

Figure1.6. Structures of the first series of derivatives.

In order to investigate the binding mode within the COX-2 binding site, two representative compounds were submitted to molecular docking calculations using the crystallographic complex between COX-2 and SC-558 as a control structure.

All the synthesized compounds were tested in vitro for evaluating their activity and selectivity towards COX-2; several derivatives showed good activities, ranging from 4 to 0.01 μM at inhibiting COX-2. Biological results, supported by molecular docking simulations, led up to the following Structure-Activity Relationship (SAR) considerations[37,38]:

- The position of the p-methylsulfonyl moiety is essential for activity: inversion of this substituent at position N1 instead of C5 caused a marked decrease of activity, due to a reorientation of the molecule in the binding site.
- The acetic chain at C3 led to more active compounds with respect to the corresponding acids and ketoesters. Conformational rigidity of ketoester derivatives influenced orientation of compounds leading to a significant loss of interactions within the binding site. Regarding acids, transformation of the ester side chain in the corresponding acid group did not influence orientation but determined a lack of positive hydrophobic interactions with the residues of the

carboxylate site and was responsible for a drop of activity.
- Substituents decorating the phenyl ring at N1 modulates activity in the following order: 3-F= 4-F> 3,4-F_2>4-OCH_3> H> 4-CF_3> 4-CH_3

1.2.1.2. Second series: α-substituted acetic esters

On these grounds, a new series of acetic esters (Fig. 1.7) was synthesized for evaluating how the introduction of either a hydroxyl or an ethoxyl substituent at the α-position of the C3 side chain could influence the activity[39,40].This substitution generated a stereogenic center, therefore the activity of each enantiomer was also evaluated in order to check any stereoselective interaction at the active site. Based on SAR of the previous series of derivatives, the sulfonylmethyl moiety decorated the phenyl ring at C5, keeping the most convenient substitutions on the phenyl ring at N1.

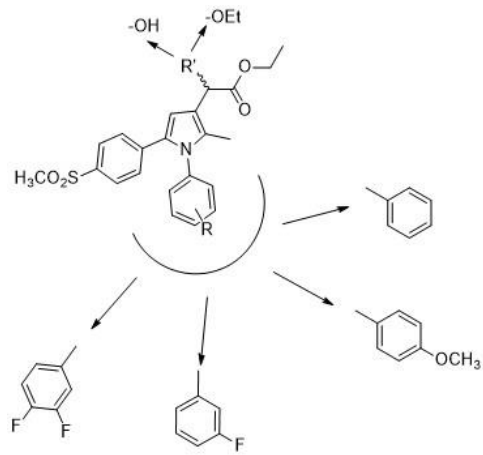

Figure 1.7. Chemical structures of the second series of derivatives.

All the tested compounds showed good activities, both *in vitro* and *in vivo*. Nonetheless, they proved to be generally less active than the previous synthesized compounds, showing that even though substitutions at C3 are more toleratedwith respect to C5 and N1, the introduction of a α-hydroxy or ethoxy group lowered activity.

1.2.1.3. Third series: ethers

In parallel, a series of 3-alkoxyethyl ether derivatives were synthesized to evaluate the influence of a completely different functional group at position C3 and to extend SAR knowledge[41] (Fig. 1.8).

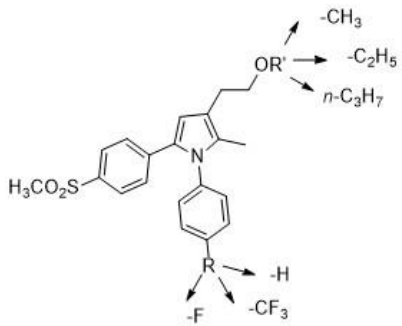

Figure 1.8. Chemical structures of the third series of derivatives.

Despite the absence of the carbonyl group, the replacement of the acetic moiety with an alkoxyethyl group retained activity. Surprisingly, the sole ether oxygen could serve for the electrostatic interactions with the carboxylate site and the presence of the more lipophilic alkoxyethyl moiety reinforced hydrophobic interactions in the above cited site. Nonetheless, these derivatives were in general less active than the esters.

1.2.1.4. Fourth series: a second generation of acetic esters

Finally, both the size and the length of C3 side chain were modified by means of introducing bulkier substituents[42]. Therefore, a new series of *i*-propyl and *n*-butyl esters were synthesized with the aim of improving hydrophobic interactions with the carboxylate site. According to SAR analysis on previous compounds, these derivatives bore an N1 phenyl ring decorated with the most convenient substituents (3-F, 3,4-F_2, H, 4-OCH_3) and a *p*-methylsulfonyl moiety at C5 (Fig. 1.9).

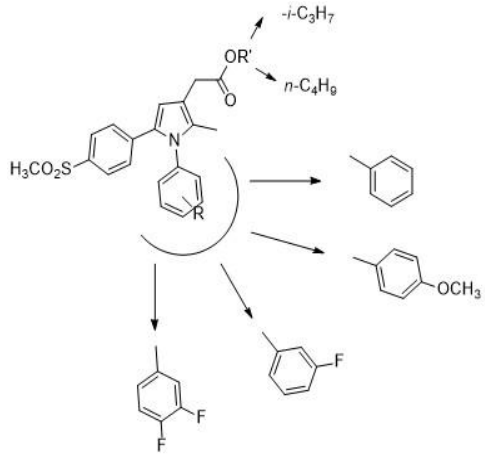

Figure 1.9. Chemical structures of the fourth series of derivatives.

These compounds showed very good potency and selectivity towards COX-2, with IC_{50} values ranging from 0.043 μM to 7 nM. The rat paw pressure and volume and the abdominal constriction tests were also performed to assess the *in vivo* anti-inflammatory and analgesic activity. The obtained results demonstrated that the tested compounds were very effective, as well as long-lasting and more potent than the corresponding ethyl esters, showing a relevant effect even two hours after the administration.

The metabolic stability was also evaluated using human liver microsomes: differently from acids, esters proved to be liable to hepatic metabolism at low concentrations (both 10^{-5} and 10^{-7} M), suggesting the hydrolysis of the ester moiety as the main metabolic pathway. Thus, MAB 48 was selected for further pharmacokinetic studies. This compound proved to be sufficiently absorbed (42% of absolute oral bioavailability) and to have a high volume of distribution and a very high value of clearance. When compared to clearance data, the extensive distribution on extravascular compartments could explain the steady state observed up to 5 h. The plasmatic concentration of the drug within 1 to 5 h was much higher than the IC_{50} of MAB 48, and could validate the long-lasting effect observed in rat. Finally, the presence of the corresponding acid was detected both after oral and intravenous administrations, confirming the hydrolysis of the ester moiety. This instability could confirm the effect observed in vivo because the long-

lasting activity could depend both on the ester itself and the acid, that was continuously released in vivo. The concentration of the acid did not depend on the administration route, proving that the hydrolysis did not occur in the gastrointestinal tract; on these grounds, we hypothesized either a hepatic or plasmatic metabolism, due to the esterase activity[42].

1.2.2. Rationale and aims

SAR analysis of the previously synthesized compounds pointed out the key parameters for activity and led to the identification of a series of ester derivatives characterized by very good values of both potency and selectivity towards COX-2 and a great activity *in vivo*. Nonetheless, pharmacokinetic studies displayed their liability to esterase; the latter led to the formation of the corresponding acid metabolite, influencing and reducing the efficacy of the esters over time. Therefore, our efforts were directed to the identification and the introduction of structural modifications at C3 in order to circumvent esterase metabolism and obtain compounds endowed with a prolonged activity.

For this purpose, we followed two different strategies:

- Replacement of the ester moiety with a group that is not sensitive to the same metabolic route, following the pathway that led from esters to ethers. Therefore, a series of small-side-chained derivatives (aldehydes, oximes and nitriles) were synthesized (compounds **1-12**, Fig. 1.10).
- Isosteric replacement of the ester moiety with the amido group, less sensitive to hydrolysis. Moreover, the methylsulfonyl moiety at position C5 was also isosterically replaced with a sulfamoyl group with the intent to further improve both activity and solubility (Compounds **13-20**, Fig. 1.10). In order to better evaluate the influence of this modification to the activity, corresponding acetic esters and acids were also synthesized and tested (Compounds **21-24**, Fig. 1.10).

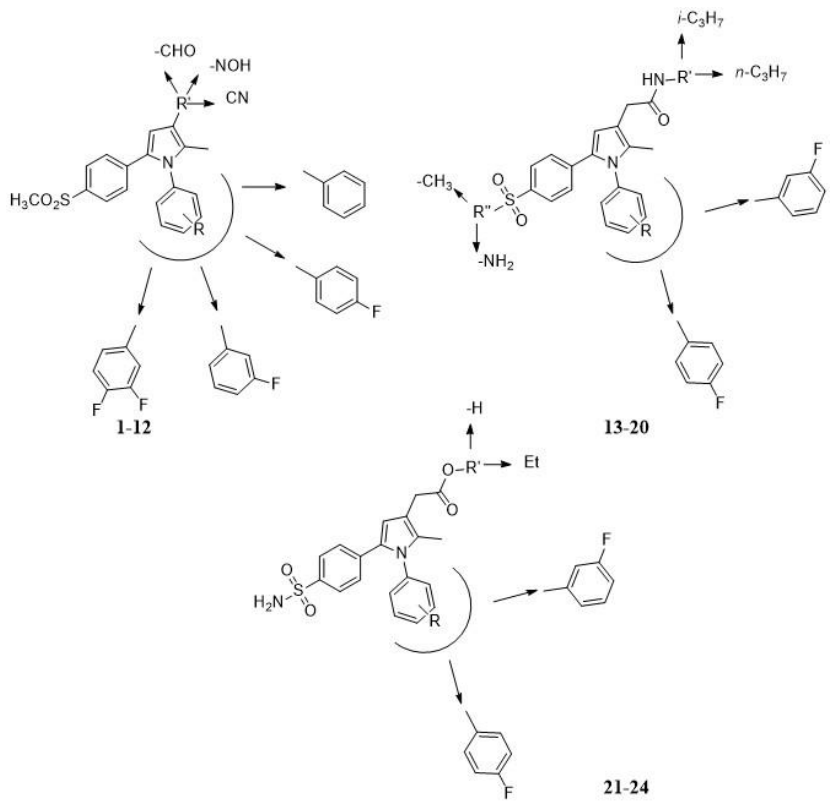

Figure 1.10. Chemical structures of compounds **1-24**

1.2.2.1. A class of pyrrole derivatives endowed with analgesic/anti-inflammatory activity

Claudio Battilocchio, Giovanna Poce, Salvatore Alfonso, Giulio Cesare Porretta, Sara Consalvi, Lidia Sautebin, Simona Pace, Antonietta Rossi, Carla Ghelardini, Lorenzo Di Cesare Mannelli, Silvia Schenone, Antonio Giordani, Luigia Di Francesco, Paola Patrignani and Mariangela Biava[44].

This first series of derivatives was developed in order to obtain a class of stable derivatives and further to evaluate the relationship between side-chain dimension and activity/selectivity. Based on the work of Khanna and co-workers[45], that described the synthesis and biological evaluations of diverse pyrrole derivatives, we synthesized three small sets of compounds: aldehydes **1-4**, oximes **5-8** and nitriles

9-12, shown in Figure 1.11.According to SAR analysis of previously synthesized compounds, the *p*-methylsulfonyl moiety at C5 was kept unchanged, and the phenyl ring at N1 was decorated with the most convenient substituents (H; 3-F; 4-F; 3,4-F_2).

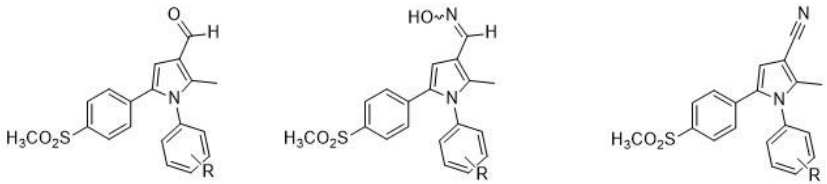

1: R=4-F
2: R=3-F
3: R=3,4-F_2
4: R=H

5: R=4-F
6: R=3-F
7: R=3,4-F_2
8: R=H

9: R=4-F
10: R=3-F
11: R=3,4-F_2
12: R=H

Figure 1.11. Chemical structures of compounds **1-12.**

Chemistry

Briefly, an umpolung reaction between 4-methylthiobenzaldehyde and methyl vinyl ketone, followed by an oxidation of the sulfur with Oxone® and a Paal-Knorr condensation with the appropriate aniline, led to the pyrrole derivatives **28 a-d**[37]. Then, a C3 formylation using the Vilsmeier's reagent provided compounds **1-4** in good yields. As determined by crude NMR, that highlighted formation of the C4 regioisomer ranging from 2 to 5%, this reaction was endowed with a good regioselectivity. Regiochemistry of the main product was established by NOE studies. Subsequently, the oximes **5-8** were obtained through a reaction of the carboxaldehyde **1-4** with hydroxylamine chloride, in the presence of sodium acetate in ethanol/water. After refluxing for one hour and a half, the mixture was cooled down, and the precipitate was filtered off, affording the oximes **5-8** in very good yields. These compounds were pure enough to progress to the next stage, and were dehydrated to corresponding nitriles **9-12** using a solution of 2,4,6-trichloro[1,3,5]triazine in dimethylformamide for 8h[46]. Finally, compounds **9-12** were purified by chromatographic column, followed by recrystallization.

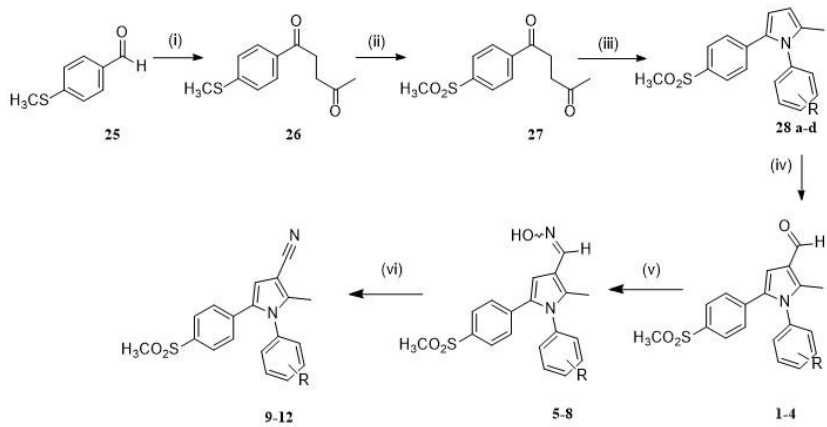

Reagents and conditions: (i) CH_2=CHCOMe, TEA, 3-ethyl-5-(2-hydroxyethyl)-4-methylthiazolium bromide, MW,15min,70% yield; (ii) Oxone, MeOH/H_2O, rt, 2 hrs, >90% yield; (iii) $RPhNH_2$, *p*-toluensulfonic acid, EtOH, MW, 45 min, 55-67% yield; (iv) Vilsmeier reagent, CH_2Cl_2, 0 °C then reflux 1h, 75-80% yield; (v) hydroxylamine, EtOH, CH_3COONa, H_2O, rt, 1.5 hrs, >90 % yield; (vi) TCT, DMF, 8hrs.
1: R=4-F; **2**: R=3-F; **3**: R=3,4-F_2; **4**: R=-H; **5**: R=4-F; **6**: R=3-F; 7: R=3,4-F_2; **8**: R=-H; **9**: R=4-F; **10**: R=3-F; **11**: R=3,4-F_2; **12**: R=-H; **28a**: R=4-F; **28b**: R=3-F; **28c**: R=3,4-F_2; **28d**: R=-H;

Scheme 1.1. Synthesis of Compounds **1-12**.

Biological and pharmacological evaluation

Following the previously adopted protocols, all the synthesized compounds were tested *in vitro* to assess selectivity and potency towards COX-1 and COX-2, in the murine monocyte/macrophage J774 cell line[47]. As shown in Table 1.1 all compounds were inactive against COX-1, while inhibited COX-2 with varying potencies.

COMPOUND	R	IC_{50} COX-1	IC_{50} COX-2
1[A]	4-F	>10	0.0340
2	3-F	>10	0.0095
3	3,4-F_2	>10	0.0700
4	-H	>10	0.0340
5	4-F	>10	0.3600
6	3-F	>10	0.4400
7	3,4-F_2	>10	0.1600
8	-H	>10	0.1900
9[B]	4-F	>10	0.0290
10	3-F	>10	0.0130
11	3,4-F_2	>10	0.0022
12	-H	>10	0.3600
CELECOXIB	-	3.84	0.0610

Table 1.1. ***In vitro*** **COX-1 and COX-2 inhibitory activities of 1-12 and celecoxib**.
[a]Khanna *et al*. reported 3.23 μM (IC_{50}) towards COX-2 isoform; [b]Khanna et al. reported 0.75 μM (IC_{50}) towards COX-2 isoform.; [c]Results are expressed as the mean (n=3 experiments) of the percentage inhibition of PGE_2 production by test compounds with respect to control samples and the IC_{50} values were calculated by GraphPad Instat program; data fit was obtained using the sigmoidal dose-response equation (variable slope) (GraphPad software

While oximes **5-8** were not endowed with good values of activity, aldehydes **1-4** and nitriles **9-12** proved to be more active, with IC_{50} values in the submicromolar range. The most active compounds were aldehyde **2** and nitrile **11** that exhibited IC_{50} values of 9.5 and 2.2 nM, respectively.

In order to assess their efficacy in analgesia, compounds **1-12** were also tested *in vivo*, following the abdominal writhing test protocol[48]. The analgesic activity was evaluated measuring the reduction of writhes induced by an intraperitoneal injection of acetic acid. Compounds **1-12** were orally administered at diverse dosages 30 minutes before the induction of writhes. Results are reported as the number of writhes and as percentage of writhes reduction with respect to the vehicle carboxymethylcellulose (CMC). As shown in Table 1.2, the most active compound of this series was aldehyde **3**, that exhibited an

efficacy in writhing reduction similar to that of celecoxib. This compound was active at the dosage of 1 mg/kg (36% reduction) and when administered at the dosage of 40 mg/kg was able to reduce writhes by 60%. Interestingly, response remained roughly the same (50 %) in the 5-20 mg/kg dosage, proving that this compound did not show a dose-dependent activity in the above-mentioned range. Regarding oximes, they were all endowed with good analgesic properties (from 41 to 57 % of writhes reduction) at a higher dosage range (20 and 40 mg/kg). On the other hand, nitriles **9** and **10** showed a moderate activity, while **11** and **12** were active (57 and 59 % respectively) at 40 mg/kg, the higher dosage tested. Surprisingly, *in vitro* results were not predictive: in fact, compounds endowed with the higher potency against COX-2 (**1, 2**, **4**,**7** and **11**) were not found to be the most active ones *in vivo*. These different *in vivo* effects could be due to a higher metabolic instability of these compounds. Thus, further studies are needed to evaluate the pharmacokinetic profile of this series of derivatives.

		NUMBER OF WRITHES (% OF WRITHES REDUCTION)				
COMPOUND	CMC	1 MGKG^{-1}	5 MGKG^{-1}	10 MGKG^{-1}	20 MGKG^{-1}	40 MGKG^{-1}
CMC	33.4±2.5	--	--	--	--	--
1	--	ND	31.7±3.6 (5)	33.6±3.7 (-)	23.3±2.9 (30)	22.9±3.0 (31)
2	--	ND	33.4±3.1 (-)	20.3±2.2* (39)	18.8±3.4* (44)	ND
3	--	21.3±2.8* (36)	16.7±3.1* (50)	15.8±2.8* (53)	16.1±2.9* (52)	13.3±2.3* (60)
4	--	ND	33.0±2.8 (-)	25.8±3.0^ (23)	22.8±3.1* (32)	23.2±2.2* (30)
5	--	ND	32.6±2.7 (2)	21.5±3.2* (36)	19.8±2.5* (41)	17.8±2.9* (47)
6	--	ND	33.1±4.0 (-)	22.6±3.5* (32)	19.2±1.7* (42)	18.2±1.7* (45)
7	--	ND	30.2±4.0 (10)	27.1±2.3 (19)	24.3±3.2^ (27)	ND
8	--	ND	28.9±2.7 (13)	24.5±3.4^ (27)	15.6±2.5* (53)	14.8±3.1* (57)
9	--	ND	29.8±2.5 (5)	21.3±2.7 (36)	22.5±3.1* (33)	18.2±3.0* (45)
10	--	ND	26.4±3.1 (21)	23.9±2.8^ (28)	22.5±3.1* (33)	20.7±2.6* (38)
11	--	ND	30.7±2.5 (8)	26.9±3.0 (19)	20.6±3.0* (38)	14.2±2.5* (57)
12	--	ND	35.4±3.3 (-)	24.1±2.3* (28)	19.3±2.8* (42)	13.8±2.9* (59)
CELECOXIB	--	19.3±2.5* (42)	16.6±2.2* (50)	42.2±2.3* (57)	13.9±2.7* (58)	10.2±2.1* (69)

Table 1.2. Effect of 1-12, celecoxib and vehicle in the mouse abdominal constriction test.

All compounds were suspended in 1% CMC and per os (po) administered 30 min before the experiment. 0.6% acetic acid was administered ip.. Each value represents the mean of 10 mice.

* P< 0.01 in comparison with CMC treated group

^ P< 0.05.

Among all the synthesized compounds, aldehyde **3,** oxime **7** and nitrile **10** were selected for evaluating inhibitory effects towards the human whole blood (HWB) assay for COX-1 and COX-2[49,50] (Fig. 1.12). This test allows to assess potency and selectivity in the presence of plasma proteins and in clinically relevant cells, such as platelets, that express only COX-1 and monocytes, expressing COX-2 in response to inflammatory stimuli. This assay has been suggested to be more useful for predicting drug efficacy in humans, because it takes into account the large number of variables that affect drug-enzyme interaction *in vivo*.

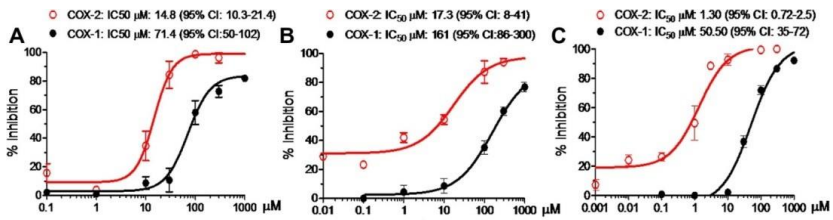

Figure 1.12. HWB inhibition curves for compounds **3 (A)**, **7 (B)** and **10 (C)**.

Compounds **3**, **7**and **10** proved to be more selective towards COX-2 than COX-1 (4.8, 9.3 and 38.8-fold, respectively) and were endowed with good values of IC_{50} (14.8, 17.3 and 1.30 μM, respectively). In contrast with its *in vivo* efficacy, nitrile **10** was found to be the most potent and selective compound; this discrepancy, even if related to one example of the entire class, could be related to a reduced bioavailability, metabolism and/or tissue distribution of nitriles.

Conclusions

Although aldehyde **3** proved to possess an antinociceptive activity comparable to that of celecoxib, these biological results showed that further modifications are needed to improve the pharmacological profile of these molecules. Moreover, since oximes **5-8** exhibited a very interesting pharmacological profile, the oxime moiety should be replaced with an isosteric moiety to get a geometrical differentiation and to evaluate any steric effect on the interaction with the receptor.

1.2.2.2. Synthesis, biological evaluation and docking analysis of a new series of methylsulfonyl and sulfamoylacetamides and ethyl acetate as potent COX-2 inhibitors

Sara Consalvi, Salvatore Alfonso, Angela Di Capua, Giovanna Poce, Adele Pirolli, Manuela Sabatino, Rino Ragno, Maurizio Anzini, Stefania Sartini, Concettina La Motta, Lorenzo Di Cesare Mannelli, Carla Ghelardini and Mariangela Biava[51].

This class of derivatives was synthesized with the aim of reducing metabolic instability of the previously synthesized compounds, by means of the isosteric replacement of the ester moiety with an amide group[51]. Thus, a series of isopropyl and propyl acetic amides (**13-16**, Fig. 1.13) was prepared; according to previous SAR results, these derivatives were characterized by a *p*-methylsulfonyl moiety at C5 and by a N1 phenyl ring decorated with fluorine substituents. Furthermore, the methylsulfonyl moiety was isosterically replaced by a sulfamoylphenyl group; this substituent was selected given the fact that arylsulfonamides generally display a greater *in vivo* profile with respect to the corresponding aryl sulfones. As reported by several studies, this is probably due to a lower logP and consequently to an improved absorption and bioavailability[52]. Moreover, this moiety decorates the phenyl ring of several coxibs, such as celecoxib and cimicoxib. To better evaluate the difference in activity, acetic ester derivatives **21** and **22** (Fig. 1.13) were also tested; hereafter, a second series of amides combining the sulfamoyl moiety with the amide function were synthesized (**17-20,** Fig.1.13). Finally, considering that both ester and amides could form the same acid derivatives *in vivo*, corresponding acids **23** and **24** were tested as well.

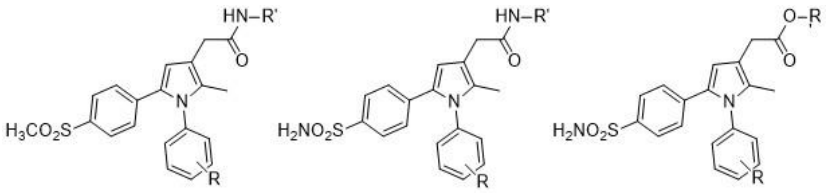

13: R=4-F; R'= *i*-pro
14: R=3-F; R'= *i*-pro
15: R=4-F; R'= *n*-pro
16: R=3-F; R'= *n*-pro

17: R=4-F; R'= *i*-pro
18: R=3-F; R'= *i*-pro
19: R=4-F; R'= *n*-pro
20: R=3-F; R'= *n*-pro

21: R=4-F; R'= -Et
22: R=3-F; R'= -Et
23: R=4-F; R'= -H
24: R=3-F; R'= -H

Figure 1.13. Chemical structures of compounds **13-24.**

Chemistry

Compounds **13-16** were prepared as shown in Scheme 1.2. Briefly, pyrroles **28 a-b** were obtained as reported in Scheme 1.1. The construction of the C3 side chain was achieved by regioselective acylation using ethoxalyl chloride and titanium tetrachloride to give corresponding ketoesters **29 a-b** that were in turn reduced to the pyrrole acetic esters **30 a-b** using triethylsilane in trifluoroacetic acid and that led to the corresponding acids **31 a-b** by treatment with 1N NaOH in MeOH for 1.5 h. Acids **31 a-b** were then coupled with the appropriate amine in the presence of 1-ethyl-3-(3-dimethylaminopropyl)carbodiimide (EDCI) and 4-dimethylaminopyridine (DMAP) afforded derivatives **13-16**.

Compounds **17-20** were synthesized following the synthetic pathway shown in Scheme 1.3. Briefly, pyrrole derivatives **28 a-b** were obtained as previously reported[37]; generation of a carbanion with butyllithium on arylmethylsulfones gave the trimethylsilylethyl intermediates **32 a-b.** Arylsulfonamides **33 a-b** were obtained by means of a desililylation with tetrabutylamonium fluoride to the corresponding sulfinic acid, followed by treatment with hydroxylamine-O-sulphonic acid in the presence of sodium acetate[52], in the microwave apparatus. A regioselective acylation of **33 a-b** using titanium tetrachloride and ethoxalyl chloride gave ketoesters **34 a-b** which in turn were reduced with triethylsilane in the presence of trifluoroacetic acid, providing esters **21** and **22**. The latter were hydrolized using sodium hydroxide in methanol and produced acid **23** and **24.** Finally, compounds **17-20** were obtained by reacting acetic acids **23** and **24** with the appropriate amine, in the presence of DMAP and EDCI.

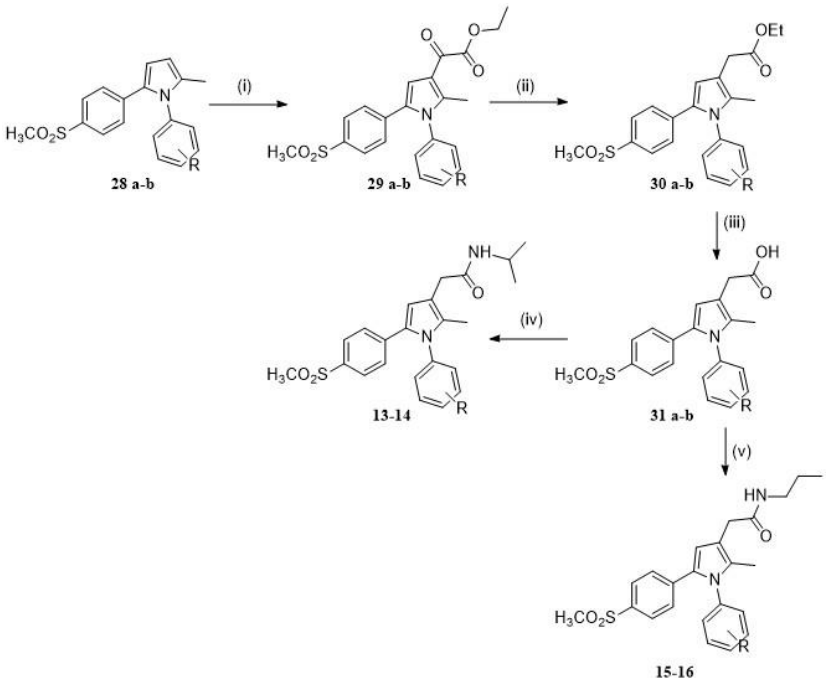

Reagents and conditions: (i) ethoxalyl chloride,$TiCl_4$, CH_2Cl_2, rt, 4h, 75-80% yield; (ii) triethylsylane, trifluoroacetic acid, rt, 2 h, 65-68% yield; (iii) NaOH, MeOH >90 % yield; (iv) *i*-Pr-NH_2, DMAP, EDCi, TEA, rt, 15h, 71-77% yield ; (v) Pr-NH_2, DMAP,EDCi,TEA,rt,15h, 74-76 % yield.

13: R=4-F; **14**: R=3-F; **15**: R=4-F; **16**: R=3-F; **28a**: R=4-F; **28b**: R=3-F; **29a**: R=4-F; **29b**: R=3-F; **30a**: R=4-F; **30b**: R=3-F; **31a**: R=4-F; **31b**: R=3-F.

Scheme 1.2. Synthesis of compounds **13-16**.

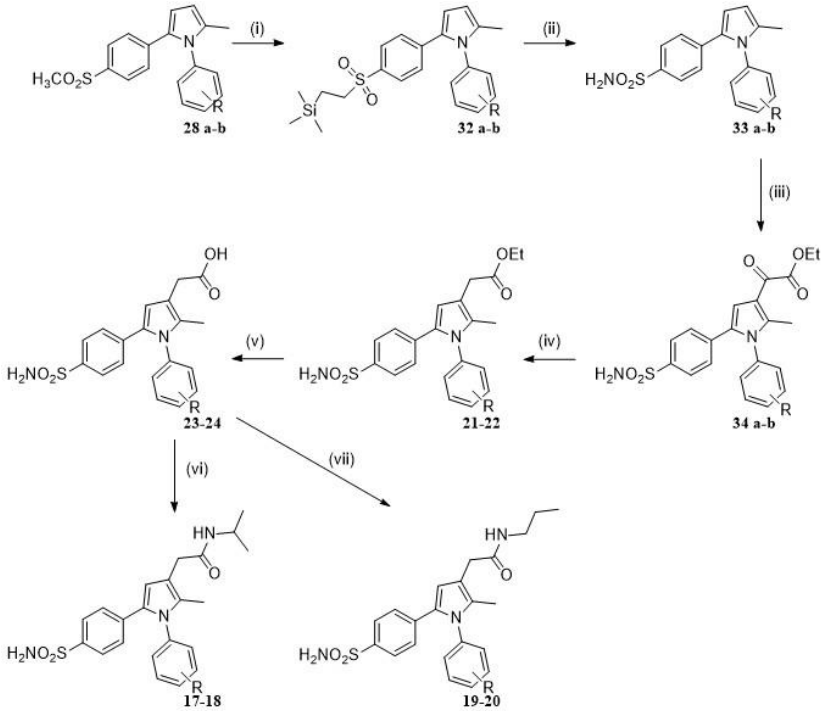

Reagents and conditions: (i) butyllithium, diisopropylamine, iodomethyltrimethylsilane, THF, -78°C-rt, 15 h, 56-60% yield; (ii) tetrabutilamoniumfluoride, hydroxylamino-O-solfonic acid, MW, 15', 78-83% yield; (iii) ethoxalyl chloride,TiCl, $CH_2Cl_2TiCl_4$, rt, 4h, 60-63% yield; (iv) triethylsylane, trifluoroacetic acid, rt, 2h, 58-67 % yield; (v) NaOH, MeOH, reflux, 1.5 h >90 % yield; (vi) *i*-Pr-NH_2, DMAP, EDCi, TEA, rt, 15h, 60-62% yield; (x) Pr-NH_2, DMAP,EDCi,TEA,rt,15h, 55-58% yield. **17**: R=4-F; **18**: R=3-F; **19**: R=4-F; **20**: R=3-F; **21**: R=4-F; **22**: R=3-F; **23**: R=4-F; **24**: R=3-F; **28a**: R=4-F; **28b**: R=3-F; **32a**: R=4-F; **32b**: R=3-F; **33a**: R=4-F; **33b**: R=3-F; **34a**: R=4-F; **34b**: R=3-F.

Scheme 1.3. Synthesis of compounds **17-24**.

Biological and pharmacological evaluation

All the synthesized compounds were tested *in vitro*, to assess their inhibitory activities towards both cyclooxygenases (COX-1 and COX-2). Tests were performed exploiting the commercially available COX Inhibitor Screening Assay (Cayman Chemical Company, Ann Arbor, MI, USA), which quantifies prostanoids produced by reaction between COX and arachidonic acid *via* an enzyme immunoassay (EIA). The inhibitory efficacy of the novel derivatives was routinely estimated at a concentration of 10 μM, and those compounds found to be active were then tested at additional concentrations between 10 μM and 10 nM, to

determine their IC_{50} values. As shown in Table 1.3, all compounds proved to be active when tested at 10 μM. Among the methylsulfonylphenyl derivatives, isopropylamide derivatives (**13-14**) proved to be more active than the corresponding propylamides (**15-16**). On the other hand, the ethyl ester function guaranteed the best activity in the sulfamoylphenyl series. In fact, both acid and amide derivatives were less active, showing that the replacement of that group with acetic acid or with an amide fragment is involved with a lack of activity. Finally, selectivity was demonstrated: in fact, the most active derivatives did not show appreciable inhibitory properties when assayed against COX-1.

	% of inhibition (10 μM)		
COMPOUND	COX-1	COX-2	IC_{50} (COX-2, μM[A])
13	36	95	4.91±0.20
14	N.T[B].	74	7.00±0.34
15	N.T.	65	N.D[C].
16	N.T.	43	N.D.
17	N.T.	48	N.D.
18	N.T.	49	N.D.
19	N.T.	62	N.D.
20	N.A[D].	96	5.78±0.30
21	N.A.	82	1.07±0.05
22	N.A.	89	0.92±0.05
23	N.T.	65	N.D.
24	N.T.	65	N.D.
SC-560	100		N.D.
DUP-697		100	

Table 1.3. *In vitro* inhibition of synthesized compounds.
[a]IC50values, means±SD, represent the concentration required to produce 50% enzyme inhibition.[b]Not tested [c]Not active [d]Not determined

Following the same protocol adopted for compounds **1-12**, all the synthesized derivatives were tested in the abdominal constriction assay to evaluate their efficacy in analgesia. As shown in Table 1.4 compound **21** exhibited the best activity (62 % of reduction when administered at the dosage of 40 mg/kg) and its efficacy is dose-dependent within the 10-40 mg/kg range. The analog 3-F derivative was less effective in reducing the number of writhes despite its similar activity *in vitro*. Among the methylsulfonyl derivatives, compound **13** proved to be the most active (48.7% of writhes reduction). Moreover, it is possible to observe a decrease of activity when going from isopropyl to propyl substituents, probably due the fact that a more branched chain is more stable at a metabolic level. Interestingly, even if administered at the different dosages, compounds **13**, **17** and **18** showed comparable activities to those of **MAB 66** and **MAB 48**, two of the most active compounds in the ester series, shown in Figure 1.14. Finally, sulfamoyl phenyl acetamido derivatives reduced the number of writhes with a moderate efficacy, except for compound **20**. The latter showed the lowest activity, nonetheless it was the most active compound *in vitro* among the sulfamoylphenyl derivatives.

TREATMENT	N° OF MICE	DOSE(MG/KG PO)	N OF WRITHES	WRITHES REDUCTION (%)
CMC	28		30.4±1.6	
13	6	10	26.7±3.6	12.2
	5	30	15.6±3.2*	48.7
14	5	10	29.3±2.8	3.6
	5	30	22.7±2.9*	25.3
15	6	1	30.6±3.7	-
	7	3	27.3±2.9	10.2
	6	10	21.3±3.4*	29.9
16	5	10	26.7±2.5	12.2
	5	30	27.4±3.3	9.9
17	6	3	25.5±3.8	16.1
	5	10	19.3±2.5*	36.5
	6	30	17.1±3.5*	43.7
18	6	3	26.9±3.1	11.5
	5	10	21.5±3.2*	29.3

	5	30	20.8±3.3*	31.6
19	6	3	29.2±3.3	3.9
	5	10	27.9±4.1	8.3
	6	30	18.5±3.6*	39.1
20	5	10	32.9±4.2	-
	5	30	26.7±3.7	12.2
21	8	10	29.2±3.1	10.4
	8	20	24.5±3.6*	24.8
	8	40	12.3±2.5*	62.3
22	5	10	22.5±2.5^	26.0
	5	30	20.2±2.8*	33.5
23	7	10	27.1±3.5	16.9
	8	20	21.8±3.2*	33.1
	9	40	16.6±3.1*	49.1
24	5	10	27.5±2.8	9.5
	6	30	31.3±3.3	-
MAB 48	8	1	33.6±3.0	-
	8	5	28.5±3.3	6
	8	15	25.5±2.8	16
MAB 66	12	5	29.5±3.8	3
	9	20	17.7±2.9	42
CELECOXIB	12	10	13.0<±2.1	57.4

Table 1.4. Effect of 13-24, celecoxib, and vehicle (CMC) in the mouse abdominal constriction test (acetic acid 0.6%). ^P < 0.05; * P < 0.01 in comparison with CMC treated group.

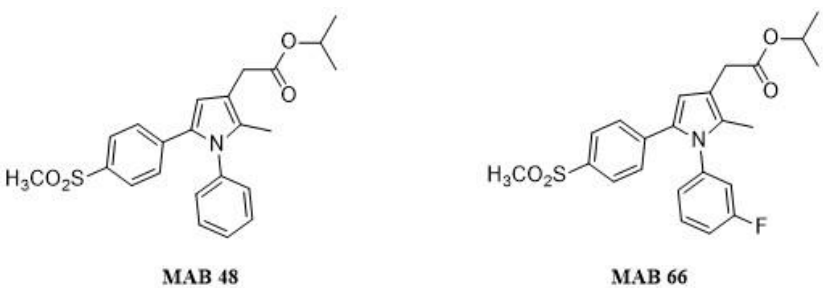

Figure 1.14. Chemical structures of MAB 48 and MAB 66

Structure-Based studies

Docking Assessment

Before performing any docking study, the most suitable docking program within a series of 8 program/scoring combinations function was assessed by a previously described cross-docking protocol[53,54]applied on the available experimental co-crystallized complexes for either COX-1 or COX-2.Briefly, each energy minimized COX complex was divided into ligand and protein. The separated ligand conformations were randomized and docked into all proteins (cross-docking), except for the native ones. The resulting lowest energy pose within all the docking runs were then compared to the experimental ones, and the root mean square deviations (RMSDs) were calculated. The calculated docking accuracy percentages (DAs %)[55]revealed Surflex-Dock[56,57] as the most suitable program to dock a modeled ligand into COX-1 showing DAs % of 58.33 while Vina performed the best for COX-2 (DA% = 67.86).In the case of COX-1, Autodock performed the same A %, but the error dispersion as calculated by the RMSD standard deviation was slightly higher than that of displayed by Surflex-Dock, with almost the same average values, furthermore Surflex-Dock is about 10 times faster than Autodock. These results clearly indicate that in the presence of a ligand able to bind either COX-1 or COX-2,the most suitable program need to be chosen ad-hoc. Based onthe docking assessment Surflex-Dock and Vinawere able to suggest their correct binding mode with the lowest errors for COX-1 and COX-2, respectively.

Binding Mode Analysis of the New Compounds

As Surflex-Dock and Vina performed the best, the titled compounds were all cross-docked by means of these programs. In particular, all the compounds found active against either COX-1 or COX-2 enzymes were modeled and cross-docked into all the available COX-1/COX-2 experimental structures following the same protocol as in the docking assessment. The lowest energy poses were selected[53] as the likely binding modes for the newly synthesized compounds. Compound **13** was the only one found with an appreciable inhibitory activity against COX-1 (36% at 10 μM) and its lowest energy bound pose was found in the proteins 2OYU. On the contrary, all the compounds

were selectively active against COX-2 at different levels and therefore were all cross-docked. Eight times (compounds **15, 16, 18**, **19**, **20**, **21**, **23** and **24**) out of twelve, 3LNI was the preferred binding site, while three times (compounds **13**, **14** and **17**) was selected the protein extracted from the 2MQE complex and compound **22** was found to best bind in 3QMO.As a matter of fact, the Vina predicted affinities against COX-2 for compounds **13, 20, 21** and **22** did not correlate with the experimental ones, likely due to the high redundancy in the scoring function associated to any docking program. On the other hand, comparing the Vina average predicted affinities, the scoring function correctly indicated compound **13** as more active against COX-2 than against COX-1. In the latter case, the enzymes' structural differences are somehow recognized by thescoring function and corroborate the previous statement.COX-2 active compounds were all docked, and their bindings examined. The COX-2 active derivatives **13-23** share a common binding mode (BM). Being compound **13** the only one exerting some activity against either enzyme BM inspection into COX-1 and COX-2 were focused on this compound. Nevertheless BM analysis revealed that compound **13** adopts similar binding modes into either isoenzyme. The main difference in binding relies on the fact that in COX-2 Arg513 side chain in the selectivity pocket makes a moderate hydrogen bond[58-59] with the sulphonyl group (distance NCOX-2-Arg513•••O4-(SO_2) = 3.10 Å), which is missing in COX-1 being residue 513 an histidine with a shorter and less flexible side chain not able to make any hydrogen bond with 4-sulphonyl group. Surprisingly, this observation is in good agreement with the 1.23 kcal/mol binding energy difference recorded for compound **13** in both COX-1 and COX-2. Furthermore, the 4-SO_2 hydrogen bonding oxygen is perfectly superimposing its analogue atom in Celecoxib SO_2 moiety as found in the bound crystal. Regarding the other titled derivatives, the overall binding modes are quite overlapping, and any further inspection would be redundant. This common BM confirms the reproducibility of the docking protocol when slightly structural differences occur. The herein application of Surflex-Dock/Vina and the cross-docking protocol are in good agreement with the earlier observations in which a different docking program (Autodock 3.0.5) and only one COX-2 structure (pdb entry code 1CX2) were used. For comparison purposes, the latest version of Autodock was applied in a parallel to cross-dock **13-24** and only slightly binding

mode differences were observed.

Conclusions

Among the synthesized compounds, some of them were endowed with a good activity against COX-2 and a good selectivity COX-2/COX-1 *in vitro* and showed a good analgesic activity *in vivo,* proving that replacement of the ester moiety with an amide group gave access to more stable derivatives, characterized by a good COX-inhibiting profile. Comparing the same dosage (10 mg/kg), sulphamoyl phenyl derivatives proved to be more active than the methylsulphonyl analogues, showing that introduction of this group led to compounds characterized by a better *in vivo* profile and a greater activity at lower dosages, probably because of their greater bioavailability. Further studies are needed to evaluate influence of that moiety on solubility and to assess the pharmacokinetic profile.

1.3. A novel class of 1,5-diphenylpyrrole acetamides endowed with NO-releasing properties

1.3.1 State of the art of the project

COX-2 inhibiting nitric oxide donors are a class of hybrid molecules that conjugates a COX-2 selective inhibiting scaffold with an NO-releasing moiety; bearing in mind NO cardioprotective effects, these agents have been developed with the aim of obtaining new anti-inflammatory and analgesic agents endowed with a safe gastrointestinal and cardiovascular profile. Following the same strategy that led to Naproxcinod, the best compounds of the selective COX-2 inhibitors series described in the previous chapter were further modified by introducing a NO donor moiety at C3.Thus, four sets of 1,5-diphenylpyrrole derivatives, shown in Fig.1.15, were previously synthesized and tested.[60–63]

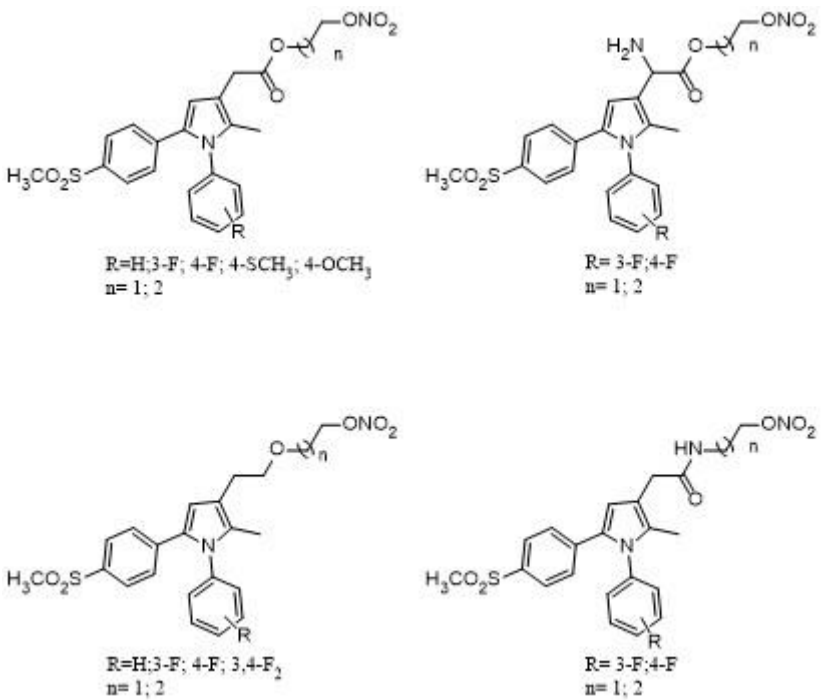

Figure 1.15. Four series of 1, 5-diphenylpyrrole nitric oxide donors.

1.3.1.1. First series: acetic esters endowed with NO-releasing properties

Taking into account SAR results coming frompreviously synthesised compounds, this first set of compounds was characterized by: *i)* a *p*-methylsulphonylphenyl moiety at position 5, responsible for selectivity; *ii)* an N1 phenyl ring decorated with the most convenient substituents; *iii)* an NO-donor alkyl ester chain with different length at position 3[60] (Fig. 1.16). Moreover, grounding on the Naproxcinod metabolism *in vivo* (Fig. 1.4), the corresponding hydroxyl derivatives were also synthesized and tested as possible metabolites.

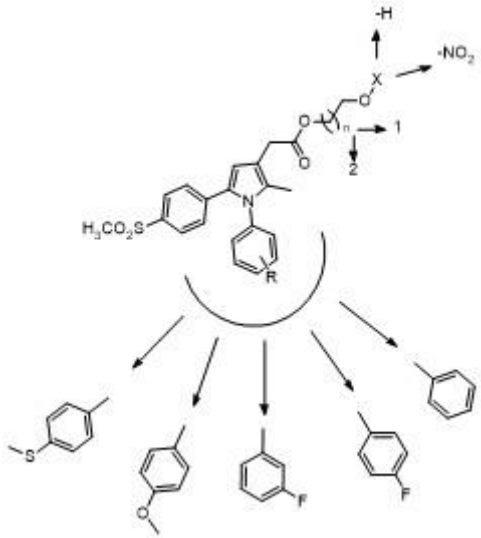

Figure 1.16. Chemical structures of the first series of derivatives.

All the synthesized compounds inhibited COX-2 at various concentrations, ranging from 1.1 micromolar to 2.4 nanomolar. Notably, nitrates compounds displayed biological activities better than the corresponding hydroxyl derivatives. Thus, differently from Naproxcinod, these compounds proved to be endowed with intrinsic anti-inflammatory properties and to not require metabolic activation.

Nitrate derivatives were further evaluated to assess their efficacy and potency in determining NO-dependent vasorelaxing responses in endothelium-denuded rat aortic rings. The obtained results showed that the two-carbons chain-bearing compounds were always endowed with vasorelaxing effects greater than the corresponding three-carbons

ones, proving that the side chain length played a pivotal role in terms of NO-releasing properties. The hydroxyl derivatives showed no vasorelaxing effects, thus demonstrating that these effects were due to the nitrooxy group. The meta-fluorine subclass of compounds was selected for the *in vivo* abdominal constriction test and the carrageenan-induced pain assay. The former pointed out that the two carbons side-chain compounds displayed a better analgesic activity, confirming the dependence of the efficacy on the side-chain length. On the other hand, the hydroxyl derivatives exhibited activities similar to that of corresponding nitrates. Even though all the tested compounds exhibited a significant efficacy *in vivo*, the activity seemed to be reduced with respect to that of predicted by *in vitro* assay. This result led us to hypothesize that the pharmacokinetic behaviour could play a fundamental role in determining the *in vivo* features of this class of molecules, therefore we went on to analyze the solubility and the metabolic stability. As expected, these compounds proved to be poorly soluble in water; moreover, the chemical and enzymatic liability of this class of molecules was taken into account as a potential responsible for that *in vitro*/*in vivo* gap of pharmacological profiles, in line with what previously reported on COX-2 inhibiting ester derivatives. Thus, our efforts were directed at improving pharmacokinetic properties[60].

1.3.1.2 Second series: glycine esters

This series of compounds was synthesized with the aim of improving solubility; for this purpose an ionizable moiety, such as an amino group, was introduced at the alpha position of the acetic side chain[61]. The phenyl ring at N1 was decorated with a fluorine atom, because of the higher degree of interaction within the binding site shown in the first series; finally, we also synthesized the nitro-free derivatives as possible metabolites (Fig. 1.17).

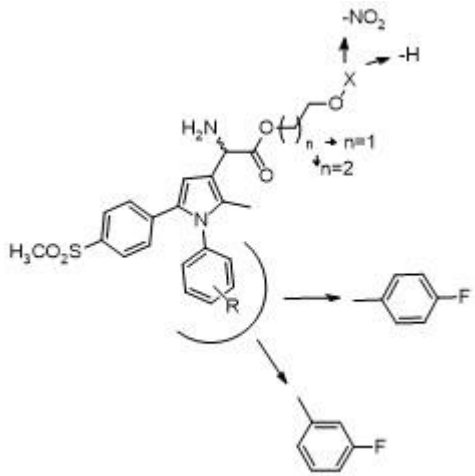

Figure 1.17. Chemical structures of the second series of derivatives.

As expected, the introduction of an amino group led to a dramatic increase in solubility; indeed, the amino derivatives proved to be more than 200-fold soluble than acetic esters (200 *vs* 1 μM), in the simulated gastric fluid (SGF). Moreover, tested compounds showed a 80-times higher (80 *vs* 1.6 μM) solubility in the phosphate buffered saline (PBS). On the other hand, such modification determined a significant lack of *in vitro* activity, as displayed by the cell-based assay. The solubility enhancement caused an increase of the *in vivo* activity; in fact, the abdominal constriction and the carrageenan tests showed quite good activities of the tested compounds. Nonetheless, the efficacy was very close to that of the first series of esters. Finally, the reduced interaction with the enzyme *in vitro* and the absence of the increase of the *in vivo* activity led us to introduce further structural modifications.

1.3.1.3. Third series: ethers

In parallel, a class of NO-releasing ethers were designed in order to overcome the metabolic instability due to the presence of the ester moiety[62] (Fig. 1.18).

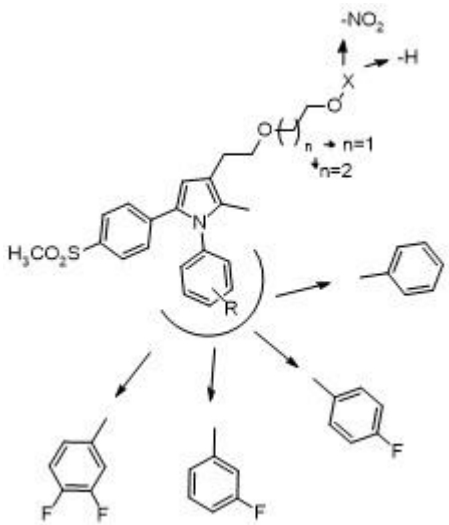

Figure 1.18. Chemical structures of the third series of derivatives.

This transformation led to active compounds, characterized by low values of IC_{50}, ranging from 8.99 micromolar to 7.30 nanomolar, significant NO-releasing properties and good *in vivo* activities. Despite their greater stability, this class of derivatives was characterized by low solubility. Consequently, we decided to further manipulate the scaffold with the aim of improving both stability and solubility.

1.3.1.4. Fourth series: amides

In order to improve both stability and solubility the ester moiety was replaced with an amide group, in line with what earlier reported on COX-2 selective inhibitors. Moreover, two subclasses of compounds decorated with either a free carboxylic substituent or a free amino group were also prepared to further enhance the solubility[63] (Fig. 1.19).

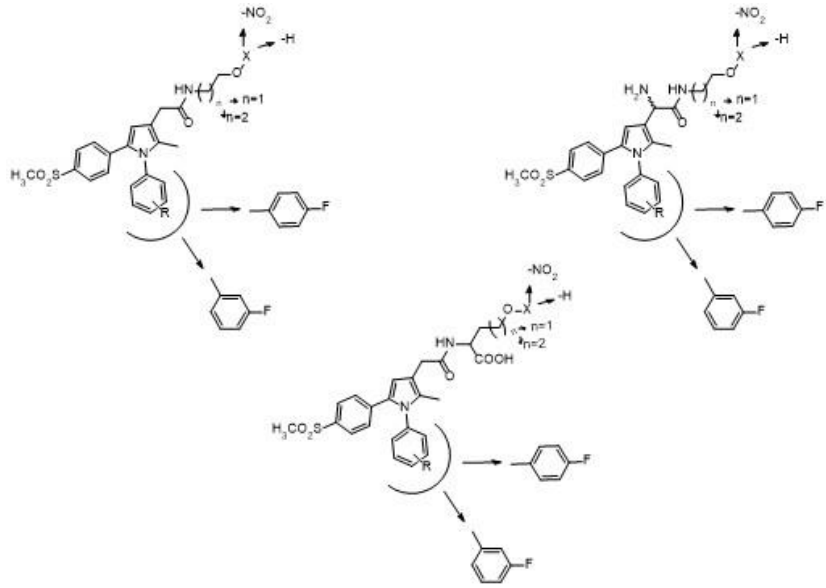

Figure 1.19. Chemical structures of the fourth series of derivatives

All the synthesized compounds displayed great COX-2 inhibitory potencies and high selectivity values in the cell-based assay. In particular, the glycine derivatives proved to be endowed with low values of IC_{50}, demonstrating that the negative effect observed with the previous class of esters was probably due to a mismatch interaction rather than to the presence of the amino group itself. The nitrooxy derivatives also showed NO-dependent vasorelaxing properties and a slow kinetic of NO release. Encouraged by such results, the anti-inflammatory and analgesic properties of selected compounds were also investigated *in vivo*, in the abdominal writhing test and in a carrageenan model of induction of pain. All the tested derivatives showed excellent and dose-dependent activities, probably because of the enhanced pharmacokinetic properties. To complete the picture, solubility and pharmacokinetic studies were also assessed. The former showed that the replacement of the ester functionality with the amide moiety gave access to more soluble molecules. Interestingly, the solubility of the carboxylate compounds was lower than expected, probably because of the participation of the carboxylic group to an intramolecular H-bond that stabilized the molecule reducing the solubility. Linear and glycine amides displayed very good values of solubility as well. Moreover, the

stability in SGF, PBS and rat plasma was also investigated: the tested compounds proved to be much more stable than both the corresponding linear and glycine esters, demonstrating that the amide moiety was less sensitive to both chemical and enzymatic hydrolysis. Finally, **MAB 137** was selected to investigate the pharmacokinetic profile; the obtained results showed that this compound was characterized by a moderate rate of clearance (0.6 L/h) and that the average finale volume of distribution was twice the rat total body water, suggesting a moderate distribution in tissues (Fig. 1.20).

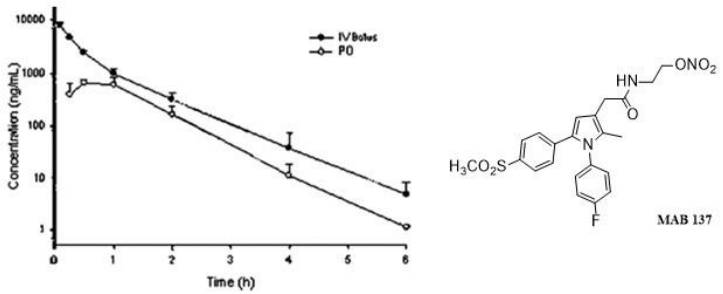

Figure 1.20. Profile of plasma concentration vs time of **MAB 137**after intravenous and oral administration.

Considering that nitro-esters could be metabolized to the corresponding alcohol **MAB145**, the presence of the hydroxyl moiety was also measured (Fig.1.21). At least 39% of the parent compound was converted into the metabolite after intravenous administration while the 99% conversion was observed after oral administration, proving that this way of administration led to a more rapid conversion of **MAB 137** into the metabolite[63].

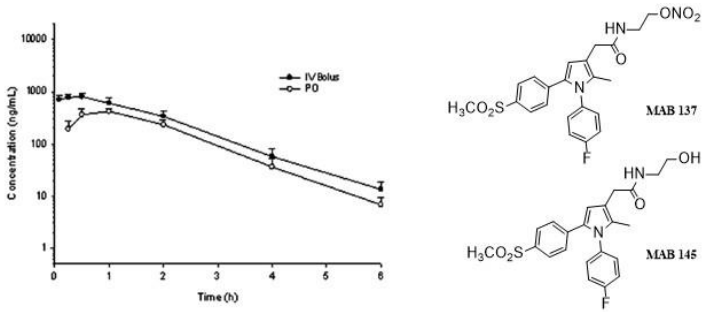

Figure 1.21. Mean plasma concentration vs time profile of **MAB 145** after intravenous and oral administration of **MAB 137**

1.3.2. Rationale and aims

The structural modifications introduced on the diphenylpyrrole acetic scaffold led to the identification of a series of amide derivatives endowed with good analgesic and anti-inflammatory efficacies and an improved pharmacokinetic profile. Encouraged by such results, we decided to modify this scaffold with the aim of further improving both potency and activity without affecting the pharmacokinetic properties. For this purpose, we decided to amend the C5 position keeping unchanged the NO-releasing amide chain at C3, responsible for both stability and solubility enhancement. The methylsulfonylphenyl moiety at C5 was then replaced by the isosteric sulfamoylphenyl function, following the same pathway described for derivatives **17-20**. Then, a novel series of NO-releasing sulfamoylphenyl amide derivatives was synthesized; consistent with SAR data emerged from the previous studies, these compounds were characterized by (compounds **35-38**, fig. 1.22):

- A sulphamoylphenyl ring at C5;
- A phenyl ring at N1 decorated with the most convenient substituents (H; 3-F; 4-F; 3,4-F_2).
- A two-carbon amide NO donor side chain at C3.
- Moreover, the corresponding hydroxyl derivatives were also synthesized and tested as possible metabolites (compounds **39-42**, fig. 1.22).

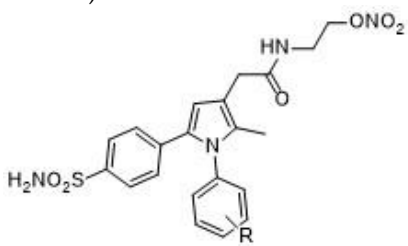

35: R=-4-F;
36: R= -3-F;
37: R= -3,4-F_2;
38: R= -H

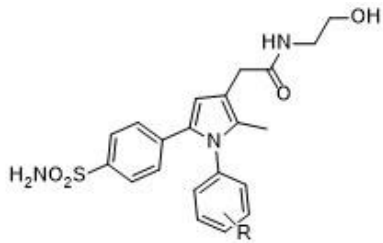

39: R=-4-F;
40: R= -3-F;
41: R= -3,4-F_2;
42: R= -H

Figure 1.22. Chemical structures of derivatives **35-42.**

1.3.3. Chemistry

The acid derivatives **43 a-d** were obtained following the same procedure seen for compounds **23** and **24**, reported in Scheme 3. The nitrooxy-ethylamine compounds **35-38** were synthesized by means of a coupling reactions between derivative **45** and the suitable acetic acids in the presence of DMAP, EDCi and TEA; compound **45** was obtained via nitration of ethanolamine using fuming nitric acid in dichloromethane and then precipitated as a nitrate salt through the addition of acetic anhydride. The hydroxyl derivatives **39-42** were obtained via an EDCi/HOBt (hydroxybenzothriazole) coupling. The synthesis of compounds **35-42** is reported in Scheme 1.4.

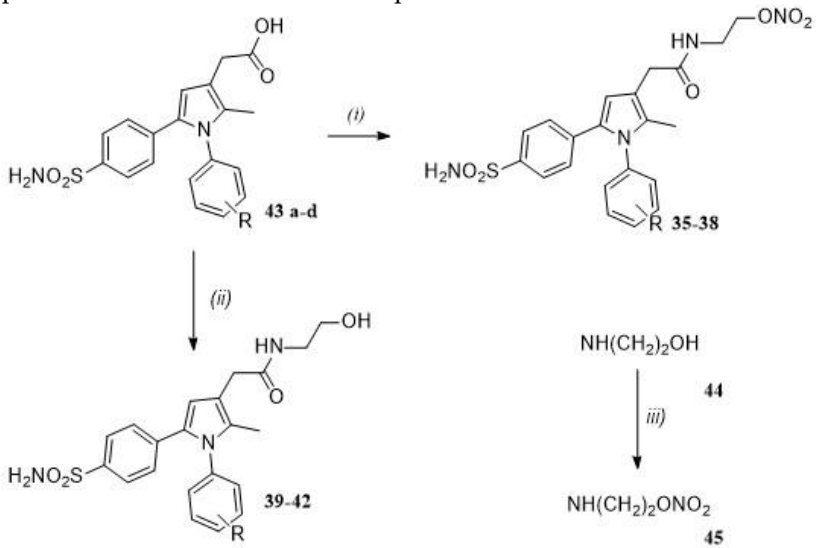

Reagents and conditions: (i) **45**, ,DMAP,EDCi,TEA,DCM/DMF,10:1,rt,15h, 47-52% yield (ii) **44**, (iii)HNO_3,CH_3COOH,$(CH_3COO)_2OAc$,EtOAc,rt,2h,45-50%yield

43a: R=4-F; **43b:** R=3-F; **43c** R=4-F; **43d:** R=3-F; **35:** R=4-F; **36:** R=3-F; **37**: 3,4-F_2; **38**:-H; **39:** R=4-F; **40:** R=3-F; **41**: 3,4-F_2; **42**:-H.

Scheme 1.4. Synthesis of compounds **35-42**.

1.3.4. Biological and pharmacological evaluation

Preliminary *in vitro* results displayed that the tested compounds inhibited COX-2 in the submicromolar range (Table 1.5), except for compound **41**. Following the same trend observed for the previous series

of compounds, the hydroxyl derivatives were found to be generally less active than the corresponding nitrooxy ones; this result confirmed that, differently from Naproxcinod, these pharmacodynamic hybrids were endowed with intrinsic antiinflammatory properties and did not require metabolic activation. Notably, derivatives **35** and **36** exhibited an IC_{50} smaller than the corresponding methylsulfonyl analogue **MAB 137** (more than one magnitude order). The latter is one of the most active compounds of the previous series, therefore this result proved that the replacement of the methylsulfonyl moiety with the sulfamoyl function improved the electronic interactions within the COX-2 selectivity site.

		% INHIBITION AT 10 μM		
COMPOUND	R	COX-1	COX-2	IC_{50} (μM)
35	-4-F	7	93	0.014
36	-3-F	5	95	0.020
37	-3,4-F_2	20	88	0.050
38	-H	17	83	0.090
39	-4-F	34	89	0.840
40	-3-F	25	88	0.45
41	-3,4-F_2	12	54	5.500
42	-H	30	82	0.60
MAB 137	-	9	100	0.250
CELECOXIB	-	65	100	0.061

Table 1.5. ***In vitro*** **activities towards COX-1 and COX-2.**

Among the nitrooxy compounds, derivatives **35-37** were endowed with the best *in vitro* potency. Therefore, they were selected to assess their capability in determining vasorelaxing responses; these derivatives were tested in a suitable experimental model of vascular smooth muscle, in particular in endothelium-denuded aortic ring precontracted with 30 mM KCl. Since NO induces vasodilator responses by activating guanylate cyclase and consequently increasing cGMP levels, the experiments were also performed in the presence of a guanylate cyclase inhibitor (1*H*-[1,2,4]oxadiazolo[4,3-*a*]quinoxalin-1-one,

ODQ), to confirm their mechanism of action. All the tested compounds were endowed with good vaso-relaxing properties and displayed a comparable efficacy (E_{max}) and a higher potency (pIC_{50}) with respect to that of the methylsulfonyl analogue **MAB 137** (Table 1.6).

COMPOUND	EMAX	pIC_{50}
35	74.9 ± 2.5	5.82 ± 0.04
36	67.5 ± 2.3	5.49 ± 0.00
37	74.9 ± 2.7	6.34 ± 0.06
MAB 137	68.0 ± 0.05	5.31 ± 0.05

Table 1.6. Nitric oxide releasing efficacy and potency for compounds 35-37.

The vasorelaxing efficacy was evaluated as the maximal vasorelaxing response (Emax), expressed as a percentage of the contractile tone induced by KCl 30 mM.The potency was expressed as pIC_{50} that was calculated as negative logarithm of the molar concentration of the tested compounds evoking a half reduction of the contractile tone induced by KCl 30 mM.

As shown in Fig. 1.23, all the tested compounds were inactive in the presence of ODQ, proving that their efficacy was due to NO release. Notably, no vasorelaxing effect was observed at low concentrations, suggesting that these compounds gradually released NO; therefore, they were not supposed to be responsible for a massive hypotensive effect *in vivo*.

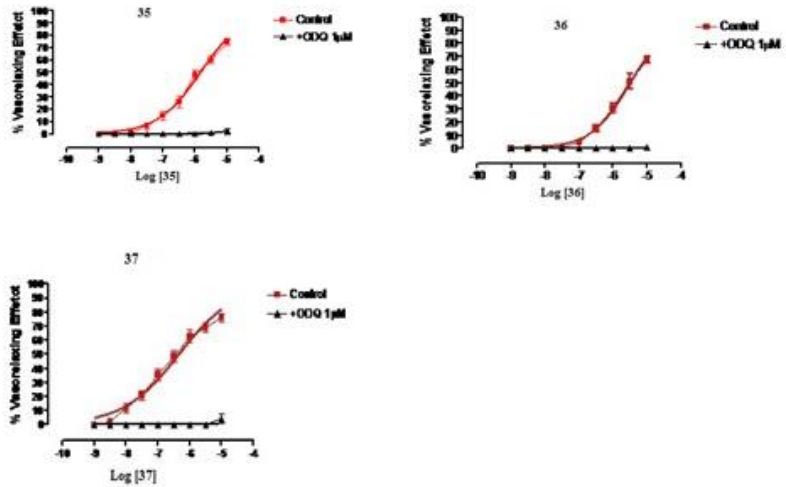

Figure 1.23. Concentration-response curves concerning the vasorelaxing effects evoked by **35**, **36** and **37**, recorded in the absence or in the presence of ODQ. The vasorelaxing responses are expressed as a percentage of the contractile effect induced by 30 mM KCl. The vertical bars indicate the standard error.

Based on their *in vitro* potencies, three nitrooxy derivatives (**35-37)** and the hydroxyl compound **40** were selected to assess their efficacies in the analgesia by means of the abdominal constriction test (Table 1.7). All the tested compounds proved to be active in reducing the abdominal writhes caused by acetic acid. In particular, derivative **36** showed a very interesting profile; since it was the most active at 5 mg/kg, its efficacy was also evaluated at lower dosages (1 and 3 mg/kg). The obtained data showed that it was even significantly effective when administered at the dose of 1 mg/kg (35% of writhes reduction), with a significantly better efficacy with respect to that of **MAB 137** and comparable to that of celecoxib. Compounds **35** and **37** proved to be moderately active; surprisingly, even though their IC_{50} values were much smaller than that of **MAB 137**, their *in vivo* activities were in general lower at the tested doses. Moreover, in both cases a costant response of writhes reduction was observed in treated animals**,** with the absence of dose-dependent activity in the 20-40 mg/kg range. Finally, the hydroxyl compound **40** was found to be less active than the corresponding nitroderivatives, confirming the trend observed for the

previously synthesized compounds.

TREATMENT	N° OF MICE	DOSE (MG/KG PO)	N°OF WRITHES	WRITHES REDUCTION (%)
CMC	28		33.6±2.2	-
35	8	5	26.7±3.3	7
	8	10	18.5±4.2	45
	8	20	15.8±3.7	53
	8	40	16.7±2.5	50
36	8	1	21.8±3.5	35
	8	3	19.4±2.9	42
	8	5	16.7±3.5	50
37	8	5	25.3±3.9	25
	7	10	17.8±3.1	47
	8	20	12.4±2.5	63
	8	40	13.7±2.8	59
40	7	3	26.4±2.5	21
	8	10	23.8±3.1	29
	9	30	21.2±2.7	37
MAB 137	10	1	NOT AC-	0
	10	5	TIVE	31
	10	10	23.1±2.8	64
	10	20	12.2±2.3	78
	10	40	7.4±1.3	76
			8.1±1.2	
CELECOXIB	10	1	19.3±2.5	42
	10	5	16.6±2.2	50
	10	10	14.2±2.3	57
	10	20	13.9±2.7	58
	10	40	10.2±2.1	70

Table 1.7. Writhes reduction for 35-37 and 40.

1.3.5. Conclusions

Preliminary *in vitro* results showed that the replacement of the methylsulphonyl moiety with the sulphamoyl one gave access to compounds endowed with higher values of potency towards COX-2. The nitrooxy derivatives also exhibited good vasorelaxing properties, due

to NO release. Among the tested compounds, derivative **36** proved to be most effective *in vivo*. The latter proved to be able to reduce writhes even at very low concentrations (1 mg/kg), with an efficacy comparable to that of celecoxib and higher than that of **MAB 137**, the most active methylsulfonyl analogue. Therefore, further studies will be carried out to assess its pharmacokinetic profile and *in vivo* anti-inflammatory activity.

1.4. Materials and methods

1.4.1. Chemistry

All chemicals used were of reagent grade. Yields refer to purified products are not optimized. A CEM Discovery microwave system apparatus was used for the synthesis of compounds **26**, **28a-d** and **33 a-b.** ^{1}H NMR spectra were recorded with a Bruker Avance DPX-400 spectrometer with the residual solvent peak as the internal reference ($CDCl_3$ = 7.26 ppm, DMSO-d6 = 2.50 ppm). ^{1}H resonances are reported to the nearest 0.01 ppm. ^{13}C NMR spectra were recorded with the same spectrometers with the central resonance of the solvent peak as the internal reference ($CDCl_3$ = 77.16 ppm, DMSOd6= 39.52 ppm). All ^{13}C resonances are reported to the nearest 0.1 ppm. The multiplicity of ^{1}H signals are indicated as: s = singlet, d = doublet, m = multiplet, or combinations of thereof. Mass spectra were recorded on a APITOF Mariner by Perspective Biosystem (Stratford, Texas, USA). Purity of compounds was assessed with elemental analysis obtained by a PE 2400 (Perkin–Elmer) analyzer. Purity of target compounds was >95%. Unless stated otherwise, reagents were obtained from commercial sources and used without purification.Sigma-Aldrich silica gel 60 (230–400 mesh) aluminum oxide (activity II–III, according to Brockmann) were used for column chromatography.

Unless otherwise stated, heating was conducted using standard laboratory apparatus. TLC analysis was performed on Merck 60 F254 silica gel plates and visualized using both short and long waved ultraviolet light in combination with standard laboratory stains such as acidic potassium permanganate. Melting points were performed on either a Stanford Research Systems MPA100 (OptiMelt) automated melting point system or a Gallenkamp melting point machine and are uncorrected.

1.4.1.1. Synthesis of 1-[4-(methylthio)phenyl]pentane-1,4-dione (26)

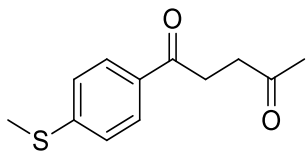

A solution of 4-methylthiobenzaldehyde **25** (11.97 mL, 0.09 mol), triethylamine (19.5 mL, 0.14 mol), methyl vinyl ketone (5.8 mL, 0.09 mol), and 3-ethyl-5-(2-hydroxyethyl)-4-methylthiazolium bromide (3.53 g, 0.014 mol), in a 20 mL vial, was microwave irradiated using a CEM apparatus for 15 min at 70 °C (150 W, internal pressure of 150 psi). The reaction mixture was treated with 2 N HCl (10 mL) and extracted with ethyl acetate; the organic layer was washed with aqueous sodium bicarbonate and brine. The organic fractions were dried over sodium sulfate, filtered, and concentrated to give an orange liquid which was crystallized from cyclohexane to give intermediate **26** as white needles (80% yield). ESI-mass: m/z 245.063 $[M+Na]^+$, mp, and ^1H NMR spectrum were consistent with those reported in the literature.[37]

1.4.1.2. Synthesis of 1-[4-(methylsulfonyl)phenyl]pentane-1,4-dione (27)

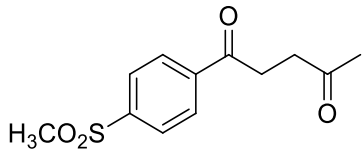

To a solution of **26** (7.8 g, 35 mmol) in methanol (150 mL), a solution of oxone (37.7 g, 61.4 mmol) in water (150 mL) was added over 5 min. After being stirred at 25 °C for 2 h, the reaction mixture was diluted with water (400 mL) and extracted with dichloromethane. The organic layer was washed with brine (200 mL) and dried over Na_2SO_4). After filtration and concentration, the crude material was chromatographed (silica gel, 3:1 hexane/ethyl acetate) to give **27** (90% yield) as a white solid. ESI-mass: m/z 277.052 $[M+Na]^+$, mp, and ^1H NMR spectrum were consistent with those reported in literature.[37]

1.4.1.3. General procedure for the preparation of 1,5-diphenylpyrroles

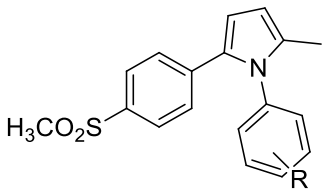

The 1,4-pentanedione **27** (2.28 mmol) and the suitable aniline (2.28 mmol) were dissolved in ethanol (2 mL) in a round-bottom flask equipped with a stirring bar in the presence of *p*-toluenesulfonic acid (30 mg, 0.17 mmol). The flask was heated in the cavity of the Discovery Microwave System apparatus (150W for 30 min, internal temperature 160° C, and internal pressure 150 psi). At the end the reaction mixture was cooled down and concentrated. The crude material was purified by chromatography on aluminum oxide with cyclohexane/ethyl acetate to give the expected 1,5-diarylpyrroles **28 a-d** as solids in satisfactory yields.

1-(4-Fluorophenyl)-2-methyl-5-(4-(methylsulfonyl)phenyl)1H-pyrrole (28a). ESI-mass: m/z 352.083 $[M+Na]^+$, mp, and ^1H NMR spectrum were consistent with those reported in literature[37].

1-(3-Fluorophenyl)-2-methyl-5-(4-(methylsulfonyl)phenyl)1H-pyrrole (28b). ESI-mass: m/z 352.091 $[M+Na]^+$, mp, and ^1H NMR spectrum were consistent with those reported in literature.[37]

1-(3,4-Difluorophenyl)-2-methyl-5-(4-methylsulfonyl)phenyl)-1H-pyrrole (28c). ESI-mass: m/z 370.075 $[M+Na]^+$, mp, and ^1H NMR spectrum were consistent with those reported in literature.[37,38]

2-Methyl-5-(4-(methylsulfonyl)phenyl)-1-phenyl-1H-pyrrole (28d). ESI-mass: m/z 334.092 $[M+Na]^+$, mp, and ^1H NMR spectrum were consistent with those reported in literature.[43,44]

1.4.1.4. General procedure for the synthesis of pyrrole-3-carbaldehydes (1-4)

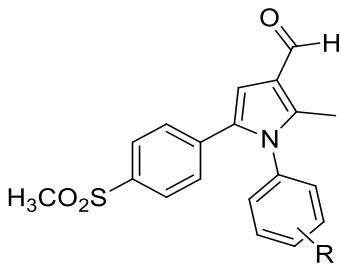

To a solution of dimethylformamide (8.3 mmol) in dichloromethane (10 mL) at 0 °C, in a round-bottomed flask equipped with a stirring bar, phosphoryl chloride (8.4 mmol) was added dropwise. After 30 min a solution of **28** (3.2 mmol in 10 mL of 100 dichloromethane) was added over 3 min and then refluxed for 1 h. The reaction mixture was cooled down to rt, diluted with saturated carbonate solution (50 mL) and extracted with dichloromethane. The organic layer was washed with brine (200 mL) and water (200 mL) and dried over sodium sulfate. After filtration and concentration, the crude material was crystallized using ethyl acetate to give the aldehyde as an off-white solid.

2-Methyl-5-[4-(methylsulfonyl)phenyl]-1-[4-fluoro-phenyl]1H-pyrrole-3-carboxaldehyde(1). White needles (>95% yield). ESI-mass: m/z 357,082 $[M+Na]^+$; Elem. Anal. for $C_{19}H_{16}FNO_3S$ calcd C, 63.85; H, 4.51; N, 3.92. Found C, 63.82; H, 4.55; N, 3.98; data, mp, ^1H and ^{13}C NMR spectra were consistent with those reported in the literature.[45]

2-Methyl-5-[4-(methylsulfonyl)phenyl]-1-[3-fluoro-phenyl]1H-pyrrole-3-carboxaldehyde (2). Off-white needles (>95% yield), mp 170 °C. ^1H NMR (DMSO-d6 400 MHz) ppm: 9.93 (s, 1H), 7.85 (m, 1H), 7.52 (m, 1H), 7.40 (m, 2H), 7.31 (m, 1H, J = 8.6 Hz), 7.08 (d, 2H, J = 8.6 Hz), 6.94 (s, 1H), 3.17 (s, 3H), 2.37 (s, 3H). ^{13}C NMR (CDCl3 100 MHz) ppm: 187.09, 163.43, 142.70, 138.91, 138.11, 137.00, 131.54, 128.84, 128.55, 117.40, 117.02, 116.03, 112.03, 107.02, 106.82, 44.33, 10.89; ESI-mass: m/z 380.073 $[M+Na]^+$.

2-Methyl-5-[4-(methylsulfonyl)phenyl]-1-[3,4-difluoro-phenyl]-1H-pyrrole-3-carboxaldehyde (3). Off-white needles (>95%yield), mp 178 °C. ^{1}H NMR (CDCl3 400 MHz) ppm: 9.97 (s, 1H), 7.77 (m, 3H), 7.55 (m, 1H), 7.36 (d, 2H, J = 8.7 Hz), 7.22 (m, 1H), 6.98 (s, 1H), 3.20 (s, 3H), 2.39 (s, 3H). ^{13}C NMR (CDCl3 100 MHz) ppm: 187.09, 163.03, 150.31, 140.70, 138.90, 138.10, 137.09, 131.50, 128.93, 128.59, 118.03, 117.33, 15 109.22, 108.8, 107.02, 44.39, 10.99; ESI-mass: m/z 398.064 $[M+Na]^{+}$.

2-Methyl-5-[4-(methylsulfonyl)phenyl]-1-phenyl-1H-pyrrole3-carboxaldehyde (4). Off-white needles (>95%yield), mp 160 °C. ^{1}H NMR (CDCl3 400 MHz) ppm: 10.00 (s, 1H), 7.73 (d, 2H, J = 8.6 Hz), 7.46 (m, 3H), 7.22 (d, 2H, J = 8.6 Hz), 7.16 (m, 2H), 6.95 (s, 1H), 3.02 (s, 3H), 2.40 (s, 3H). ^{13}C NMR ($CDCl_3$ 100 MHz) ppm: 186.69, 161.30, 140.30, 139.33, 138.04, 135.89, 133.70, 129.04, 128.55, 128.44, 125.40, 111.10, 109.57, 44.20, 11.44. ESI-mass: m/z 362.083 $[M+Na]^{+}$.

1.4.1.5. General procedure for the synthesis of pyrrole-3-carboximes (5-8)

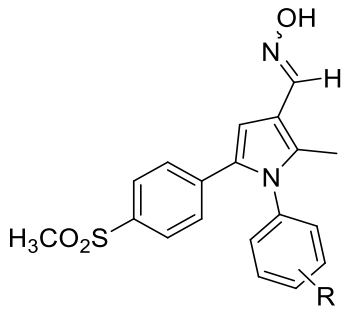

To a solution of the suitable aldehyde (**1-4**) (1 mmol) in ethanol (5 mL), hydroxylamine chloride water solution (1 mmol in 4 mL of water) and sodium acetate (1 mmol) were added. The reaction was refluxed for 1 h and a half. At the end the precipitated formed was filtered and collected to give oximes **5-8** as white powders.

2-Methyl-5-[4-(methylsulfonyl)phenyl]-1-[4-fluoro-phenyl]1H-pyrrole-3-carboxime(5). White powder (>95%yield). ^{1}H NMR (400 MHz, DMSO-d6): (ppm) 10.94 (s, 1H), 10.61 (s, 1H), 8.11 (s, 1H), 7.70 (d, 4H, J = 40 8.4 Hz), 7.42– 7.31 (m, 9H), 7.21 (d, 4H, J = 8.4 Hz), 6.74 (s,

2H), 3.15 (s, 6H), 2.13 (s, 6H); ^{13}C NMR (CDCl3 100 MHz) ppm: 159.66, 148.20, 138.92, 138.11, 136.73, 135.19, 133.30, 128.81,128.50, 123.22, 117.13, 116.10, 106.98, 47.88, 10.96; ESI-mass: m/z 395.084 $[M+Na]^+$.

2-Methyl-5-[4-(methylsulfonyl)phenyl]-1-[3-fluoro-phenyl]1H-pyrrole-3-carboxime (6). White powder (>95%yield). ^{1}H NMR (400 MHz, DMSO-d6) ppm: 10.98 (s, 1H), 10.65 (s, 1H), 8.14 (s, 1H), 7.78 (d, 4H, J = 8.6 Hz), 7.53–7.43 (m, 2H), 7.36–7.33 (m, 6H), 7.18 (d, 4H, J = 8.4 Hz), 6.77 (s, 2H), 3.19 (s, 6H), 2.19 (s, 6H). ^{13}C NMR (CDCl3 100 MHz) ppm: 163.55, 149.00, 143.00, 138.88, 138.21, 55 135.20, 133.10, 131.00, 128.77, 128.43, 117.21, 117.10, 112.28, 107.28, 106.90, 47.99, 11.06. ESI-mass: m/z 395.084 $[M+Na]^+$.

2-Methyl-5-[4-(methylsulfonyl)phenyl]-1-[3,4-ifluorophenyl]-1H-pyrrole-3-carboxime (6). White powder (>95%yield). ^{1}H NMR (400 MHz, DMSO-d6): (ppm) 10.98 (s, 1H), 10.66 (s, 1H), 8.14 (s, 1H), 7.79 (d, 4H, J = 8.5 Hz), 7.64–7.69 (m, 2H), 7.66 (m, 2H), 7.43–7.23 (m, 5H), 7.15 (m, 2H), 6.77 (s, 2H), 3.19 (s, 6H), 2.19 (s, 6H). ^{13}C NMR (CDCl3 100 MHz) ppm: 153.35, 148.33, 146.30, 138.98, 138.56, 138.31, 135.10, 133.13, 128.87, 128.53, 118.61, 117.70, 117.44, 108.88, 106.89, 48.01, 11.12. ESI-mass: m/z 413.075 $[M+Na]^+$.

2-Methyl-5-[4-(methylsulfonyl)phenyl]-1-phenyl-1H-pyrrole3-carboxime (7). White powder (>95%yield). ^{1}H NMR 400 MHz, DMSO-d6): (ppm) 10.92 (s, 1H), 10.59 (s, 1H), 8.10 (s, 1H), 7.68 (d, 4H, J = 8.6 Hz), 7.45–7.32 (m, 11H), 7.23 (d, 4H, J = 8.6 Hz), 6.76 (s, 2H), 3.10 (s, 6H), 2.15 (s, 6H). ^{13}CNMR (CDCl3 100 MHz) ppm: 148.23, 141.22, 138.98, 138.16, 135.11, 133.17, 129.43, 128.89, 128.63, 80 125.66, 121.65, 106.91, 117.24, 47.66, 11.02. ESI-mass: m/z 377.094 $[M+Na]^+$.

1.4.1.6. General procedure for the synthesis of pyrrole-3-carbonitriles (9-12)

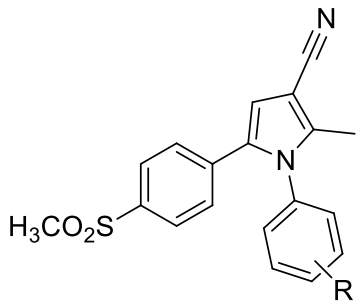

A solution of 2,4,6-trichloro[1,3,5]triazine (1 mmol) in 0.2 mL of dimethylformamide was stirred for 30 min at room temperature. Carboxime **5** (1 mmol), dissolved in 1.5 mL of dimethylformamide, was added, and the reaction mixture was stirred at room temperature for 8 h. The reaction mixture was then diluted with water (2 mL), extracted with ethyl acetate (50 x 3 mL), washed with saturated carbonate solution (50 mL), 1 N HCl (50 mL) and brine (50 mL). After filtration and concentration, the crude mixture obtained was purified by chromatography on silica gel with 4:1 cyclohexane/ethylacetate mixture as eluent, to give compounds **9-12** as white solids. Recrystallization from ethanol gave **9-12** as white crystals.

2-Methyl-5-[4-(methylsulfonyl)phenyl]-1-[4-fluoro-phenyl]1H-pyrrole-3-carbonitrile (9). White needles (80% yield). ESI-mass: m/z 377.073 $[M+Na]^+$. mp, ^1H and ^{13}C NMR spectra were consistent with those reported in the literature.[45]

2-Methyl-5-[4-(methylsulfonyl)phenyl]-1-[3-fluoro-phenyl]1H-pyrrole-3-carbonitrile (10). White needles (76.8% yield), mp 219 °C. ^1H NMR (400 MHz, CDCl3): (ppm) 7.78 (d, 2H, J = 8.4 Hz), 7.50–7.44 (m, 1H), 7.23 (d, 2H, J = 8.4 Hz), 105 6.99– 6.92 (m, 3H), 6.71 (s, 1H), 3.05 (s, 3H), 2.35 (s, 3H). ^{13}C NMR (CDCl3 100 MHz) ppm: 159.59, 140.66, 138.94, 138.01, 137.50, 133.41, 129.23, 128.89, 128.56, 117.55, 117.39, 116.00, 111.25, 108.02, 106.77, 45.00, 11.21; ESI-mass: m/z 377.074 $[M+Na]^+$.

2-Methyl-5-[4-(methylsulfonyl)phenyl]-1-[3,4-difluoro-phenyl]-1H-pyrrole-3-carbonitrile (11). White needles (78.0% yield), mp 220 °C. ^{1}H NMR (400 MHz, CDCl3): (ppm) 7.79 (d, 2H, J = 8.3 Hz), 7.29–7.25 (m, 1H), 7.21 (d, 2H, J = 8.3 Hz), 7.06–7.02 (m, 1H), 6.95–6.93 (m, 1H), 6.68 (s,1H), 3.05 (s, 3H), 2.30 (s, 3H). ^{13}C NMR (CDCl3 100 MHz) ppm: 159.66, 146.76, 138.64, 138.38, 137.53, 132.91, 128.78, 128.77, 117.44, 116.60, 08.14, 107.00, 44.89, 11.11. ESI-mass: m/z 395.064 $[M+Na]^{+}$.

2-Methyl-5-[4-(methylsulfonyl)phenyl]-1-phenyl-1H-pyrrole3-carbonitrile (12). White needles (79.3% yield), mp 197 °C. ^{1}H NMR (400 MHz, CDCl3): (ppm) 7.45 (d, 2H, J = 8.4 Hz), 7.30 (m, 3H), 7.20 (m, 2H), 7.18 (d, 2H, J = 8.4 Hz), 6.70 (s, 1H), 3.05 (s, 3H), 2.19 (s, 3H). ^{13}C NMR (CDCl3 100 MHz) ppm: 138.90, 138.51, 133.57, 133.09, 129.42, 129.68, 128.40, 128.44, 125.55, 121.13, 117.38, 112.05, 110.65, 44.80, 11.55. ESI-mass: m/z 359.083 $[M+Na]^{+}$.

1.4.1.7. General procedure for the preparation of Ethyl 1,5-Diarylpyrrol-3-yl-glyoxylic Esters (29a,b)

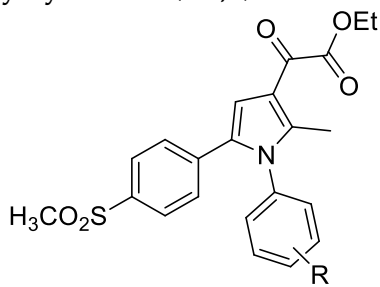

To a solution of the appropriatepyrrole**28 a-d** in anhydrous dichloromethane,(4.82 mmol)under a nitrogen flow, $TiCl_4$ (0.53 mL,4.82 mmol) and ethoxalyl chloride (0.54 mL, 4.82 mmol) at 0 °C were added. The solution was stirred for 4 h at room temperature. The mixture was then washed with water and extracted with $CHCl_3$. The organic solution was washed with a saturated aqueous NaCl solution, dried, and evaporated in vacuo. Purification of the residue by flash chromatography with $CHCl_3$ as the eluant gave a solid which, after recrystallization from hexane, afforded the expected products **29a-b**.

Ethyl-2-methyl-5-[4-(methylsulfonyl)phenyl]-1-(4-fluoro-phenyl)-1Hpyrrole-3-glyoxylate (**29a**). White needles (74% yield). Analytical data, the melting point, and the ^{1}H NMR spectrum were consistent with those reported in the literature[42].

Ethyl-2-methyl-5-[4-(methylsulfonyl)phenyl]-1-(3-fluoro-phenyl)-1Hpyrrole-3-glyoxylate (**29b**). White needles (76% yield). Analytical data, the melting point, and the ^{1}H NMR spectrum were consistent with those reported in the literature[42].

1.4.1.8. General procedure for the Preparation of 1,5-Diarylpyrrole-3-acetic esters (30a,b)

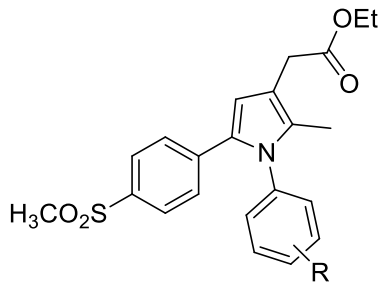

To a solution of the suitable keto ester **29** (2.3 mmol) in TFA (9 mL, 0.12 mol) stirred at 0°C under a nitrogen flow was slowly added triethylsilane (0.75 mL,4.7 mmol), and the mixture was stirred for 2 h at room temperature. At the end of the reaction, the mixture was made alkaline with 40% aqueous ammonia (10 mL) and extracted with $CHCl_3$. The organic solution was dried and evaporated in vacuo. The resulting residue was chromatographed on silica gel eluting with CHCl3 to give a solid which, after recrystallization from hexane, afforded the desired products **30a,b**.

Ethyl-2-methyl-5-[4-(methylsulfonyl)phenyl]-1-(4-fluoro-phenyl)-1Hpyrrole-

3-acetate (30a). White solid (68% yield). Analytical data, the melting point, and the 1H NMR spectrum were consistent with those reported in the literature[38].

Ethyl-2-methyl-5-[4-(methylsulfonyl)phenyl]-1-(3-fluoro-phenyl)-1Hpyrrole-3-acetate (30b). White solid (65% yield). Analytical data, the melting point, and the 1H NMR spectrum were consistent with those reported in the literature[38].

1.4.1.9. General procedure for the preparation of 1,5-Diarylpyrrole-3-acetic acids (31 a,b)

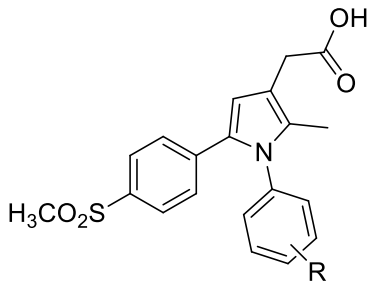

To a solution of the appropriate ethyl 1,5-diarylpyrrole-3-acetic esters 31 a,b (0.30 g,0.67 mmol) in methanol (4.83 mL) was added 4.83 mL of 1 N NaOH. The resulting mixture was refluxed for 1 h, cooled, and concentrated in vacuo. The residue was solubilized in water and then acidified with concentrated HCl. The precipitate was filtered to give the desired acids **31a** and **b** as white solids.

2-Methyl-5-[4-(methylsulfonyl)phenyl]-1-(4-fluorophenyl)-1H-pyrrol-3-acetic Acid (31a). White solid (>90% yield). Analytical data, the melting point, and the ^{1}HNMR spectrum were consistent with those reported in the literature[38]

2-Methyl-5-[4-(methylsulfonyl)phenyl]-1-(3-fluorophenyl)-1H-pyrrol-3-acetic Acid (31b). White solid (>90% yield). Analytical data, the melting point, and the ^{1}HNMR spectrum were consistent with those reported in the literature[38]

1.4.1.10. General procedure for the preparation of 4-methylsulphonylphenyl acetamides (13-16)

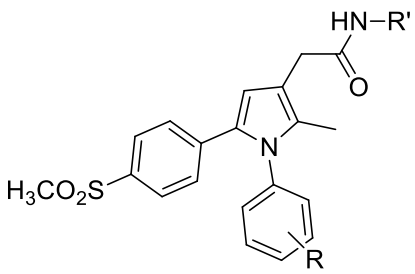

To a solution of the appropriate acid (**31a,b**) (0.51 mmol) in DCM (10 mL), the suitable amine (2.04 mmol), DMAP (0.61 mmol, 00.07g) and EDCI (0.82 mmol, 0.16g) were added in sequence. The reaction mixture was stirred at room temperature for 15h and then it was diluted with water, and the two phases were separated with dichlorometane. The organic layers were washed with 2N HCl, $NaHCO_3$ saturated solution and brine, then was dried Na_2SO_4, filtered and concentrated *in vacuo*. The obtained crude products were purified by column chromatography on silica gel using cyclohexane/ethyl acetate 1:1, as eluent. After recrystallization from ethyl acetate the desired products **13-16** were obtained.

2-(1-(4-Fluorophenyl)-2-methyl-5-(4-(methylsulfonyl) phenyl)-1*H*-pyrrol-3-yl)-*N*-isopropylacetamide (13).

White powder, mp 178°C (yield 74%). ^{1}H-NMR (400MHz, DMSO-d_6) δ ppm: 7.76 (d, 1H), 7.68 (d, 2H), 7.30-7.28 (m, 4H), 7.17 (d, 2H), 6.49 (s, 1H), 3.85-3.79 (m, 1H), 3.20 (s, 2H), 3.13 (s, 3H), 1.98 (s, 3H), 1.05 (d, 6H). ^{13}C-NMR (100 MHz, DMSO-d_6) δ (ppm): 171.9, 160.0, 147.3, 145.1, 141.5, 135.2, 129.3, 128.5, 126.3, 122.2, 121.3, 116.9, 114.3, 48.2, 44.0, 23.5, 10.2. MS-ESI: m/z 451.15 $[M + Na]^+$.

2-(1-(3-Fluorophenyl)-2-methyl-5-(4-(methylsulfonyl) phenyl)-1*H*-pyrrol-3-yl)-*N*-isopropylacetamide (14).

White powder, mp 175°C (yield 71%). ^{1}H-NMR (400MHz, DMSO-d_6) δ ppm: 7.80 (d, 1H),7.69 (d, 2H), 7.51-7.46 (m, 1H), 7.30-7.21 (m, 2H), 7.17 (d, 2H), 7.03 (d, 1H), 6.50 (s, 1H), 3-86-3.78 (m, 1H), 3.21 (s, 2H), 3.14 (s, 3H), 2.02 (s, 3H), 1.06 (d, 6H). ^{13}C-NMR (100 MHz, DMSO-d_6) δ

(ppm): 171.8, 159.9, 144.2, 143.0, 140.4, 134.4, 130.0, 128.3, 128.0, 124.8, 120.6, 115.8, 113.1, 112.3, 106.5, 46.7, 44.3, 33.5, 23.1, 9.7. MS-ESI: m/z 451.15 $[M + Na]^+$.

2-(1-(4-Fluorophenyl)-2-methyl-5-(4-(methylsulfonyl) phenyl)-1*H*-pyrrol-3-yl)-*N*-propylacetamide (15).

White powder, mp 168°C (yield 76%). ^{1}H-NMR (400MHz, DMSO-d_6) δ ppm: 7.86 (t, 1H), 7.69 (d, 2H), 7.32-7.30 (m, 4H), 7.19 (d, 2H), 6.52 (s, 1H), 3.26 (s, 2H), 3.15 (s, 3H), 3.03 (q, 2H), 2.01 (s, 3H), 1.45-1.41 (m, 2H), 0.86 (t, 3H). ^{13}C-NMR (100 MHz, DMSO-d_6) δ (ppm): 171.6, 159.2, 146.2, 144.0, 141.3, 134.0, 128.6, 128.0, 125.8, 121.9, 121.2, 115.8, 112.9, 46.3, 41.9, 34.3, 23.1, 11.0, 9.8. MS-ESI: m/z 451.15 $[M + Na]^+$.

2-(1-(3-Fluorophenyl)-2-methyl-5-(4-(methylsulfonyl) phenyl)-1*H*-pyrrol-3-yl)-*N*-propylacetamide (16).

White powder, mp 164°C (yield 77%). ^{1}H-NMR (400MHz, DMSO-d_6) δ ppm: 7.87 (t, 1H), 7.68 (d, 2H), 7.51-7.46 (m, 1H), 7.31-7.26 (m, 2H), 7.18 (d, 2H), 7.04 (d, 1H), 6.51 (s, 1H), 3.24 (s, 2H), 3.14 (s, 3H), 3.01 (q, 2H), 2.02 (s, 3H), 1.44-1.39 (m, 2H), 0.84 (t, 3H). ^{13}C-NMR (100 MHz, DMSO-d_6) δ (ppm): 171.6, 161.4, 144.4, 143.7, 141.3, 134.6, 131.2, 128.8, 128.4, 125.8, 121.0, 116.3, 113.5, 112.7, 107.2, 47.3, 42.6, 34.0, 23.4, 14.6, 10.0. MS-ESI: m/z 451.15 $[M + Na]^+$.

1.4.1.11. General procedure for the preparation of 2-methyl-5-(4-((2-(trimethylsilyl) ethyl)sulfonyl) phenyl)-1H-pyrroles (32 a-b)

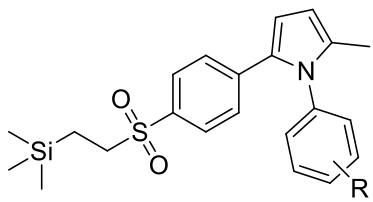

A butyllithium solution (3.38 mmol, 1.38 mL, 2.5 M in hexane) was slowly added to a mixture of DIPA (4.03 mmol, 0.58 mL) in dry THF (10 mL), at 0°C and under nitrogen flow. The reaction mixture was stirred for thirty minutes and was cooled down to -78°C, then a solution of the suitable pyrrole (**28a,b**) (2.9 mmol) in dry THF (10 mL) was

added dropwise. After 1,5 hour stirring, iodomethyltrimethylsilane (4.03 mmol, 0.61 mL) was added and the mixture was allowed to warm up to room temperature and to stir for 15 h. The reaction mixture was quenched with water and the pH was adjusted (pH=2) with 1N HCl. The resulting mixture was extracted with ethyl acetate and the organic layers were washed with brine and dried over Na_2SO_4. After concentration *in vacuo* the crude products were purified by chromatography on silica gel using cyclohexane/ethylacetate 15:1 (v/v) as eluent to give the expected products **32a,b** as white powder.

1-(4-fluorophenyl)-2-methyl-5-(4-((2- (trimethylsilyl)ethyl) sulfonyl)phenyl)-1*H*-pyrrole (32 a).

White powder, mp 75°C (60 %yield). ^{1}HNMR (400 MHz, $CDCl_3$) δ (ppm): 7.63 (d, 2H), 7.15-7.08 (m, 6H), 6.51 (d, 1H), 6.13 (d, 1H), 2.98-2.93 (m, 2H), 2.13 (s, 3H), 0.93-0.86 (m, 2H), 0.03 (s, 9H). ^{13}C-NMR (100 MHz, $CDCl_3$) δ (ppm): 160.1, 146.3, 142.8, 139.3, 133.2, 128.6, 128.3, 127.9, 122.4, 117.9, 113.1, 110.2, 58.2, 15.4, 13.3, 2.1. MS-ESI: *m*/*z* 438.13 $[M + Na]^+$.

1-(3-fluorophenyl)-2-methyl-5-(4-((2-(trimethylsilyl) ethyl) sulfonyl)phenyl)-1*H*-pyrrole (32b).

White powder, mp 78°C (60 %yield). ^{1}HNMR (400 MHz, $CDCl_3$) δ (ppm): 7.66 (d, 2H), 7.40-7.36 (m, 1H), 7.20 (d, 2H), 7.14-7.09 (m, 1H), 6.97-6.95 (m, 1H), 6.91-6.89 (m, 1H), 6.52 (d, 1H), 6.14 (d,1H), 2.98-2.93 (m, 2H), 2.18 (s, 3H), 0.92-0.88 (m, 2H), 0.03 (s, 9H). ^{13}C-NMR (100 MHz, $CDCl_3$): δ (ppm) 163.2, 144.8, 142.9, 139.3, 133.2, 131.5, 129.1, 128.7, 128.3, 117.5, 112.6, 112.1, 110.3, 108.6, 58.4, 15.3, 13.2, 2.1. MS-ESI: *m*/*z* 438.13 $[M + Na]^+$.

1-(3,4-difluorophenyl)-2-methyl-5-(4-((2- (trimethylsilyl)ethyl) sulfonyl)phenyl)-1*H*-pyrrole.

White powder, (58% yield); mp. 80°C; $C_{22}H_{25}F_2NO_2SSi$; ^{1}H-NMR (400MHz, $CDCl_3$) ppm: 7.68 (d, 2H), 7.21 (m, 3H), 7.03 (m, 1H), 6.93 (m, 1H), 6.50 (d, 1H), 6.14 (d, 1H), 2.98 (m, 2H), 2.15 (s, 3H), 0.91 (m, 2H), 0.03 (s, 9H). 133.4, 118.0, 112.8, 107.7, 109.2, 138.9, 150.1, 146.3, 128.5, 139.1, 144.6, 128.8 , 108.8, 117.7, 117.4, 129.1, 128.8, 58.7, 15.1, 1.8, 12.7.

1-phenyl-2-methyl-5-(4-((2- (trimethylsilyl)ethyl)

sulfonyl)phenyl)-1*H*-pyrrole.

White powder, (56 % yield) $C_{22}H_{27}NO_2SSi$; ^{1}H-NMR (400MHz, $CDCl_3$) ppm: 7.63 (d, 2H), 7.41 (m, 3H), 7.17 (m, 4H), 6.54 (d, 1H), 6.15 (d, 1H) 2.95 (m, 2H), 2.15 (s, 3H), 0.90 (m, 2H), 0.03 (s, 9H);151.0, 144.6, 138.9, 133.4, 129.3, 129.2, 128.8, 128.6, 128.5, 125.5, 121.3, 118.0, 112.8, 109.2, 58.7, 15.1, 1.8.

1.4.1.12. General procedure for the preparation of sulfonamide pyrroles (33a,b)

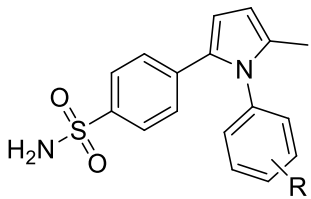

A solution of tetrabutilamonium fluoride in hexane (3,6 mmol, 3.6 mL) was added to the appropriate trimethylsilylpyrrole **32 a,b** (1.2 mmol) and was microwave irradiated at 120 °C for 15 minutes (power 150W, pressure 170 psi), then a solution of sodium acetate (3,6 mmol, 0.29 g) in water (3.6 mL) and hydroxylamine-*O*-sulfonic acid (3.6 mmol, 0.41 g) were added; the mixture was again irradiated for 10 minutes at 50°C(power 150 W, pressure 170 psi). The reaction mixture was then quenched with water and was then extracted with ethylacetate and washed with brine. The organic layers were dried over Na_2SO_4, filtered of and concentrated *in vacuo*. The obtained crude products were purified by cromatography on silica gel using petroleum ether/ethylacetate 2:1 (v/v) as eluent. After recrystallization from diethyl ether the expected products were obtained.

4-(1-(4-Fluorophenyl)-5-methyl-1*H*-pyrrol-2-yl) benzenesulfonamide (33a).

White powder, mp 126°C (83 % yield). ^{1}H-NMR (400MHz, $CDCl_3$) δ (ppm): 7.67 (d, 2H), 7.13-7.09 (m, 6H), 6.48 (d, 1H), 6.13 (d, 1H), 4.71 (s broad, 2H), 2.13 (s, 3H). ^{13}C-NMR (100 MHz, $CDCl_3$) δ (ppm): 163.8, 146.1, 144.1, 141.5, 133.3, 130.8, 129.1, 128.8, 116.9, 114.2, 111.3, 108.8, 12.8. MS-ESI: *m*/*z* 353.07 $[M + Na]^+$.

4-(1-(3-fluorophenyl)-5-methyl-1*H*-pyrrol-2-yl) benzenesulfonamide (33b).

White powder, mp 115°C (80 % yield). ^{1}H-NMR (400MHz, $CDCl_3$) δ (ppm): 7.67 (d, 2H), 7.46-7.42 (m, 1H), 7.28-7.26 (m, 2H),7.07-7.03 (m, 1H), 6.94-6.91 (m, 1H), 6.89-6.86 (m, 1H), 6.48 (d, 1H), 6.15 (d, 1H), 4.81 (s, broad, 2H), 2.14 (s, 3H). ^{13}C-NMR (100 MHz, $CDCl_3$) δ (ppm): 163.3, 145.6, 143.1, 141.9, 134.3, 131.6, 129.1, 128.3, 126.9, 116.9, 113.2, 112.9, 110.4, 108.1, 12.6. MS-ESI: *m*/*z* 353.07 $[M + Na]^+$.

4-(1-(3,4-difluorophenyl)-5-methyl-1*H*-pyrrol-2-yl) benzenesulfonamide; (78% yield); m.p. 110°C; $C_{17}H_{14}F_2N_2O_2S$ ^{1}H-NMR (400 MHz, $CDCl_3$) ppm: 7.70 (d, 2H), 7.21 (m, 1H), 7.13 (d, 2H), 7.04 (m, 1H), 6.99 (d, 1H), 6.43 (d, 1H), 6.10 (d, 1H), 5.41 (s broad, 2H), 2.14 (s, 3H);^{13}C-NMR (100 MHz, $CDCl_3$) δ (ppm):150.1, 146.3, 143.7, 142.8, 139.1, 133.4, 128.5, 127.8, 118.0, 117.7, 117.4, 112.8, 109.2, 108.8, 12.7. MS-ESI: *m*/*z* 371.07 $[M + Na]^+$.

4-(1-phenyl)-5-methyl-1*H*-pyrrol-2-yl) benzenesulfonamide; (79% yield) mp: 115°C;$C_{17}H_{15}FN_2O_2S$; ^{1}H-NMR (400MHz, $CDCl_3$) ppm: 7.67 (d,2H), 7.17 (m, 6H), 6.48 (d, 1H), 6.15 (d, 1H), 4.81 (s broad, 2H), 2.14 (s, 3H).^{13}C-NMR (100 MHz, $CDCl_3$) δ (ppm):133.4, 128.5, 112.8, 109.2, 143.7, 151.0, 142.8, 127.8, 121.3, 121.3, 129.3, 129.6, 125.5, 12.7.

1.4.1.13. General procedure for the preparation of 1,5-Diarylpyrrol-3-glyoxylic esters (34a,b)

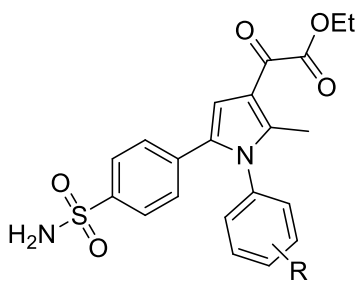

Ethoxalyl chloride (3.0 mmol) and $TiCl_4$ (3.0 mmol) were added in sequence, at 0 °C and under nitrogen atmosphere, to a solution of the appropriate pyrrole (**33 a,b**) (3.0 mmol) in dry dichloromethane (10

mL). The resulting solution was allowed to warm up to room temperature and stirred for 4 h. The mixture was then diluted with water and the two phases were separated with dichloromethane. The organic layers were washed with brine, dried over Na_2SO_4, and evaporated *in vacuo*, then the crude material was purified by chromatography on silica gel employing petroleum ether/ethyl acetate, 3:1 (v/v) as eluent. After recrystallization from diethyl ether the expected products **34 a,b** were obtained.

Ethyl-2-(1-(4-fluorophenyl)-2-methyl-5-(4-sulfamoylphenyl)-1*H*-pyrrol-3-yl)-2-oxoacetate (34a).

White powder, mp 177°C (60% yield). ^{1}H-NMR (400MHz, $CDCl_3$) δ ppm: 7.72 (d, 2H), 7.16-7.13 (m, 6H), 7.05 (s, 1H), 4.72 (s broad, 2H), 4.41 (q, 2H), 2.44 (s, 3H), 1.42 (t, 3H). ^{13}C-NMR (100 MHz, CDCl3) δ (ppm): 183.0, 166.4, 162.9, 146.4, 143.8, 142.3, 134.9, 131.4, 128.2, 122.8, 121.3, 117.6, 112.8, 106.5, 62.1, 13.8, 12.7. MS-ESI: m/z 453.09 $[M + Na]^+$.

Ethyl-2-(1-(3-fluorophenyl)-2-methyl-5-(4-sulfamoylphenyl)-1H-pyrrol-3-yl)-2-oxoacetate (34b).

White powder, mp 175°C, (60% yield). ^{1}H-NMR (400MHz, $CDCl_3$) δ ppm: 7.75 (d, 2H), 7.45-7.43 (m, 1H), 7.20-7.17 (m, 3H), 7.07 (s, 1H), 6.97 (d, 1H), 6.89 (m, 1H), 4.75 (s broad, 2H), 4.42 (q, 2H), 2.47 (s, 3H), 1.43 (t, 3H). ^{13}C-NMR (100 MHz, CDCl3) δ (ppm): 183.2, 166.2, 162.9, 145.8, 144.2, 142.3, 135.2, 133.4, 131.4, 129.3, 128.6, 117.1, 113.7, 112.1, 107.2, 106.8, 61.7, 13.6, 12.8. MS-ESI: m/z 453.09 $[M + Na]^+$.

Ethyl-2-(1-(3,4-difluorophenyl)-2-methyl-5-(4-sulfamoylphenyl)-1H-pyrrol-3-yl)-2-oxoacetate (34c).

White powder, mp 180°C, (63% yield). $C_{17}H_{14}F_2N_2O_2S$ (PM=348.37); ^{1}H-NMR (400 MHz, $CDCl_3$) ppm: 7.70 (d, 2H), 7.21 (m, 1H), 7.13 (d, 2H), 7.04 (m, 1H), 6.99 (d, 1H), 6.43 (d, 1H), 6.10 (d, 1H), 5.41 (s broad, 2H), 2.14 (s, 3H); ^{13}C-NMR (100 MHz, CDCl3) δ (ppm): 185.6, 164.1, 150.1, 146.3, 143.7, 142.8, 139.1, 134.9, 133.4, 127.8, 127,3, 127.2, 126.9, 118.0, 117.7, 117.4, 113.0, 108.8, 106.8, 60.8, 13.8, 12.6. MS-ESI: m/z 471.09 $[M + Na]^+$.

Ethyl-2-(1-phenyl)-2-methyl-5-(4-sulfamoylphenyl)-1H-pyrrol-3-yl)-

2-oxoacetate.

White powder, mp 165°C, (61% yield). $C_{21}H_{20}N_2O_5S$; ^{1}H-NMR (400MHz, DMSO) ppm: 7.68 (d, 2H), 7.59 (m, 3H), 7.43 (m, 4H), 7.29 (d,2H),7.02 (s, 1H), 4.44 (q, 2H), 2.41 (s, 3H), 1.39 (t, 3H).^{13}C-NMR (100 MHz, CDCl3) δ (ppm):185.3, 164.1, 151.0, 143.7, 142.8, 134.9, 133.4, 129.3, 128.9, 127.8, 127.4, 127.0, 126.8, 125.5, 121.3, 121.1, 113.0, 106.8, 60.8, 13.8, 12.6. MS-ESI: m/z 435.09 $[M + Na]^+$.

1.4.1.14. General procedure for the preparation of 1,5-Diarylpyrrol aceticesters (21-22)

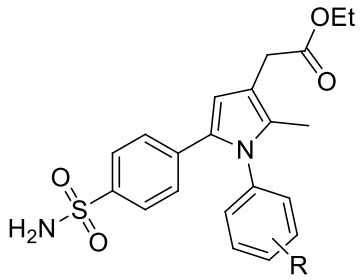

To a solution of the appropriate glyoxylic ester **34** (2.3 mmol) in trifluoroacetic acid (16.1 mL) at 0° C and under nitrogen atmosphere, thriethylsilane (6.9 mmol, 1.1 mL) was slowly added. The mixture was allowed to warm up to room temperature and stirred for two hours, then was diluted with water and was made alkaline (pH=12) using a solution of 40 % aqueous ammonia. The mixture was then extracted with dichlorometane, washed with brine, dried over Na_2SO_4, filtered, and evaporated *in vacuo*. The crude products were purified by chromatography on silica gel, using as eluent petroleum ether/ethyl acetate 2:1 (v/v). After recrystallization from diethyl ether the acetic esters were obtained.

Ethyl 2-(1-(4-fluorophenyl)-2-methyl-5-(4-sulfamoylphenyl)-1*H*-pyrrol-3-yl)acetate (21).

White powder, mp 149°C (67% yield). ^{1}H-NMR (400MHz, $CDCl_3$) δ ppm: 7.67 (d, 2H), 7.13-7.08 (m, 6H), 6.50 (s, 1H), 4.72 (s broad, 2H), 4.20 (q, 2H), 3.51 (s, 2H), 2.06 (s, 3H), 1.29 (t, 3H). ^{13}C-NMR (100 MHz, $CDCl_3$) δ (ppm): 169.1, 160.9, 146.8, 143.4, 142.5, 134.4, 128.8, 127.7,

125.6, 122.3, 121.4, 116.2, 113.3, 61.4, 34.5, 14.6, 10.2. MS-ESI: m/z 439.11 $[M + Na]^+$.

Ethyl 2-(1-(3-fluorophenyl)-2-methyl-5-(4-sulfamoylphenyl)-1*H*-pyrrol-3-yl)acetate(22).

White powder, mp 164°C (65% yield). ^{1}H-NMR (400MHz, $CDCl_3$) δ ppm: 7.66 (d, 2H), 7.38-7.34 (m, 1H), 7.13-7.08 (m, 3H), 6.96-6.87 (m, 2H), 6.45 (s, 1H), 4,86 (s broad, 2H), 4.08 (q, 2H), 3.48 (s, 2H), 2.01 (s, 3H), 1.20 (t, 3H). ^{13}C-NMR (100 MHz, $CDCl_3$) δ (ppm): 169.2, 163.8, 144.8, 143.7, 142.3, 134.2, 131.4, 129.3, 128.6, 125.9, 122.3, 116.1, 113.5, 111.9, 107.4, 61.3, 34.2, 13.6, 10.8. MS-ESI: m/z 439.11 $[M + Na]^+$.

Ethyl 2-(1-(3,4-difluorophenyl)-2-methyl-5-(4-sulfamoylphenyl)-1*H*-pyrrol-3-yl)acetate.

White powder, mp 160°C (63% yield). ^{1}H-NMR (400MHz, $CDCl_3$) δ ppm:7.65 (d, 2H), 7.11 (m, 6H), 6.48 (s, 1H), 4.88 (s broad, 2H), 4.18 (q, 2H), 3.50 (s broad, 2H), 2.06 (s, 3H), 1.28 (m, 3H). ^{13}C-NMR (100 MHz, $CDCl_3$) δ (ppm):169.2, 150.1, 143.7, 146.3, 142.8, 139.1, 134.4, 128.1, 127.8, 127.5, 127.3, 125.9, 121.4, 117.7, 117.4, 113.3, 108.8, 61.3, 34.2, 141, 10.2. MS-ESI: m/z 457.11 $[M + Na]^+$.

Ethyl 2-(1-phenyl)-2-methyl-5-(4-sulfamoylphenyl)-1*H*-pyrrol-3-yl)acetate.

White powder, mp 148°C (58% yield).^{1}H-NMR (400MHz, $CDCl_3$) δ ppm:7.58 (d, 2H), 7.47 (q, 1H), 7.28 (m, 1H), 7.13 (d, 2H), 7.02 (d, 2H), 6.45 (s, 1H), 4.87 (s broad, 2H) 4.08 (q, 2H), 3.48 (s, 2H), 2.01 (s, 3H), 1.20 (t, 3H).^{13}C-NMR (100 MHz, $CDCl_3$) δ (ppm):169.2, 151.0, 143.7, 142.8, 134.4, 129.6, 129.3, 128.3, 127.8, 127.2, 127.1, 125.9, 125.5, 121.4, 121.3, 113.3, 61.3, 34.2, 14.1, 10.2.MS-ESI: m/z 421.11 $[M + Na]^+$.

1.4.1.15. General procedure for the preparation of 1,5-Diarylpyrrol acetic acids (23-24)

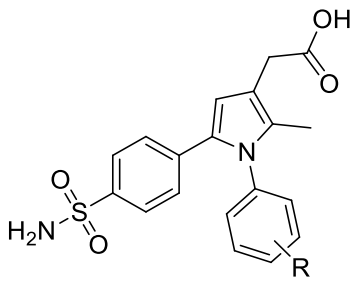

After dissolution of the appropriate acetic ester (1.3 mmol) in ethanol (9.4 mL), a solution of NaOH (0.38 g) in water (9.4 mL)was added dropwise. The mixture was refluxed for two hours and then the residue was solubilized in water (5 mL) and then concentrated HCl was added dropwise until a precipitate was formed. The precipitate was filtered off to give the expected acids as a white solids.

2-(1-(4-Fluorophenyl)-2-methyl-5-(4-sulfamoylphenyl)-1*H*-pyrrol-3-yl)acetic acid (23).

White powder, mp 181°C (>90% yield). ^{1}H-NMR (400MHz, DMSO-d_6) δ ppm: 12.15 (s broad, 1H), 7.59 (d, 2H), 7.39-7.27 (m, 6H), 7.13 (d, 2H), 6.48 (s, 1H), 3.41 (s, 2H), 2.03 (s, 3H).^{13}C-NMR (100 MHz, DMSO-d_6) δ (ppm): 176.1, 157.3, 146.8, 142.4, 142.0, 134.1, 127.8, 126.4, 125.0, 121.3, 119.3, 116.1, 113.3, 35.8, 10.1. MS-ESI: m/z 411.08 $[M+Na]^+$.

2-(1-(3-Fluorophenyl)-2-methyl-5-(4-sulfamoylphenyl)-1*H*-pyrrol-3-yl)acetic acid (24).

White powder, mp 182°C (>90% yield). ^{1}H-NMR (400MHz, DMSO-d_6) δ ppm: 12.17 (s broad, 1H), 7.59 (d, 2H), 7.28-7.23 (m, 4H), 7.14 (d, 2H), 7.04-7.03 (m, 1H), 6.46 (s, 1H), 3.31 (s, 2H), 2.01 (s, 2H). ^{13}C-NMR (100 MHz, DMSO-d_6) δ (ppm): 176.3, 163.5, 143.8, 142.9, 142.0, 134.2, 130.6, 128.1, 127.8, 125.4, 121.3, 116.1, 113.3, 112.0, 107.2, 36.2, 10.2. MS-ESI: m/z 411.08 $[M+ Na]^+$.

2-(1-(3,4-difluorophenyl)-2-methyl-5-(4-sulfamoylphenyl)-1*H*-pyrrol-3-yl)acetic acid.

White powder, mp 191°C (>90% yield). ^{1}H-NMR (400MHz, DMSO-d_6) δ ppm:12.18 (s broad, 1H), 7.59 (d, 2H), 7.30 (m, 4H), 7.24 (s broad, 2H), 7.14 (d, 2H), 6.47 (s, 1H), 3.41 (s, 2H), 2.00 (s, 3H).^{13}C-NMR (100 MHz, DMSO-d_6) δ (ppm): 174.2, 150.1, 146.3, 143.7, 142.8, 139.1, 134.4, 127.8, 127.2, 126.8, 125.9, 121.4, 117.7, 117.4, 113.3, 108.8, 36.4 10.2. MS-ESI: m/z 429.08 $[M+ Na]^+$.

2-(1-(4-Fluorophenyl)-2-methyl-5-(4-sulfamoylphenyl)-1*H*-pyrrol-3-yl)acetic acid.

White powder, mp 131°C (>90% yield). ^{1}H-NMR (400MHz, DMSO-d_6) δ ppm:12.15 (s broad, 1H), 7.59 (d, 2H), 7.51 (m, 1H), 7.30 (m, 5H), 7.13 (d, 2H), 6.48 (s, 1H), 3.41 (s, 2H), 2.03 (s, 3H) ^{13}C-NMR (100 MHz, DMSO-d_6) δ (ppm): 174.8, 151.2, 148.2, 143.5, 142.8, 139.0, 133.9, 128.0, 127.2, 126.8, 125.9, 121.4, 117.7, 117.4, 113.3, 108.8, 36.4, 10.2. MS-ESI: m/z 393.08 $[M+ Na]^+$.

1.4.1.16. General procedure for the preparation of 4-sulfamoylphenyl acetamides 17-20

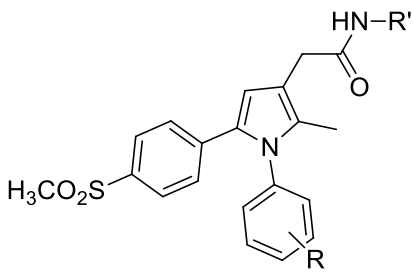

To a solution of the suitable acetic acid (**23** and **24**) (0.51 mmol) in a mixture of DCM/DMF 10:1 (v/v) under nitrogen flow, the appropriate amine (2.04 mmol), DMAP (0.61 mmol, 0.07 g) and EDCI (0.82 mmol, 0.16 g) were added in sequence. The reaction mixture was stirred at room temperature for 15h and then it was diluted with water, and the two phases were separated with dichlorometane. The organic layers were washed with 2N HCl, $NaHCO_3$ saturated solution and brine, then was dried Na_2SO_4, filtered and concentrated *in vacuo*. The

obtained crude products were purified by column chromatography on silica gel using cyclohexane/ethyl acetate 1:1, as eluent. After recrystallization from ethyl acetate the desired products **17-20** were obtained.

2-(1-(4-Fluorophenyl)-2-methyl-5-(4-sulfamoylphenyl)-1*H*-pyrrol-3-yl)-*N*-isopropylacetamide (17).

White powder, mp 194°C (yield 60 %). ^{1}H-NMR (400MHz, DMSO-d_6) δ ppm: 7.78 (d, 1H), 7.57 (d, 2H), 7.30-7.20 (m, 6H), 7.10 (d, 2H), 6.41 (s, 1H), 3.84-3.79 (m, 1H), 3.19 (s, 2H), 1.98 (s, 3H), 1.05 (d, 6H). ^{13}C-NMR (100 MHz, DMSO-d_6) δ (ppm): 171.3, 159.7, 147.2, 143.5, 142.8, 134.3, 129.2, 127.7, 126.4, 122.3, 121.2, 116.3, 113.3, 44.5, 34.8, 23.2, 10.0. MS-ESI: m/z 452.14 $[M + Na]^+$.

2-(1-(3-Fluorophenyl)-2-methyl-5-(4-sulfamoylphenyl)-1*H*-pyrrol-3-yl)-*N*-isopropylacetamide (18).

White powder, mp 186°C (yield 62%). ^{1}H-NMR (400MHz, DMSO-d_6) δ ppm: 7.81 (d, 1H), 7.58 (d, 2H), 7.48-7.46 (m, 1H), 7.29-7.19 (m, 4H), 7.12 (d, 2H), 7.01 (d, 1H), 6.43 (s, 1H), 3.85-3.79 (m, 1H), 3.20 (s, 2H), 1.98 (s, 3H), 1.06 (d, 6H). ^{13}C-NMR (100 MHz, DMSO-d_6) δ (ppm): 171.3, 164.2, 143.7, 143.5, 143.0, 134.4, 131.3, 130.0, 127.9, 126.2, 121.6, 117.1, 113.1, 112.2, 107.5, 44.3, 34.5, 23.1, 9.8. MS-ESI: m/z 452.14 $[M + Na]^+$.

2-(1-(4-Fluorophenyl)-2-methyl-5-(4-sulfamoylphenyl)-1*H*-pyrrol-3-yl)-*N*-propylacetamide (19).

White powder, mp 183°C (yeld 55%). ^{1}H-NMR (400MHz, DMSO-d_6) δ ppm: 7.86 (t, 1H), 7.58 (d, 2H), 7.31-7.24 (m, 6H), 7.11 (d, 2H), 6.44 (s, 1H), 3.24 (s, 2H), 3.02 (m. 2H), 2.00 (s, 3H), 1.43 (q, 2H), 0.85 (t, 3H). ^{13}C-NMR (100 MHz, DMSO-d_6) δ (ppm): 171.2, 159.3, 146.6, 143.3, 142.0, 133.9, 129.2, 128.0, 125.8, 121.8, 121.0, 115.8, 112.6, 42.5, 33.8, 23.0, 11.0, 9.8. MS-ESI: m/z 451.15 $[M + Na]^+$.

2-(1-(3-Fluorophenyl)-2-methyl-5-(4-sulfamoylphenyl)-1*H*-pyrrol-3-yl)-*N*-propylacetamide (20).

White powder, mp 192°C (yield 58%). ^{1}H-NMR (400MHz, DMSO-d_6) δ ppm: 7.85 (t, 1H), 7.57 (d, 2H), 7.50-7.45 (m, 1H), 7.23-7.19 (m, 3H), 7.12 (d, 2H), 7.02 (d, 1H), 6.44 (s, 1H), 3.23 (s, 2H), 3.01 (q, 2H), 1.44 (m,

2H), 0.84 (t, 3H). ^{13}C-NMR (100 MHz, DMSO-d_6) δ (ppm): 171.8, 164.8, 144.2, 143.8, 143.1, 134.9, 131.2, 127.9, 127.6, 126.4, 121.8, 117.5, 113.8, 112.7, 108.0, 43.3, 34.6, 23.5, 11.8, 10.2 MS-ESI: m/z 452.14 $[M + Na]^+$.

1.4.1.17. General procedure for the Preparation of 1,5-diarylpyrrole-3-acetic nitro-oxyalkyl amides (35-38)

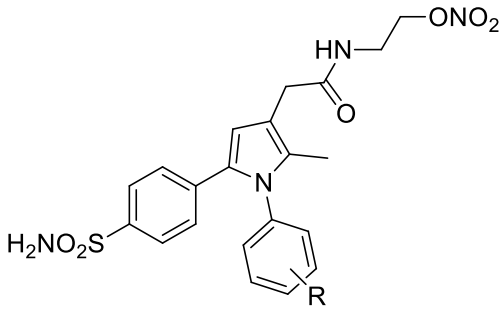

Nitroxyalkylamine **45**, nitrate salt (0.3 mmol), DMAP(0.1 mmol), and EDCI (0.2 mmol) were added in sequence to a solution of the acid partner (16) (0.1 mmol) dissolved in DCM/DMF 10:1 (v/v) (5 mL),under nitrogen atmosphere. An excess of triethylamine(0.35 mmol) was added dropwise and the reaction was stirred atrt for 12 h. Then the mixture was quenched with water (10 mL)and extracted with chloroform (50 mL X 3). The organic layer was washed with 1 N HCl (50 mL), $NaHCO_3$ saturated solution (50 mL),brine (50 mL) and dried over Na_2SO_4. After filtration and concentration of the organic phase a crude material was obtained. The material was then purified by chromatography on silica gel/alumina(1:1) using petroleum ether/chloroform/ethyl acetate, 4:4:1(v/v/v), as the eluent to give the desired product in good yield.

2-(nitrooxy)ethyl 2-(1-(4-fluorophenyl)-2-methyl-5-(4-sulfamoylphenyl)-1H-pyrrol-3-yl)acetate (35): (50 % yield) mp 107°C ; $C_{21}H_{20}N_3O_7FS$ **;** ^{1}H-NMR (400MHz, $CDCl_3$) ppm:7.66 (d, 2H), 7.11-7.05 (m, 6H), 6.47 (s, 1H), 4.81 (s, broad, 2 H), 4.70 (m, 2H), 4.42 (m, 2H), 3.55 (s, 2H), 2.05 (s, 3H); ^{13}C-NMR (100 MHz, $CDCl_3$) δ (ppm): 169.5, 158.8, 146.6, 143.4, 142.5, 134.9, 127.8, 126.4, 123.1, 122.6, 121.8, 117.0, 114.4, 66.2, 62.3, 34.8, 10.3. ESI-Mass: *m*/*z* 500.09 $[M + Na]^+$.

2-(nitrooxy)ethyl 2-(1-(3-fluorophenyl)-2-methyl-5-(4-sulfamoylphenyl)-1H-pyrrol-3-yl)acetate (36): (51% yield)mp 105°C; $C_{21}H_{20}N_3O_7FS$;^{1}H-NMR (400MHz, $CDCl_3$) ppm: 7.68 (d, 2H), 7.39-7.37 (m, 1H), 7.15-7.13 (m, 3H), 6.96 (d,1H), 6.91 (d, 1H), 6.48 (s, 1H), 4.75 (s broad, 2H), 4.71 (m, 2H), 4.43 (m, 2H), 3.55 (s, 2H), 2.08 (s, 3H); ^{13}C-NMR (100 MHz, $CDCl_3$) δ (ppm):169.3, 163.5, 144.0, 143.2, 142.3, 134.4, 131.5, 130.6, 127.8, 125.6, 120.8, 117.2, 112.7, 111.6, 106.5, 65.9, 62.1, 34.8, 10.2;ESI-Mass: *m/z* 500.09 $[M + Na]^+$.

2-(nitrooxy)ethyl 2-(1-(3,4-difluorophenyl)-2-methyl-5-(4-sulfamoylphenyl)-1H-pyrrol-3-yl)acetate (37):(52% yield) m 110 °C; $C_{21}H_{19}N_3O_7F_2S$7.79(m, 2H), 7.32-7.30 (m, 1H), 7.19-7.17 (m, 2H), 7.05-7.02 (m, 2H), 6.50 (s, 1H), 4.75 (s broad, 2H), 4.68 (m, 2H), 4.40 (m, 2H), 3.58 (s, 2H), 2.05 (s, 3H);^{13}C-NMR (100 MHz, $CDCl_3$) δ (ppm): 171.0, 150.0, 144.6, 140.1, 139.1, 134.4, 128.8, 128.5, 118.0, 125.9, 118.0, 117.4,128.8, 121.4, 113.3, 108.8, 107.7, 66.0, 47.7, 37.3, 34.0, 9.8.

2-(nitrooxy)ethyl 2-(1-phenyl-2-methyl-5-(4-sulfamoylphenyl)-1H-pyrrol-3-yl)acetate (38):(47% yield) mp 129°C; $C_{21}H_{21}N_3O_7S$; $C_{21}H_{22}N_4O_6S$ (PM=458.49); ^{1}H-NMR (400MHz, $CDCl_3$) ppm: 7.68 (d, 2H), 7.20 (m, 1H), 7.15 (m, 6H), 6.47 (s, 1H), 6.12 (s broad, 1H), 4.74 (s broad, 2H), 4.60 (m, 2H), 3.65 (m, 2H), 3.52 (s, 2H), 2.07 (s, 3H).^{13}C-NMR (100 MHz, $CDCl_3$) δ (ppm):171.6, 151.0, 143.7, 142.8, 134.4, 129.3, 127.8, 121.3, 125.9, 125.5, 121.4,118.0, 113.3, 107.7, 66.0, 37.3, 34.0, 14.7, 9.8.

1.4.1.18. General procedure for the Preparation of 1,5-diarylpyrrole-3-acetic hydroxy-alkyl amides (39-42)

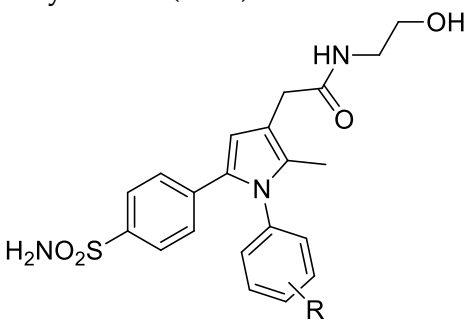

Ethanolamine (**44**) (1.0 mmol), HOBt (0.9 mmol), and EDCi (1.2

mmol) were added in sequence to a solution of the suitable 1,5-diarylpyrrole-3-acetic acid (0.7 mmol) in a mixture of DCM/DMF 10:1 (20 mL), under nitrogen atmosphere. An excess of triethylamine (2.0 mmol) was added dropwise and the reaction was stirred at rt for 12 h. Then the mixture was quenched with water(10 mL) and extracted with chloroform (50 mL X 3). The organic layer was washed with 1 N HCl (50 mL), $NaHCO_3$ saturated solution(50 mL), brine (50 mL) and dried over Na_2SO_4. After filtration and concentration of the organic phase a crude material was obtained. The material was then purified by chromatography on silica gel using petroleum ether/chloroform/ethyl acetate, 3:2:1(v/v/v), as the eluent to give the desired product in good yield.

2-(1-(4-fluorophenyl)-2-methyl-5-(4-sulfamoylphenyl)-1H-pyrrol-3-yl)-N-(2-hydroxyethyl)acetamide (39): (yield 50%) mp 148 °C; $C_{21}H_{21}FN_3O_4S$; ^{1}H-NMR (400MHz, DMSO) ppm:7.83 (t, 1H), 7.56 (d, 2H), 7.26-7.20 (m, 6H), 7.11 (d, 2H), 6.44 (s, 1H), 4.63 (s broad, 1H), 3.41-3.38 (m, 2H), 3.28 (s, 2H), 3.12-3.10 (m, 2H), 2.05 (s, 3H); ^{13}C-NMR (100 MHz, CDCl3) δ (ppm):171.9, 160.2, 147.0, 144.0, 142.9, 134.6, 128.0, 127.3, 126.2, 121.9, 121.5, 116.0, 113.7, 66.9, 41.8, 33.9,10.1; ESI-Mass: *m*/*z* 454.12 $[M + Na]^+$.

2-(1-(3-fluorophenyl)-2-methyl-5-(4-sulfamoylphenyl)-1H-pyrrol-3-yl)-N-(2-hydroxyethyl)acetamide (40): (yield 50%) mp 152 °C; $C_{21}H_{21}FN_3O_4S$; ^{1}H-NMR (400MHz, DMSO) ppm: 7.89 (t, 1H), 7.60 (d, 2H), 7.51-7.49 (m, 1H), 7.31-7.26 (m, 4H), 7.15 (d, 2H), 7.04 (s, 1H), 6.48 (s, 1H), 4.69 (s broad, 1H), 3.43-3.42 (m, 2H), 3.27 (s, 2H), 3.115-3.14 (m, 2H), 2.04 (s, 3H).^{13}C-NMR (100 MHz, CDCl3) δ (ppm): 171.3, 162.9, 142.0, 142.5, 141.6, 133.6, 129.2, 127.8, 126.5, 125.0, 120.9, 116.8, 112.6, 111.9, 106.8, 60.9, 40.8, 33.2, 9.6; ESI-Mass: *m*/*z* 454.12 $[M + Na]^+$.

2-(1-(3,4-difluorophenyl)-2-methyl-5-(4-sulfamoylphenyl)-1H-pyrrol-3-yl)-N-(2-hydroxyethyl)acetamide (41): (yield 48%) $C_{21}H_{21}F_2N_3O_4S$;^{1}H-NMR (400MHz, DMSO) ppm: 7.80 (t, 1H), 7.50 (d, 2H), 7.14 (m, 5H), 7.11(d, 2H), 6.47 (s, 1H), 6.60 (m broad, 1H) 3.40 (t, 2H),3.10 (t, 2H), 2.40 (s, 2H), 2.09 (s, 3H). ^{13}C-NMR (100 MHz, CDCl3) δ (ppm):171.6, 150.1, 146.3, 143.7, 142.8, 139.1, 134.4, 128.5, 127.8, 125.9,

121.4, 118.0, 117.7, 117.4, 113.3, 108.8, 107.7, 61.0, 41.6, 34.0, 9.8.

2-(1-phenyl)-2-methyl-5-(4-sulfamoylphenyl)-1H-pyrrol-3-yl)-N-(2-hydroxyethyl)acetamide (42): (yield 45%) mp 147°C; $C_{21}H_{23}N_3O_4S$;^{1}H-NMR (400MHz, DMSO) ppm: 7.80 (t, 1H), 7.58 (d, 2H), 7.20 (m, 1H), 7.15 (m, 6H), 6.98 (d, 2H), 6.47 (s, 1H), 6.60 (m broad, 1H), 3.47 (t, 2H), 3.19 (t, 2H), 2.44 (s, 2H), 2.09 (s, 3H).171.6, 151.0, 143.7, 142.8, 134.4, 129.3, 128.5, 128.2, 127.8, 127.3, 127.2, 126.9, 125.9, 125.5, 121.4, 121.3, 121.0, 118.4, 118.0, 113.3, 107.7, 106.5, 61.0, 41.6, 34.0, 9.8.

1.4.1.19. General procedure for the Preparation of nitro-oxyalkylamine (45)

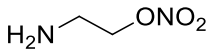

Fuming nitric acid (3 mL) was added to dichloromethane in a100 mL round-bottomed flask. The solution was allowed to reach0°C and then ethanolamine (**44**) (16 mmol) was added dropwise. After 50 min of stirring, acetic anhydride (2 mL) was added dropwise over 2 min. After 45 min a precipitate was formed and then filtered. The solid was then crystallizedwith hot chloroform/ethanol to give the product as nitrate salt.

1-(4-Fluorophenyl)-2-methyl-5-(4-(methylsulfonyl)phenyl)1H-pyrrole (45). 2-(Nitro-oxy)ethyl amine nitrate salt. mp and ^{1}H NMR spectrum were consistent with those reported in literature.

1.4.2. Biology and pharmacology

1.4.2.1. In vitro anti-inflammatory studies

The inhibitory activity of compounds **13-24** against both cyclooxygenases, COX-1 and COX-2, was determined by the commercially available COX Inhibitor Screening Assay (Cayman Chemical, Ann Arbor, MI, USA, catalogue no. 560131), which exploits an enzyme immunoassay to measure PGE_{2a} produced by stannous chloride reduction of $PGEH_2$, derived in turn by reaction between the target enzyme and the substrate, arachidonic acid.According to manufacturer's protocol, test compounds (10 μL) were incubated for 10 min at 37 °C with assay buffer (0.1 M Tris-HCl, pH 8, 160 μL), Heme (10 μL), and either ovine

COX-1 or human recombinant COX-2 enzyme solution (10 μM). Arachidonic acid (10 μL) was then added, and the resulting mixture was incubated for 2 min at 37°C. Enzyme catalysis was stopped by adding HCl (1M, 10 mL) and the obtained $PGEH_2$ were converted to PGE_{2a} with saturated stannous chloride solution (20 μL). Prostanoids were finally quantified by EIA and their amount was determined through interpolation from a standard curve. The % inhibition of target enzyme by test compounds was calculated by comparingPGE_{2a}produced in compound-treated samples with that of the compound-free, control sample. The highly selective COX-1 inhibitor SC-560 and the highly selective COX-2 inhibitor Dup-697 were used as reference compounds. All the test compounds, **13-24**, were dissolved into dilute assay buffer, and their solubility was facilitated by using DMSO, whose concentration never exceeded 1% in the final reaction mixture. The inhibitory effect of test compounds was routinely estimated at a concentration of 10 μM. Those compounds found to be active were tested at additional concentrations between 10 μM and 10 nM. The determination of the IC_{50} values was performed by linear regression analysis of the log-dose response curve, which was generated using at least five concentrations of the inhibitor causing an inhibition between 10% and 90%, with three replicates at each concentration.

1.4.2.2. In vitro cell-based assay

The *in vitro* profiles of compounds **1-12** and **35-42,** related to their inhibitory activity towards both COX-1and COX-2 isoenzymes, were evaluated through cell-based assay employing murine monocyte/macrophage J774 cell lines. The cell line was grown in DMEM supplemented with 2 mM glutamine,25 mM HEPES, 100 units/mL penicillin, 100 lg/mL streptomycin,10% fetal bovine serum (FBS), and 1.2% sodium pyruvate. Cells were plated in 24-well culture plates at a density of 2.5 X105cells/mL or in 60 mm diameter culture dishes (3 X106 cells per3 mL per dish) and allowed to adhere at 37 °C in 5% CO2 for 2 h. Immediately before the experiments, culture medium was replaced with fresh medium and cells were stimulated as describedpreviously.26–28,33–40 The evaluation of COX-1 inhibitory activity was achieved pre-treating cells with test compounds (10 μM) for15 min and then incubating them at 37 °C for 30 min with 15 μM arachidonic acid

to activate the constitutive COX. For the compounds with COX-1% inhibition higher than 50% (at 10 μM), the cells were treated also with lower concentrations (0.01–1 μM). At the end of the incubation, the supernatants were collected for the measurement of prostaglandin E2 (PGE2) levels by a radioimmunoassay(RIA). To evaluate COX-2 activity, cells were stimulated for 24 h with Escherichia coli lipopolysaccharide (LPS, 10 μg/mL) to induce COX-2, in the absence or presence of test compounds(0.01–10 μM). Celecoxib was utilized as a reference compound for the selectivity index. The supernatants were collected for the measurement of PGE2 by means of RIA. Throughout the time the experiments lasted, triplicate wells were used for the various conditions of treatment. Results are expressed as the mean, for three experiments, of the percent inhibition of PGE2 production by test compounds with respect to control samples. The IC50 values were calculated with GraphPadInstat, and the data fit was obtained using the sigmoidal dose-response equation (variable slope) (GraphPad).

1.4.2.3. Ex vivo vasorelaxing activity

All the experimental procedures were carried out following the guidelines of the European Community Council Directive 86-609.The effects of the compounds were tested on isolated thoracic aortic rings of male normotensive Wistar rats (250–350 g). After a light ether anaesthesia, rats were sacrificed by cervical dislocation and bleeding. The aortae were immediately excised, freed of extraneous tissues and the endothelial layer was removed by gently rubbing the intimal surface of the vessels with a hypodermic needle. Five mm wide aortic rings were suspended, under a preload of 2 g, in 20 mL organ baths, containing Tyrode solution(composition of saline in mM: NaCl 136.8; KCl 2.95; $CaCl_2$ 1.80;$MgSO_4$ 1.05; NaH_2PO_4 0.41; $NaHCO_3$ 11.9; glucose 5.5), thermostated at 37 °C and continuously gassed with a mixture of O_2(95%) and CO_2 (5%). Changes in tension were recorded by means of an isometric transducer (Grass FTO3), connected with a computerised system (Biopac). After an equilibration period of60 min, the endothelium removal was confirmed by the administration

of acetylcholine (ACh) (10 μM) to KCl (30 mM)-precontracted vascular rings. A relaxation <10% of the KCl-induced contraction was considered representative of an acceptable lack

of the endothelial layer, while the organs, showing a

relaxationP10% (i.e. significant presence of the endothelium), were discarded. From 30 to 40 min after the confirmation of the endothelium removal, the aortic preparations were contracted by a single concentration of KCl (30 mM) and when the contraction reached a stable plateau, 3-fold increasing concentrations of the tested compounds(1 nM–10 μM) were added. Preliminary experiments

showed that the KCl (30 mM)-induced contractions remained in a stable tonic state for at least 40 min. The same experiments were carried out also in the presence of a well-known GC inhibitor: ODQ 1 μM which was incubated in aortic preparations after the endothelium removal confirmation. The vasorelaxing efficacy was evaluated as maximal vasorelaxing response (Emax), expressed as a percentage (%) of the contractile tone induced by KCl 30 mM. When the limit concentration 10 M (the highest concentration, which could be administered) of the tested compounds did not reach the maximal effect, the parameter of efficacy represented the vasorelaxing response, expressed as a percentage (%) of the contractile tone induced by KCl 30 mM, evoked by this limit concentration. The parameter of potency was expressed as pIC_{50},calculated as negative logarithm of the molar concentration of the tested compounds evoking a half reduction of the contractile tone induced by KCl 30 mM. The pIC50 could not be calculated for those compounds showing an efficacy parameter lower than50%. The parameters of efficacy and potency were expressed as mean ± standard error, for 6-10 experiments. Two-way ANOVA was selected as statistical analysis, $P < 0.05$ was considered representative of significant statistical differences. Experimental data were analysed by a computer fitting procedure (software: Graph-Pad Prism 4.0).

1.4.2.4. In vivo analgesic and anti-inflammatory study

In vivo anti-inflammatory activity of the new compounds wasalso assessed. Male Swiss albino mice (23–25 g) and Sprague-Dawleyor Wistar rats (150–200 g) were used. The animals were fed with a standard laboratory diet and tap water ad libitum and keptat 23 (1 °C with a 12 h light/dark cycle, light on at 7 a.m.) The paw pressure test was performed by inducing an inflammatory processby the intraplantar (ipl) carrageenan administration 4 h before the test. In the administered intraplantar (ipl) carrageenan 4 h beforethe test. The

carrageenan-induced paw oedema test was also performed, evaluating the paw volume of the right hind paw 4 h after the injection of carrageenan and comparing it with saline/carrageenan-treated controls. The analgesic activity of compounds was also assessed by performing the abdominal constriction test, using mice into which a 0.6% solution of acetic acid (10 mL/kg)had been injected intra-peritoneal (ip). The number of stretching movements was counted for 10 min, starting 5 min after administration.

1.4.3. Molecular modelling

Molecular docking calculations were carried out with several programs selected among those as open source or free to academics: Autodock,[64]Vina,[65]Plants,[66]PARADOCKS[67] and Surflex-Dock.[56]

1.4.3.1. Docking assessment protocol

A cross-docking protocol was set up for eight docking program/scoring function combination, during the cross-docking each ligand extracted from the experimental COX complex was docked into all the not native proteins for each isoenzyme.

1.4.3.2. Ligand and protein preparation

The experimental complexes (PDB entries listed in Tables 3 and 4),[58] upon hydrogen addition, were minimized by means of GROMACS[68] with the AMBER force field59 in explicit water (box expanding 10 Å from each external complex coordinate) using the Powell method with an initial Simplex optimization (500 iterations) followed by 1000 iterations of conjugated gradient termination at 0.01 kcal/(mol Å). Ligand's random conformations were generated from the bound conformation extracted from the minimized COX-1/COX-2 experimental co-crystallized complexes. Using OpenBabel 2.3.2[69] version, hydrogen atoms were added, and charges were loaded using the Gasteiger and Marsili charge calculation method, then their center of mass were centered at x,y,z 0.0 coordinates, finally the OpenBabel ob conformer tools was used to generate a minimized random conformation for each ligand. Input ligands file format was mol2 for all the docking programs except for Autodock and Vina that required a pdbqt format; a total of 8 docking/scoring function combinations were used.

1.4.3.3. AutoDock/Vina setting

Intermediary steps, such as pdbqt files for protein and ligand preparation were completed using different AutoDock Tools (ADT) Scripts. AutoGrid was used for the preparation of the grid map using a grid box. The grid size was expanded 10 Å beyond any external ligand atoms with grid spacing of 0.375 Å and centered at the mean molecules' center of mass. For each calculation, twenty poses were obtained and ranked according to the scoring-functions of either Autodock or Vina.

1.4.3.4. Plants settings

The docking of the target protein with the ligand was performed using Plants v1.2 version with three different scoring functions at default speed (SPEED1). The docking tools generated 20 conformation for each docked ligand. The docking binding site was centered the molecules' mean center and enlarging to a radius of 15 Å.

1.4.3.5. Paradocks settings

Both Paradocks-pscore and Paradocks-pmf04 scoring functions were used in their default configuration (Iteration 15000, particle count 20, constricting the inertia start 1.0, constricting inertia end 0.2, cognitive weight 1.0 and social weight 3.4).

1.4.3.6. Surflex-Dock settings

Version 2.0.1 of the program was used; the input file was built using the mol2 prepared protein structure. The protocol was generated using all the ligands structures with a threshold of 0.50 and bloat set to 0 (default settings). Ligand were prepared as describes above and docked as mol2 files.

1.4.3.7. New COX inhibitor preparation and docking.

Ligand's 3D conformations were generated from scratch. Marvin was used for drawing, displaying and characterizing chemical structures, Marvin 14.7.7.0, 2014, ChemAxon (http://www.chemaxon.com). For homogeneity purposes, OpenBabel was used to generate a random conformation similarly as described in the docking assessment section.

The 1-12 generated random conformations were cross-docked using Surflex-Dock and Vina for COX-1 and COX-2, respectively. The

same setting used for the docking assessment protocolwere applied. All the protein structures were used in this step.

References

1.Dubois, R. N. *et al.*Cyclooxygenase in biology and disease. *FASEB J.* **12,** 1063-1073 (1998).

2.Luong, C. *et al.* Flexibility of the NSAID binding site in the structure of human cyclooxygenase-2. *Nat. Struct. Biol.* **3,** 927-933 (1996).

3.Kiefer, J. R. *et al.* Structural insights into the stereochemistry of the cyclooxygenase reaction. *Nature* **405,** 97-101 (2000).

4.Smith, W. L., *et al.* R. M. Cyclooxygenases: structural, cellular, and molecular biology. *Annu. Rev. Biochem.* **69,** 145-182 (2000).

5.Patrignani, P. & Patrono, C. Cyclooxygenase inhibitors: From pharmacology to clinical read-outs. *Biochim. Biophys. Acta* **1851**, 422-432 (2015).

6.Wood, A. J. J. *et al.* The Coxibs, Selective Inhibitors of Cyclooxygenase-2. *N. Engl. J. Med.* **345,** 433-442 (2001).

7.Richy, F. Time dependent risk of gastrointestinal complications induced by non-steroidal anti-inflammatory drug use: a consensus statement using a meta-analytic approach. *Ann. Rheum. Dis.* **63,** 759-766 (2004).

8.Murata, T. *et al.* Altered pain perception and inflammatory response in mice lacking prostacyclin receptor. *Nature* **388,** 678-682 (1997).

9.Nakao, K. *et al.* CJ-023,423, a Novel, Potent and Selective Prostaglandin EP4 Receptor Antagonist with Antihyperalgesic Properties. *J. Pharmacol. Exp. Ther.* **322,** 686-694 (2007).

10.Smyth, W. *et al.* Prostanoids in health and disease. *J. Lipid Res.* **50,** S423-428 (2009).

11.Ghosh, N., Chaki, R., Mandal, V. & Mandal, S. C. COX-2 as a target for cancer chemotherapy. *Pharmacol. Rep.* **62,** 233-244 (2010).

12.Wang, D. & DuBois, R. N. The role of COX-2 in intestinal inflammation and colorectal cancer. *Oncogene* **29,** 781-788 (2010).

13.Gupta, R. A. & Dubois, R. N. Colorectal cancer prevention and treatment by inhibition of cyclooxygenase-2. *Nat. Rev. Cancer* **1,** 11-21 (2001).

14.Wang, D. & DuBois, R. N. Eicosanoids and cancer. *Nat. Rev. Cancer* **10,** 181-193 (2010).

15.Yiu, G. K. & Toker, A. NFAT Induces Breast Cancer Cell Invasion by Promoting the Induction of Cyclooxygenase-2. *J. Biol. Chem.* **281,** 12210-12217 (2006).

16.Chen, S.-F. *et al.* Caveolin-1 facilitates cyclooxygenase-2 protein degradation. *J. Cell. Biochem.* **109,** 356-362 (2010).

17.Rizzo, M. T. Cyclooxygenase-2 in oncogenesis. *Clin. Chim. Acta* **412,** 671-687 (2011).

18.Oshima, M. *et al.*Suppression of intestinal polyposis in Apc delta716 knockout mice by inhibition of cyclooxygenase 2 (COX-2). *Cell* **87,** 803-809 (1996).

19.Bresalier, R. S. *et al.* Cardiovascular Events Associated with Rofecoxib in a Colorectal Adenoma Chemoprevention Trial. *N. Engl. J. Med.* **352,** 1092-1102 (2005).

20.Arber, N. *et al.* The APC and PreSAP Trials: A Post Hoc Noninferiority Analysis Using a Comprehensive New Measure for Gastrointestinal Tract Injury in 2 Randomized, Double-Blind Studies Comparing Celecoxib and Placebo. *Clin. Ther.* **34,** 569-579 (2012).

21.Cheng, Y. *et al.* Role of prostacyclin in the cardiovascular response to thromboxane A2. *Science* **296,** 539-541 (2002).

22.Dogné, J.-M. *et al.* D. Adverse Cardiovascular Effects of the Coxibs. *J. Med. Chem.* **48,** 2251-2257 (2005).

23.Coxib and traditional NSAID Trialists' (CNT) Collaboration Vascular and upper gastrointestinal effects of non-steroidal anti-inflammatory drugs: meta-analyses of individual participant data from randomised trials. *Lancet* **382,** 769-779 (2013).

24.Baron, J. A. *et al.* Cardiovascular events associated with rofecoxib: final analysis of the APPROVe trial. *Lancet* **372,** 1756-1764 (2008).

25.Mason, R. P. *et al.* Rofecoxib increases susceptibility of human LDL and membrane lipids to oxidative damage: a mechanism of cardiotoxicity. *J. Cardiovasc. Pharmacol.* **47**, S7-14 (2006).

26.Reddy, L. R. & Corey, E. J. Facile air oxidation of the conjugate base of rofecoxib (Vioxx™), a possible contributor to chronic human toxicity. *Tetrahedron Lett.* **46,** 927-929 (2005).

27.Martelli, A. *et al.* NO-releasing hybrids of cardiovascular drugs. *Curr. Med. Chem.* **13,** 609-625 (2006).

28.Breschi, M. C. *et al.* New NO-releasing pharmacodynamic hybrids of losartan and its active metabolite: design, synthesis, and biopharmacological properties. *J. Med. Chem.* **49,** 2628-2639 (2006).

29.Decker, M. *et al.* Synthesis and vasorelaxant properties of hybrid molecules out of NO-donors and the beta-receptor blocking drug propranolol. *Bioorg. Med. Chem. Lett.* **14,** 4995-4997 (2004).

30.Konter, J. *et al.* J. NO-donors. Part 17: Synthesis and antimicrobial activity of novel ketoconazole-NO-donor hybrid compounds. *Bioorg. Med. Chem.* **16,** 8294-8300 (2008).

31.Ignarro, L. J. Nitric oxide as a unique signaling molecule in the vascular system: a historical overview. *J. Physiol. Pharmacol. Off. J. Pol. Physiol. Soc.* **53,** 503-514 (2002).

32.Cheng, H. *et al.* Nitric oxide in cancer metastasis. *Cancer Lett.* **353,** 1-7 (2014).

33.Geusens, P. Naproxcinod, a new cyclooxygenase-inhibiting nitric oxide donator (CINOD). *Expert Opin. Biol. Ther.* **9,** 649-657 (2009).

34.Cicala, C. *et al.* NO-naproxen modulates inflammation, nociception and downregulates T cell response in rat Freund's adjuvant arthritis. *Br. J. Pharmacol.* **130,** 1399-1405 (2000).

35.Cuzzolin, L. *et al.* Anti-inflammatory potency and gastrointestinal toxicity of a new compound, nitronaproxen. *Pharmacol. Res. Off. J. Ital. Pharmacol. Soc.* **31,** 61-65 (1995).

36.Karlsson, J. *et al.* Efficacy, Safety, and Tolerability of the Cyclooxygenase-Inhibiting Nitric Oxide Donator Naproxcinod in Treating Osteoarthritis of the Hip or Knee. *J. Rheumatol.* **36,** 1290-1297 (2009).

37.Biava, M. *et al.* 1,5-Diarylpyrrole-3-acetic acids and esters as novel classes of potent and highly selective cyclooxygenase-2 inhibitors. *J. Med. Chem.* **48,** 3428-3432 (2005).

38.Biava, M. *et al.* Cyclooxygenase-2 inhibitors. 1,5-diarylpyrrol-3-acetic esters with enhanced inhibitory activity toward cyclooxygenase-2 and improved cyclooxygenase-2/cyclooxygenase-1 selectivity. *J. Med. Chem.* **50,** 5403-5411 (2007).

39.Biava, M. *et al.* Synthesis, in vitro, and in vivo biological evaluation and molecular docking simulations of chiral alcohol and ether derivatives of the 1,5-diarylpyrrole scaffold as novel anti-inflammatory and analgesic agents. *Bioorg. Med. Chem.* **16,** 8072-8081 (2008).

40.Biava, M. *et al.* HPLC enantioseparation and absolute

configuration of novel anti-inflammatory pyrrole derivatives. *Chirality* **20,** 775-780 (2008).

41.Anzini, M. *et al.* Synthesis, Biological Evaluation, and Enzyme Docking Simulations of 1,5-Diarylpyrrole-3-Alkoxyethyl Ethers as Selective Cyclooxygenase-2 Inhibitors Endowed with Anti-inflammatory and Antinociceptive Activity. *J. Med. Chem.* **51,** 4476-4481 (2008).

42.Biava, M. *et al.* Novel ester and acid derivatives of the 1,5-diarylpyrrole scaffold as anti-inflammatory and analgesic agents. Synthesis and in vitro and in vivo biological evaluation. *J. Med. Chem.* **53,** 723-733 (2010).

43.Biava, M. *et al.* Enlarging the NSAIDs family: ether, ester and acid derivatives of the 1,5-diarylpyrrole scaffold as novel anti-inflammatory and analgesic agents. *Curr. Med. Chem.* **18,** 1540-1554 (2011).

44.Battilocchio, C. *et al.* A class of pyrrole derivatives endowed with analgesic/anti-inflammatory activity. *Bioorg. Med. Chem.* **21,** 3695-3701 (2013).

45.Khanna, I. K. *et al.* 1,2-Diarylpyrroles as potent and selective inhibitors of cyclooxygenase-2. *J. Med. Chem.* **40,** 1619-1633 (1997).

46.De Luca, L. *et al.*Beckmann Rearrangement of Oximes under Very Mild Conditions. *J. Org. Chem.* **67,** 6272-6274 (2002).

47.Swinney, D. C. Differential Allosteric Regulation of Prostaglandin H Synthase 1 and 2 by Arachidonic Acid. *J. Biol. Chem.* **272,** 12393-12398 (1997).

48.Jones, C. K. Efficacy of Duloxetine, a Potent and Balanced Serotonergic and Noradrenergic Reuptake Inhibitor, in Inflammatory and Acute Pain Models in Rodents. *J. Pharmacol. Exp. Ther.* **312,** 726-732 (2004).

49.Patrono, C. *et al.* Low dose aspirin and inhibition of thromboxane B2 production in healthy subjects. *Thromb. Res.* **17,** 317-327 (1980).

50.Patrignani, P. *et al.* Biochemical and pharmacological characterization of the cyclooxygenase activity of human blood prostaglandin endoperoxide synthases. *J. Pharmacol. Exp. Ther.* **271,** 1705-1712 (1994).

51.Consalvi, S. Synthesis, biological evaluation and docking analysis of a new series of methylsulfonyl and sulfamoylacetamides and ethyl acetate as potent COX-2 inhibitors. *Bioorg. Med. Chem.* **23**, 810-820 (2015)

52.Khanna, I. K. *et al.* Selective Cyclooxygenase-2 Inhibitors: Heteroaryl Modified 1,2-Diarylimidazoles Are Potent, Orally Active

Antiinflammatory Agents. *J. Med. Chem* .**43,** 3168-3185 (2000).

53.Musmuca, I. *et al.* Combining 3-D Quantitative Structure−Activity Relationship with Ligand Based and Structure Based Alignment Procedures for in Silico Screening of New Hepatitis C Virus NS5B Polymerase Inhibitors. *J. Chem. Inf. Model.* **50,** 662-676 (2010).

54.Caroli, A. *et al.* R. Hsp90 Inhibitors, Part 2: Combining Ligand-Based and Structure-Based Approaches for Virtual Screening Application. *J. Chem. Inf. Model.* **54,** 970-977 (2014).

55.Ragno, R. *et al.* HIV-Reverse Transcriptase Inhibition: Inclusion of Ligand-Induced Fit by Cross-Docking Studies. *J. Med. Chem.* **48,** 200-212 (2005).

56.Spitzer, R. & Jain, A. N. Surflex-Dock: Docking benchmarks and real-world application. *J. Comput. Aided Mol. Des.* **26,** 687-699 (2012).

57.Jain, A. N. Surflex-Dock 2.1: Robust performance from ligand energetic modeling, ring flexibility, and knowledge-based search. *J. Comput. Aided Mol. Des.* **21,** 281-306 (2007).

58.Steiner, T. The Hydrogen Bond in the Solid State. *Angew. Chem. Int. Ed.* **41,** 48-76 (2002).

59.Pettersen, E. F. *et al.* UCSF Chimera—A visualization system for exploratory research and analysis. *J. Comput. Chem.* **25,** 1605-1612 (2004).

60.Biava, M. *et al.* Novel analgesic/anti-inflammatory agents: diarylpyrrole acetic esters endowed with nitric oxide releasing properties. *J. Med. Chem.* **54,** 7759-7771 (2011).

61.Biava, M. *et al.* Improving the solubility of a new class of anti-inflammatory pharmacodynamic hybrids, that release nitric oxide and inhibit cycloxygenase-2 isoenzyme. *Eur. J. Med. Chem.* **58,** 287-298 (2012).

62.Anzini, M. *et al.* Novel analgesic/anti-inflammatory agents: 1,5-diarylpyrrole nitrooxyalkyl ethers and related compounds as cyclooxygenase-2 inhibiting nitric oxide donors. *J. Med. Chem.* **56,** 3191-3206 (2013).

63.Biava, M. *et al.* Enhancing the pharmacodynamic profile of a class of selective COX-2 inhibiting nitric oxide donors. *Bioorg. Med. Chem.* **22,** 772-786 (2014).

64.Morris, G. M. *et al.* Using AutoDock for Ligand-Receptor Docking *Curr. Protoc. Bioinform.* **24**,8.14.1-8.14.40 (2008).

65.Trott, O. & Olson, A. J. AutoDock Vina: Improving the speed and accuracy of docking with a new scoring function, efficient optimization, and multithreading. *J. Comput. Chem.* **31,** 455-461 (2010).

66.Korb, O., Stützle, T. & Exner, T. E. Empirical Scoring Functions for Advanced Protein–Ligand Docking with PLANTS. *J. Chem. Inf. Model.* **49,** 84-96 (2009).

67.Meier, R. *et al.* ParaDockS: A Framework for Molecular Docking with Population-Based Metaheuristics. *J. Chem. Inf. Model.* **50,** 879-889 (2010).

68.Van Der Spoel, D. *et al.* GROMACS: Fast, flexible, and free. *J. Comput. Chem.* **26,** 1701-1718 (2005).

69.O'Boyle, N. M. *et al.* Open Babel: An open chemical toolbox. *J. Cheminformatics* **3,** 33, 1-14 (2011).

2. Development of a novel BRD9 chemical probe

2.1. Introduction

The post-translational modifications (PTM) of histones include phosphorylation, acetylation, ubiquitination, methylation, biotinylation, cytrullination, ribosylation and crotonilation[1]. Such chemical modifications affect the integrity of the genome architecture and modulate the gene transcription control by acting mainly in two ways: *i)* altering the chromatin structure by changing physical interaction with DNA and consequently its ability of being transcribed; *ii)* recruiting other proteins that can directly or indirectly influence transcription[2]. PTMs are usually orchestrated by three types of protein: "writers", that add chemical marks; "readers", that bind to these marks thus influencing gene expression; "erasers", that remove such marks[3].

The histone lysine acetylation is one of the most studied PTMs. This process is highly regulated by two enzyme families endowed with opposite mechanisms of action: the histone acetyltransferase (HAT) and the histone deacetylase (HDAC). The former is an acetylation "writer" and catalyzes the transfer of an acetyl group to the ε-amino group of the lysine side chains, thus neutralizing the positive charge of the amino group and weakening interactions between the histones and DNA. On the other hand, HDAC act as an "eraser": indeed, these proteins restore positive charge on lysine residues and stabilize chromatin architecture by reversing lysine acetylation[2]. Aberrant ly-

sine acetylation levels have been linked to many diseases, particularly to cancer. Indeed, HAT and HDAC inhibitors have arisen as promising antitumor agent.

Bromodomains (BRDs) are a family of well-conserved protein interaction modules that selectively recognize ε-*N*-lysine acetylation motifs, serving as "readers" of these epigenetic marks. 61 different BRDs are encoded by the human proteome and are present in 46 different cytoplasmic and nuclear proteins. According to structure-based alignments, they refer to eight distinct groups[4] and comprise transcriptional co-activators and mediators, bromodomain and extraterminal proteins (BETs), P300/CBp associated factor and bromodomain containing protein 9 (BRD9), chromatin remodelling complexes and HATs and HAT associated proteins, histone methyltransferase, helicases and nuclear scaffolding proteins. [5].All these proteins share a largely conserved fold. The BRD fold is constituted by four left-handed bundle helices (α_Z, α_A, α_B, α_C). The interhelical ZA and BC loops are of variable length and measures and delimitthe binding pocket of acetyl-lysine,which is in turn anchored by means of a hydrogen bond to an asparagine residue[6,7].Some members of BRDs families, such as BET, can bind to two acetylated histones at the same time. Since the acetylated lysine is neutral-charged, this binding pocket is mostly hydrophobic, making this target particularly attractive for the design and the development of small molecules that compete with this protein-protein interaction.

BRD containing proteins are involved in many biological processes and exert broad effects. They are implicated in recruiting general and specific transcription factors, thus playing a crucial role in oncogenic rearrangements and in the development of a number of extremely aggressive types of cancer, such as the nuclear protein in testis midline carcinoma (NMC). Moreover, BRDs interact with the acetylated NF-kB (nuclear factor kappa-light-chain-enhancer of activated B cells) and stimulate the transcription of NF-kB regulated genes[5,8]. In addition, they modulate responses to viral infections; indeed they can regulate the transcription of viral proteins and are involved in the viral genome replication of several viruses, including Human Immunodeficiency Virusand Human Papilloma Virus. As a consequence, they arise as possible targets for treating inflammatory pathologies and auto-immune disorders, viral infections and cancer[5].

In order to deeper understand the biology of these proteins, a series of highly selective small molecule inhibitors, also known as chemical probes, has been developed. These molecules allow to establish a relationship between a molecular target and its biological function[9] and represent a useful tool to validate new treatment strategies for diseases characterized by very complex mechanisms. According to a fragment-based approach, a number of small molecule fragments, mimicking the binding mode of acetylated lysine within the binding pocket, have been identified (Fig. 2.1.). These scaffolds constituted the starting points for the design of new inhibitors, taking advantage of molecular docking and crystal-structure-guided lead optimization studies[10,11].

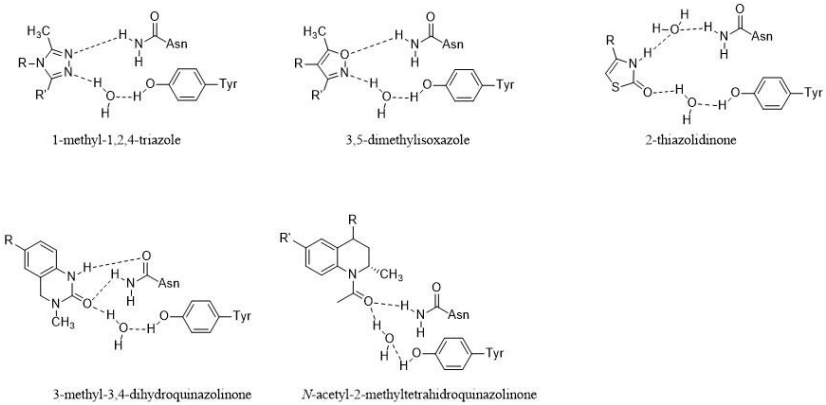

Figure 2.1. Schematic representation of acetyl-lysine mimic fragments within the binding pocket.

Several BRD inhibitors have been developed in the last decade, particularly against the BET subclass. Few examples are represented in figure 2.2.[10,12].

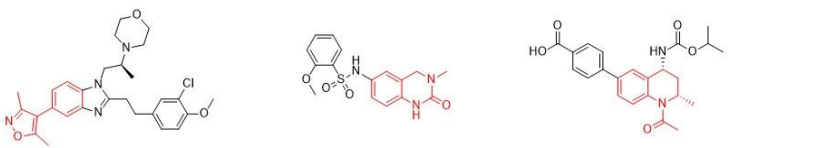

Figure 2.2. Chemical structures of some BRD inhibitors and corresponding activities. Starting fragments are highlighted in red.

A number of BRD inhibitors are currently under clinical investigation. Given the efficacy in animal models, the BET inhibitors I-BET762 (GSK-525762, Fig. 2.3) and TEN-010 are in Phase I clinical trial targeting NMC, a rare and aggressive form of cancer that strictly depend on the *BRD3-NUT* and/or *BRD4-NUT* oncogene. CPI-0610 and OTX-015are currently in Phase I for exploring their efficacy against acute leukaemia and lymphoma, respectively[11].

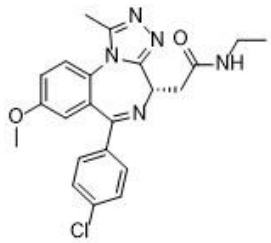

GSK-525762

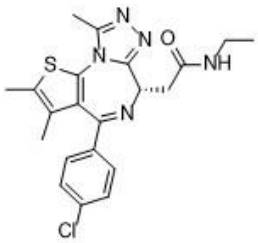

OTX-015

Figure 2.3. Chemical structures of BRD inhibitors in clinical trials.

While BET proteins have been extensively investigated and many inhibitors have been developed, the coverage of the entire BRD family has not been completed, and the biological role of many of them has not been elucidated yet. Given the importance of chemical probes in disclosing BET role in diseases, it is clear that further efforts are needed in targeting non-BET BRDs for disclosing their functions and their therapeutic potentials[13].

2.2. Rationale and aims

The BRD9 containing protein function needs to be elucidated; keeping in mind significant results obtained with BET proteins, it seems clear that the development of a novel BRD9 chemical probes could be useful for disclosing its biological role. The research group of Dr. Paul Brennan and Prof. Darren Dixon has obtained a series of BRD7/BRD9 inhibitors endowed with outstanding activities. **BDOQI000075a**, one of the best hits, arose from the quinolin-2-one fragment **BDOQI000061a** (Fig. 2.4.).

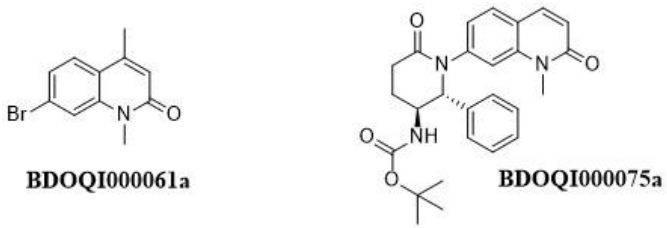

Figure 2.4. Chemical structures of BDOQI**000061a** and **BDOQI000075a.**

On these grounds, this project focuses on designing and synthesizing two small sets of derivatives with the aim of further improving the binding affinity of these compounds and for extending SAR knowledge.

Firstly, the fragment hit **BDOQI000061a** was modified for evaluating the importance of such scaffold for the activity (Fig. 2.5.). Therefore, an ethyl group was alternatively placed either at N1 or C4 of the quinolone scaffold (compounds **46** and **47**); moreover, the derivative **48** was synthesized to investigate the importance of the carbonyl moiety at C2.

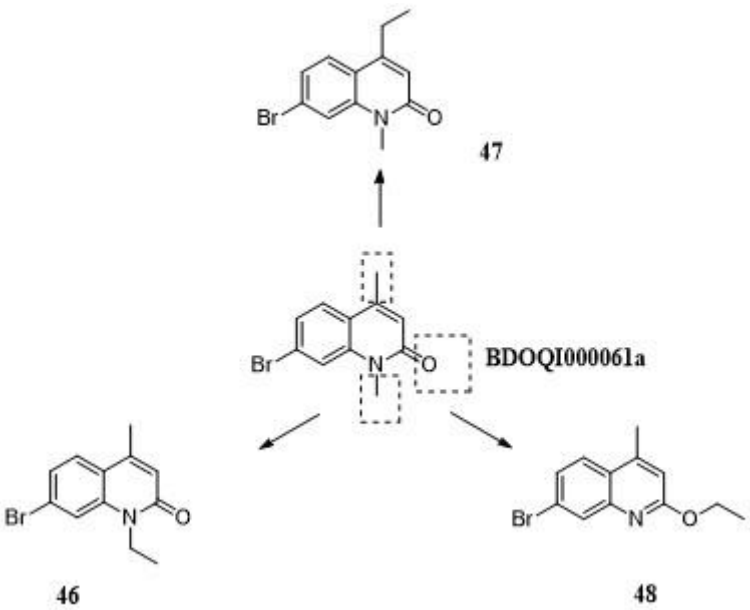

Figure 2.5. First set of modifications on the quinoline scaffold.

Thereafter, **BDOQI000075a** was modified by replacing the six-member lactam at position 7 of the quinoline ring with a five-member one, for evaluating the influence of the ring size on the binding affinity for BRD9 (Fig.2.6). In line with **BDOQI000075a,** the pyrrolidine ring was decorated with a *tert*-butyl carbamate at C3 and a phenyl ring at C5 (derivatives **49-50**). The two racemic mixtures **49** and **50,** (the *trans* and the *cis* diastereoisomer, respectively), were individually tested; the obtained results showed that the *trans* mixture was the most active one. Therefore, the single enantiomers were isolated to evaluate the influence of the stereochemistry for binding affinity. Derivative **49** was further modified by introducing a chlorine substituent (compound **51**) at the phenyl ring at C4 of the pyrrolidine ring, in order to investigate the influence of an electron withdrawing group in this position. Finally, to assess the importance of the *tert*-butyl carbamate substituent for the activity, the amino derivative **52**, as well as the carbamate **53**, the ureas **54** and **55**, the sulphonamides **56** and **57** and the amides **58** and **59** were also synthesized.

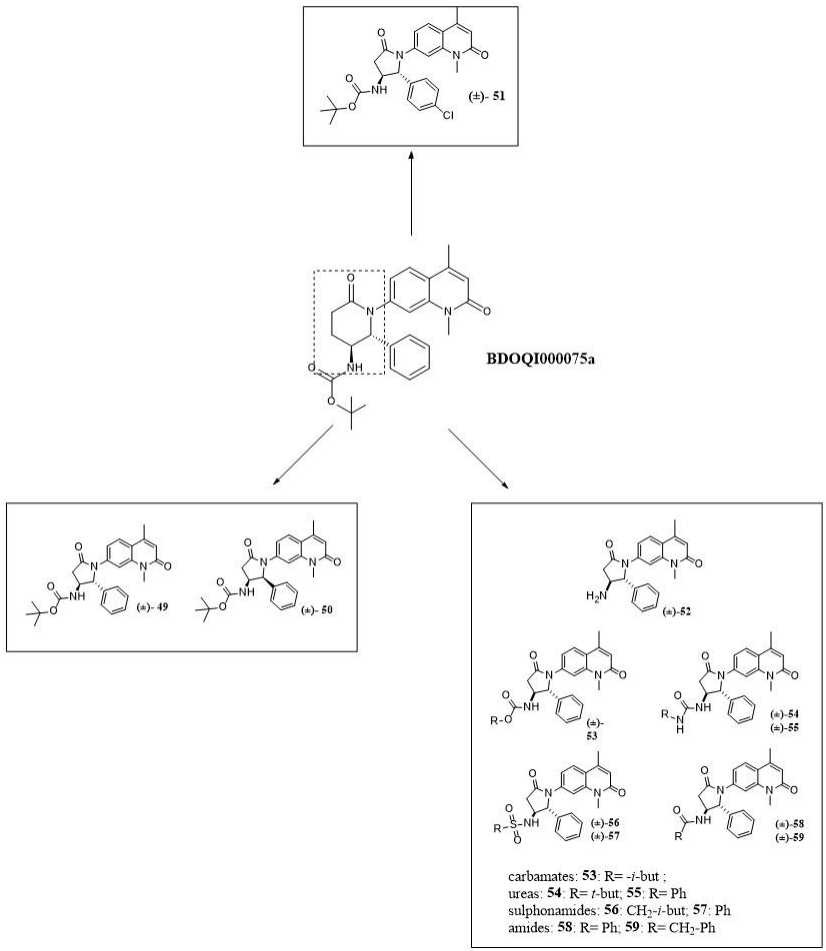

Figure 2.6. Second set of modifications.

2.3. Chemistry

The quinoline fragment was synthesized according to the procedure indicated in Scheme 2.1. Briefly, a reaction between the bromoaniline **60** and the diketene **61** led to the β-ketoamide **62** in a 73 % yield[14]; the ketoamide was then reacted with sulphuric acid at 120 °C, giving the quinoline **63** in good yields[15]. Derivative **46** was obtained through a reaction between the quinoline **63** and ethyl iodide in the presence of potassium carbonate (25% yield) and was accompanied by the side-product **48**, isolated in a 10% yield. The reaction between the bromoaniline and ethyl-3-oxopentanoate **64** provided the β-ketoamide **65** that was cyclized to the quinoline **66** using sulphuric acid at 120°C[15]. Finally, the nitrogen was methylated by means of a reaction with methyl iodide in the presence of potassium carbonate and provided derivative **47**in a satisfactory yield (74%).

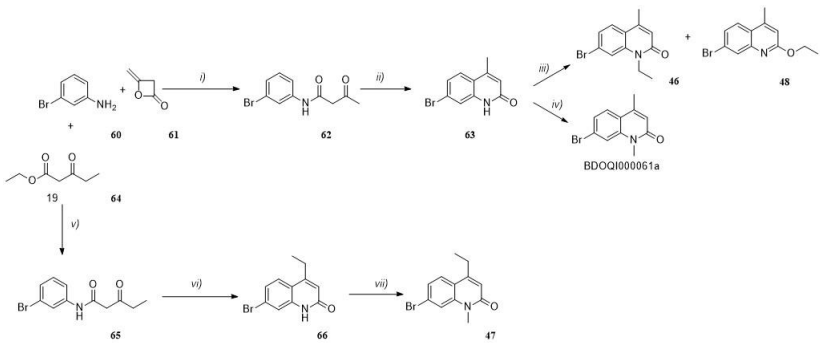

Reagents and conditions: i) toluene, 2h, RT, 74% yield. ii) H_2SO_4, reflux, 3 h, >90% yield; iii) iodoethane, K_2CO_3, MeOH, reflux, 24 h 25% yield for compound **46**, 10 yield for compound **48** ; iv) iodomethane, K_2CO_3, MeOH, reflux, 24 h 67 % yield.; v) toluene, reflux, 15 h, 30 % yield; vi) H_2SO_4, reflux, 3 h, >90% yield; vii) iodomethane, K_2CO_3, MeOH, reflux, 24 h 71% yield.

Scheme 2.1. Synthesis of derivatives **46-48**.

Derivatives **49-59** were synthesized following the synthetic procedure reported in Scheme 2. The nitroester **70** was obtained according to a procedure reported inliterature[16,17]. The imines **71 a-b** were synthesized with excellent yields (>95%) by means of a reaction between the suitable benzaldehyde and *p*-anisidine. A reaction between derivatives **71 a-b** and the nitroester **70** in the presence of a catalytic amount of benzoic acid afforded the *p*-methoxyphenyl (PMP) protected nitrolactams **72 a-b** as a mixture of two diastereoisomers (40-55 yield%). As determined by crude NMR, the diastereomeric ra-

tio of this reaction was 20:1 in favor of the *trans* diastereoisomer. Compounds **72 a-b** were deprotected by means of ceric ammonium nitrate, affording the nitrolactams **73 a-b**[18]. At this stage, the two diastereoisomers were easily separated by flash column chromatography (FCC). The nitrolactams **73 a-b** were then reduced using sodium borohidride and nickel chloride hexahydrate, quickly providing the corresponding aminoderivatives that reacted *in situ* with di-*tert*-butyl dicarbonate, affording*N*-BOC lactams **74 a-b** in good yields. Derivatives **49-51** were then obtained through a coupling reaction between **74 a-b** and **BDOQI000061a** in the presence of copper iodide, trans-dicyclohexylamine and potassium phosphate (86-87% yields)[19]**.** The enantiomers of compound **49** were then separated by HPLC, using a Chiralcel Semi-Preparative AD column and a 60:40 hexane: iso-propanol eluent system. The purity of each enantioenriched sample was determined by HPLC analysis (Chiralcel OG, hexane/iso-propanol 85:15). To date, the absolute stereochemistry has not been assigned. Derivative **49** was deprotected using HCl in dioxane and provided compound **52**in excellent yields (> 90 %)**;** the latter reacted with *i*-butylchloroformate to afford the carbamate **53** and with *tert*-butyl-isocyanate and phenylisocyanate to obtain ureas **54** and **55**, respectively. Finally, a reaction between **52** and the suitable acyl chloride or sulphonyl chloride in the presence of TEA provided compounds **56-59**.

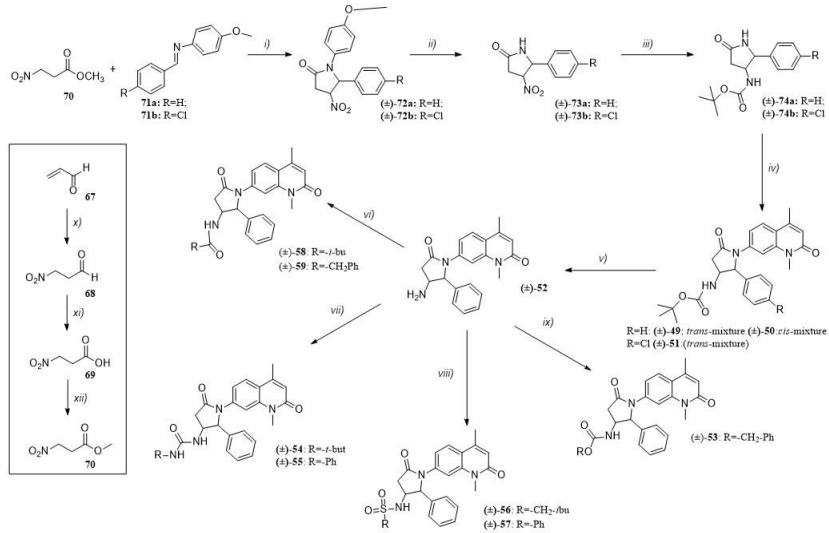

Reagents and conditions: i) benzoic acid, toluene, 80°C, 40-55% yield., 20:1 dr ; ii) ceric ammonium nitrate, CH_3CN/H_2O, 0°C, 67-73% yield; iii) nickel chloride hexahydrate, sodium borohydride, Boc-anhydride, MeOH, 15 h, RT, 67-87% yield; iv) **BDOQI000061a**, CuI, trans-dicycloexylamine, K_3PO_4, dioxane, 100°C, 42 h, 67-76 % yield; v) HCl, dioxane (4M), 15 h, rt, 90% yield; vi)*(±)*-**58**: benzoyl chloride, DCM, TEA, 3h, rt, 19% yield; *(±)*-**59**: 2-chloro-1-phenylethanone, DCM, TEA, rt, 3h, 19% yield; vii) *(±)*-**54** *tert*-butyl isocyanate, DCM, 15 h, rt, 24% yield; *(±)*-**55** phenyl isocyanate, DCM, 15 h, rt, 34% yield; viii)*(±)*-**54** isobutanesulfonyl chloride, DCM, TEA, rt, 27% yield; *(±)*-**55** phenylsulfonyl chloride, DCM, TEA, 3 h, rt, 23% yield *ix) (±)*-**53**: isobutylchloroformate, DCM, TEA, 3 h, 21 % yield *x)* sodium nitrite, acetic acid, THF/H_2O, RT, 4h, 85 % yield;xi) NaH_2PO_4, H_2O_2, $NaClO_2$, 0°C-RT, 15 h, >90 % yield; xii) H_2SO_4, MeOH, reflux, 15 h, 70 % yield.

Scheme 2.2. Synthesis of derivatives **49-59**

2.4. Biological evaluation

In order to evaluate the binding affinity for BRD9, compounds **46-50** and **52** were tested using the differential scanning fluorimetry[20], a method that relates the differences in denaturation midpoint temperatures (ΔT_m) in the presence and in the absence of the ligand with the binding affinity. The unfolding temperatures are measured taking advantage of the increase in fluorescence of a dye with affinity for hydrophobic parts of the protein exposed when protein unfolds. Results concerning the fragments **46-48** in comparison with **BDOQI000061a** are shown in Table 2.1.

COMPOUND	DSF ΔT_M (°C) BRD9
BDOQI000061A	4.80
46	5.87
47	-0.13
48	1.18

Table 2.1. ΔT_m (°C) measured by DSF against BRD9

Compounds **47** and **48** proved to be completely inactive, proving the importance of the methyl group at position 1 and the carbonyl group at position 2 forthe binding affinity. On the other hand, the presence of the ethyl group at C4 slightly increased ΔT_m with respect to **BDOQI000061a**, suggesting that substitutions at such position are more tolerated.

Thereafter, compounds **49**, **50** and **52** were tested as racemic mixtures (Table 2.2.).

COMPOUND[A]	DSF ΔTM (°C) BRD9
BDOQI000075A	6.60
49	9.11
50	2.90
52	4.24

Table2.2. ΔTm(°C) measured by DSF against BRD9. [a]All compounds are racemic mixtures.

The replacement of the six member lactam with a five-member one resulted in a high increase of ΔT_m, thus demonstrating that the ring size influenced the binding affinity for BRD9. Notably, compound **50**, corresponding to the *cis* diastereoisomer, was endowed with a lower activity, proving that the activity resided in the *trans* form. Finally, compound **52** determined a decrease in ΔT_m, thus demonstrating that the presence of a substituent on the nitrogen is responsible for an increase of activity. Biological evaluation of derivatives **51** and **53-59** is ongoing.

Given the excellent results obtained in the DSF assay, the derivative **49** was analysed by Isothermal Titration Calorimetry (ITC), for evaluating its potency. The obtained results showed two different K_d of 250 μM and 30 nM respectively, suggesting us that each enantiomer was endowed with a different activity. Biological evaluation of the single enantiomers is ongoing.

2.5. Conclusions

Preliminary results were very encouraging and led to the following SAR consideration:

- Regarding the quinoline fragment **BDOQI000061a**, both the presence of a methyl moiety at C4 and of the carbonyl function at C2 are essential for activity; on the other hand, substituents at the nitrogen are more tolerated.
- The replacement of the six-member lactam of **BDOQI000075a** with a five-member one increases the binding affinity.
- Stereochemistry influences the activity; the *trans* racemic mixture is endowed with a much higher binding affinity.
- The presence of a substituent on the nitrogen at C5 of the lactam is important for activity.

The racemic mixture **49** was endowed with an outstanding binding affinity. As assessed by ITC, this compound was characterized by two distinct values of K_d, each corresponding to a different enantiomer. One of these was in the nanomolar range, suggesting the potential use of this derivative as a chemical probe, and prompting us to further develop this scaffold.

2.6. Materials and methods

2.6.1. Chemistry

Reagents used were obtained from commercial suppliers or purified according to standard procedures. Petroleum ether (PE) refers to distilled light petroleum of fraction 30 - 40 °C. Anhydrous 1,4-dioxane was dried over 3Å molecular sieves. Degassing was achieved by bubbling argon through the reaction mixture for 15 minutes with sonication. Reactions were monitored by thin layer chromatography (TLC) using Merck silica gel 60 F254 plates and visualized by fluorescence quenching under UV light. In addition, TLC plates were stained with potassium permanganate solution. Chromatographic purification was performed on VWR 60 silica gel 40 - 63 μm using technical grade solvents that were used as supplied. Methyl-3-nitropropanoate was prepared according to literature methods[16,17]. Melting points were obtained on a Leica Galen III Hot-stage melting point apparatus and microscope and on a Kofler hot block and are reported uncorrected. NMR spectra were recorded on a Bruker Spectrospin spectrometer operating at 200, 400 or 500 MHz (^{1}H acquisitions), and 100 or 125 MHz (^{13}C acquisitions). Chemical shifts (δ) are reported in ppm with the solvent resonance as the internal standard (e.g. Chloroform δ 7.27 ppm for ^{1}H and 77.0 ppm for ^{13}C). Two-dimensional spectroscopy (COSY, HSQC and HMBC) was used to assist in the assignment and the data is not reported. High-resolution mass spectra (ESI) were recorded on Bruker Daltonics MicroTOF mass spectrometer. Optical rotations were recorded using a Perkin Elmer 341 polarimeter; absolute optical rotation are quoted $[\alpha]_D^T$ where concentrations (c) are quoted in g/100 mL, D refers to the D-line of sodium (589 nm), and temperatures (T) are given in degrees Celsius (°C). The enantiomeric excesses were determined by HPLC analysis on an Agilent 1200 Series instrument employing a chiral stationary phase column specified in the individual experiment and by comparing the samples with the appropriate racemic mixtures, separated under the same conditions specified in the experiments.

2.6.1.1. Synthesis of N-(3-bromophenyl)-3-oxobutanamide (62)

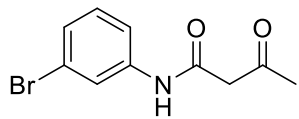

A solution of 4-bromoaniline **60** (5.8 mmol) and of diketene **61** (8.7 mmol) was refluxed in toluene. After two hours the mixture was cooled, extracted with ethyl acetate (EtOAc), washed with brine and dried over Na_2SO_4. The combined filtrates were concentrated in vacuo leaving a crude residue that was purified by FCC (EP/EtOAc 6:1, v/v) to give the desired product **62** (1.1 g, 74% yield) as white needles.

N-(3-bromophenyl)-3-oxobutanamide (66): white needles mp: 108 °C(74% yield); ^{1}H-NMR (400MHz, $CDCl_3$)δppm: 9.29 (br s, 1H,) 7.83 (s, 1H,), 7.44 (d, 1H,), 7.25 (d, 1H,), 7.18 (t, 1H,), 3.60 (s, 2H,), 2.33 (s, 3H,); ^{13}C-NMR (100MHz, $CDCl_3$): δ ppm 205.3, 163.5, 138.7, 130.2, 127.5, 123.0, 122.6, 118.6, 49.3, 31.3; LR-ESI-MS: $C_{10}H_{10}BrNO_2$ $[M+H]^+$*m*/*z* found 256.0, calcd 255.9.

2.6.1.2. General procedure for the preparation of 7-bromo-quinolin-2(1H)-one (63 and 66)

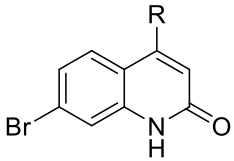

A suspension of **62** (3.1 mmol) in sulphuric acid (14.1 mL, 0.8 M) was heated for two hours at 120 °C. The reaction mixture was cooled and water was slowly added. The resulting precipitate was filtered off affording desired products as white solids.

7-bromo-4-methylquinolin-2(1H)-one (63): white solid mp: 108 °C (74% yield); ^{1}H-NMR (400MHz, $CDCl_3$) δ ppm:11.68 (br s, 1H), 7.65 (d, 1H), 7.47 (d, 1H), 7.35 (dd, 1H), 6.43 (d, 1H), 2.40 (d, 3H);^{13}C-NMR (100MHz, DMSO-*d6*): δppm: 161.5, 147.7, 139.8, 126.8, 124.4, 123.3, 121.3, 118.7, 117.5, 18.4; LR-ESI-MS: $C_{10}H_9BrNO$ [M+H]+ *m*/*z* found 237.9, calcd 238.0.

7-bromo-4-ethylquinolin-2(1H)-one (66): white solid mp: 124 °C (68% yield); ^{1}H-NMR (400MHz, $CDCl_3$) ppm:11.72 (s broad, 1 H), 7.72

(d, 1H), 7.51 (d, 1H), 7.37-7.35 (dd, 1H), 6.40 (s, 1H), 2.82 (q, 2H), 1.25 (t, 3H); ^{13}C-NMR (100MHz, $CDCl_3$): δ ppm 162.1, 153.3, 140.5, 126.9, 124.5, 123.7, 119.8, 118.3, 93.6, 24.7, 13.4.

2.6.1.3. Synthesis of 7-bromo-1,4-dimethylquinolin-2(1H)-one (BDOQI000061a)

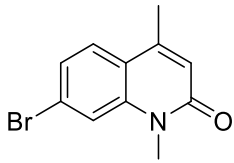

Compound **63** (1.136g, 4.8 mmol) and methyl iodide (0.75 mL, 5.3 mmol) were suspended in MeOH (48 mL, 0.1M), then potassium carbonate (1.32 g, 9.6 mmol) was added and the reaction was allowed to reflux for 12 hours. The reaction was quenched with NaOH (2 mL, 1M) then water and EtOAc were added. The organic phase was separated and the aqueous phase was extracted with EtOAc three times. The combined organic phases were dried over Na_2SO_4 and concentrated under reduced pressure to give a crude residue that was purified by FCC (EP/EtOAc 3:1 v/v) providing the desired product (915 mg, 76%) as white crystals.

7-bromo-4-dimethylquinolin-2(1H)-one (*BDOQI000061a.):* white solid mp: 124 °C (76% yield); ^{1}H-NMR (400MHz, $CDCl_3$) δ ppm:7.55 (d, 1H), 7.53 (s, 1H), 7.37 (dd, 1H), 6.61 (d, 1H), 3.68 (s, 3H), 2.45 (d, 3H); ^{13}C-NMR (100MHz, $CDCl_3$): δ ppm 161.9, 146.0, 139.2, 126.5, 125.1, 124.8, 121.4, 120.3, 117.4, 29.4, 18.9; LR-ESI-MS: $C_{11}H_{11}BrNO$ $[M+H]^+$*m/z* found 252.0, calcd 252.0; HR-ESI-MS: $C_{11}H_{11}BrNO$ $[M+H]^+$*m/z* found 252.0033, calcd 252.0019.

2.6.1.4. Synthesis of 7-bromo-1-ethyl-4-methylquinolin-2(1H)-one (46) and 7-bromo-2-ethoxy-4-methylquinoline (48)

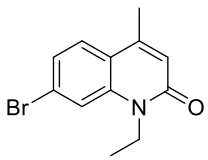

46

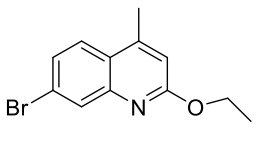

48

Compound **63** (0.500 g, 2.1 mmol) and ethyl iodide (0.19 mL, 2.3 mmol) were suspended in MeOH (21 mL, 0.1M), then potassium carbonate (0.96 g, 4.2 mmol) was added and the reaction was allowed to reflux for 12 hours. The reaction was quenched with NaOH 1M, then water and EtOAc were added. The organic phase was separated and the aqueous phase was extracted with EtOAc three times. The combined organic phases were dried over $Na_2SO_4$and concentrated under reduced pressure to give a crude residue that was purified by FCC (EP/EtOAc 3:1 v/v) providing **46** as a white solid (0.13 g, 25 % yield) and **48** as an amorphous solid (0.05 g, 9% yield).

7-bromo-1-ethyl-4-methylquinolin-2(1H)-one (46): white solid (25% yield) mp: 132 °C; ^{1}H-NMR (400MHz, MeOD-*d*4) ppm: 7.73 (d, 2H), 7.43 (d, 2H), 6.54 (s, 1H), 4.32 (q, 2 H), 2.46 (s, 3H), 1.28 (t, 2H). ^{13}C-NMR (100MHz, $CDCl_3$): δ ppm161.4, 145.9, 139.7, 126.7, 124.5, 121.4, 120.5, 117.1, 37.2, 18.9, 12.7.
7-bromo-2-ethoxy-4-methylquinoline (48): amorphous solid (9% yield)^{1}H-NMR (400MHz, $CDCl_3$) δ ppm: 7.94(d, 1H), 7.63 (d, 1H), 7.40-7.38 (dd, 1H), 6.67 (s, 1H), 4.42 (q, 2H), 2.54 (s, 3H), 2.10 (s, 3H), 1.36 (t, 2H). ^{13}C-NMR (100MHz, $CDCl_3$): δ ppm 206.0, 161.6, 145.5, 129.1, 125.9, 123.1, 122.2, 112.6, 60.6, 28.7, 17.6, 13.5.

2.6.1.5. Synthesis of 7-bromo-4-ethyl-1-methylquinolin-2(1H)-one (47)

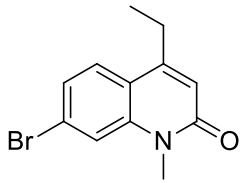

Compound **66** (1.1g, 4.4 mmol) and methyl iodide (0.93 mL, 6.6 mmol) were suspended in MeOH (44 mL, 0.1M), then potassium carbonate (1.21 g, 8.8 mmol) was added and the reaction was allowed to reflux for 12 hours. The reaction was quenched with NaOH then water and EtOAc were added. The organic phase was separated and the aqueous phase was extracted with EtOAc three times. The combined organic phases were dried over Na_2SO_4 and concentrated under reduced pressure to give a crude residue that was purified by FCC (EP/EtOAc 3:1 v/v) providing the desired product (0.8g, 70%) as

white crystals.

7-bromo-4-ethyl-1-methylquinolin-2(1H)-one (47): white solid; mp: 170 °C (70% yield); ^{1}H-NMR (400MHz, $CDCl_3$) δ ppm: 7.60 (d, 1H), 7.53 (d, 1H), 7.35 (dd, 1H), 6.61 (s, 1H), 3.77 (s, 3 H), 2.46 (q, 2H), 1.28 (t, 3H). ^{13}C-NMR (100MHz, $CDCl_3$): δ ppm161.4, 145.9, 139.7, 126.7, 124.5, 121.4, 120.5, 117.1, 37.2, 18.9, 12.7.

2.6.1.6. General procedure for the preparation of methyl-3-nitropropanaote (70)

Synthesis, ^{1}H NMR spectra and ESI mass are consistent with literature data[16,17]

2.6.1.7. General procedure for the preparation of imines (71 a-b)

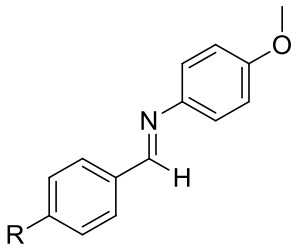

p-anisidine (97.5 mmol) and the suitable benzaldehyde (97.5mmol) were dissolved in DCM, then $MgSO_4$ (184.6mmol) was added and the mixture was allowed to stir for 15 hours at room temperature. After 15 h the mixture was filtered and was concentrated in vacuo to afford **71 a-b** in a 99% yield.

N-benzylidene-4-methoxyaniline (71a): brownish solid; mp: 55 °C (99% yield); ^{1}H-NMR (400MHz, $CDCl_3$) δ ppm: 8.41 (s, 1H), 7.83-7.80 (m, 2H), 7.40 (m, 2H), 7.18 (d, 2H), 6.87 (d, 2H), 3.76 (s, 3H); ^{13}C-NMR (100MHz, $CDCl_3$): δ ppm158.5, 158.3, 144.9, 136.5, 131.1, 128.8, 128.7, 122.2, 114.4, 55.53.

N-(4-chlorobenzylidene)-4-methoxyaniline (71b): brownish solid; mp: 107 °C (99% yield); ^{1}H-NMR (400MHz, $CDCl_3$) δ ppm: 8.47 (s, 1H), 7.85 (d, 2H), 7.47 (d, 2H), 7.28 (d, 2H), 6.98 (d, 2H), 3.86 (s, 3H). ^{13}C-NMR (100MHz, $CDCl_3$): δ ppm 158.5, 156.7, 144.5, 137.0, 135.0, 129.8, 129.0, 122.3, 114.4, 55.5.

2.6.1.8. General procedure for the preparation of the PMP-protected nitrolactams (72 a-b)

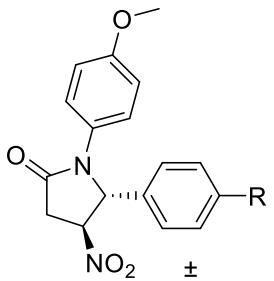

Methyl-3-nitropropanoate **70** (2.96 mmol) was dissolved in toluene, then the suitable imine **71** (4.44 mmol) and benzoic acid (0.3 mmol) were added in sequence. The mixture was degassed for 15 minutes and was allowed to stir at 70°C for 3 days. The reaction was quenched with Na_2CO_{3aq} and was then extracted with EtOAc for three times. The organic phases were washed with brine, dried over Na_2SO_4 and concentrated *in vacuo*, affording a crude mixture that was purified by means of FCC (DMC/EtOAc 10% v/v) providing a mixture of the two diastereoisomers (20:1 ratio in favour of the *trans* diastereoisomer) as brown oils.

(4S*,5R*)-1-(4-methoxyphenyl)-4-nitro-5-phenylpyrrolidin-2-one (72a):brown oil (55 % yield); NMR (400MHz, $CDCl_3$)δppm: 7.29 (d, 2H), 7.15 (m, 4H), 6.74 (d, 2H), 5.56 (d, 1H), 4.86-4.83 (dt, 1H), 3.65 (s, 3H), 3.24-3.20 (dd, 1H), 3.19-3.07 (dd, 1H); ^{13}C-NMR (100MHz, $CDCl_3$): δppm 169.2, 157.8, 135.3, 135.2, 129.9, 127.6, 124.4, 114.4, 114.3, 84.6, 67.6, 55.4, 34.9.

(4S*,5R*)-1-(4-methoxyphenyl)-4-nitro-5-(4-chlorophenyl)pyrrolidin-2-one (72b): brown oil (40 % yield) NMR (400MHz, $CDCl_3$) δ ppm:7.32 (d, 2H), 7.18-7.15 (m, 4H), 6.76 (d, 2H), 5.57 (d, 1H), 4.87-4.85 (dt, 1H), 3.68, (s, 3H), 3.23-3.20 (dd, 1H), 3.17-3.05 (dd, 1H); ^{13}C-NMR (100MHz, $CDCl_3$): δppm 169.4, 157.6, 136.7, 129.7, 126.1, 124.3,114.3 114.2, 84.9, 68.3, 55.4, 35.0.

2.6.1.9. General procedure for the preparation of the nitrolactams (73 a-b)

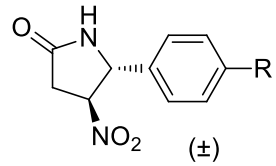

72 a (1.3 mmol) was dissolved in acetonitrile (39 mL, 0.3M) and cooled; ceric ammonium nitrate (3.9 mmol) was dissolved in water (13 mL, 0.1M) and was added dropwise. After 30 minutes the reaction was allowed to warm at room temperature, then was extracted with EtOAc. The organic fractions were washed with brine, dried over Na_2SO_4 and evaporated under reduced pressure giving a crude mixture. The latter was purified by FCC (DCM/MeOH 1% v/v) affording **73 a** as yellowish needles.

(4S*,5R*)-4-nitro-5-phenylpyrrolidin-2-one (73a): yellowish needles (67 %, 41% yieldas single diastereoisomer), mp: 105°C ; ^{1}HNMR (400MHz, $CDCl_3$)δppm: 8.62 (s, 1H), 7.47-7.39 (m, 5H), 5.28-5.25 (m, 1H), 5.18, (d, 1H), 3.00-2.94 (dd, 1H), 2.91-2.86 (dd, 1H). ^{13}C-NMR (100MHz, $CDCl_3$): δ ppm 172.9, 140.2, 129.3, 126.7, 87.4, 61.5, 39.3, 34.6.

(4S*,5R*)-4-nitro-5-(4-chlorophenyl)pyrrolidin-2-one (73b): yellowish needles (73% yield, 33% yield as single diastereoisomer), mp: 140°C ; ^{1}H NMR (400MHz, $CDCl_3$) δ ppm: 7.40 (d, 2H), 7.24 (d, 2H), 6.42 (s, 1H), 5.18 (d, 1H), 4.88-4.84 (m, 1H), 3.11-3.05 (dd, 1H), 2.93-2.86 (dd, 1H); ^{13}C-NMR (100MHz, $CDCl_3$): δ ppm 172.9, 139.2, 133.5, 129.3, 128.9, 128.85, 87.0, 60.7, 40.6, 39.3,34.6, 31.2.

2.6.1.10. General procedure for the preparation of the BOC-protected nitrolactams (74 a-b)

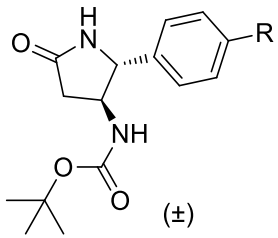

The suitable nitrolactam (2.0 mmol) was dissolved in MeOH (0.15M) and the solution was cooled to 0°C. Nickel (II) chloride hexahydrate (0.01 mmol) was added and the reaction was stirred for five minutes. Sodium borohydride (8.0 mmol) was added portionwise over 30 minutes, then the reaction was stirred at 0°C for 30 minutes. Di-*tert*-butyl dicarbonate (2.4 eq) was added and the reaction was allowed to warm to ambient temperature with stirring for 12 hours. The reaction mixture was poured into a mixture of 2:1:2 brine: $NaHCO_{3(sat\ aq)}$: EtOAc and the organic phase was removed. The aqueous phase was extracted with EtOAc three times, then the organic phases were combined, dried over Na_2SO_4 and concentrated under reduced pressure. The crude material was purified with FCC (EtOAc) to yield the title compound (67-87 % yield).

***tert*-butyl ((2S*,3R*)-2-phenyl-5-oxopyrrolidin-3-yl)carbamate (74a):** white powder (87% yield), mp: 173°C ; ^{1}H NMR (400MHz, $CDCl_3$) δ ppm: 7.41-7.38 (m, 5H), 5.92 (s, 1H), 4.94 (s broad, 1H), 4.66 (s broad, 1H), 4.14-4.08 (m, 1H), 2.84-2.81 (dd, 1H), 2.79-2.77 (dd, 1H), 1.45 (s, 9H). ^{13}C-NMR (100MHz, $CDCl_3$): δ ppm 171.2, 155.6, 141.8, 128.9, 128.0, 126.4, 78.6, 53.8, 40.6, 39.9, 26.8.

tert-butyl ((2S*,3R*)-2-(4-chlorophenyl)-5-oxopyrrolidin-3-yl)carbamate (74b): white powder (67% yield); ^{1}H NMR (400MHz, $CDCl_3$) δ ppm: 7.31-7.28 (m, 4 H), 5.92 (s, 1 H), 4.87 (d, 1H), 4.59 (s broad, 1 H), 4.02-3.98 (m, 1H), 2.74-2.67 (dd, 1H), 2.17-2.13 (d, 1H), 1.38 (s, 9H).

2.6.1.11. General procedure for the preparation of the 1-tert-butyl (-1-(1,4-dimethyl-2-oxo-1,2-dihydroquinolin-7-yl)-5-oxo-2-phenylpyrrolidin-3-yl) carbamate (49-51)

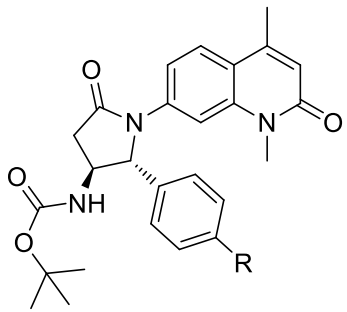

1,4-Dioxane (0.1M) was added to the appropriate lactam **74 a** (1.8 mmol), **BDOQI000061a** (2.7 mmol) and K_3PO_4 (3.6 mmol) and the mixture was degassed for 15 minutes. CuI (1.8 mmol) and (+/-)-*trans*-1,2-diaminocyclohexane (1.8 mmol) were added under inert conditions, and the reaction was sealed and heated at 100°C for 42 h. The reaction mixture was filtered through celite, which was then washed with DCM. The filtrate was concentrated under reduced pressure and purified with FCC (15% IPA/hexane then 30% IPA/hexane) to yield the title compound.

The enantiomers of the *trans*-racemic mixture were separated by HPLC (Semipreparative Chiralcel AD, 10 mm ID, hexane/iso-propanol 60:40, λ 220 nm, 5.0 mL/min). The purity of each enantioenriched sample was determined by HPLC analysis (ChiralcelOG, hexane/iso-propanol 85:15, λ 220 nm, 1 mL/min). t (**49a**)= 13.2 minutes; t(**49b**): 16.1 min. >99% ee. To date, the absolute stereochemistry hasn't been assigned yet.

***tert*-butyl ((2R*,3S*)-1-(1,4-dimethyl-2-oxo-1,2-dihydroquinolin-7-yl)-5-oxo-2-phenylpyrrolidin-3-yl)carbamate (49):** white solid (76% yield), mp: 195°C ; ^{1}HNMR (400MHz, $CDCl_3$) δ ppm: 7.98 (s broad, 1H), 7.45 (d, 1H), 7.31-7.29 (m, 4H), 7.28-7.25 (m, 1H), 7.07 (d, 1H), 6.42 (s, 1H), 5.26 (s, 1 H), 5.19 (s, 1H), 4.09-4.06 (m, 1H), 3.49 (s, 3H), 3.07-3.00 (dd, 1H), 2.40 (d, 1H), 1.42 (s, 9H).

***tert*-butyl((2S*,3S*)-1-(1,4-dimethyl-2-oxo-1,2-dihydroquinolin-7-yl)-5-oxo-2-phenylpyrrolidin-3-yl)carbamate (50)**: amorphous solid; ^{1}HNMR (400MHz, $CDCl_3$) δ ppm: 8.02 (s broad, 1H), 7.48(d, 1H), 7.33-7.30 (m, 4H), 7.27-7.24 (m, 1H), 7.07 (d, 1H), 6.38 (s, 1H), 5.26 (s, 1

H), 5.32 (d, 1H), 4.78-4.75 (m, 1H), 4.15 (m, 1H), 3.49 (s, 3H), 2.98 (m, 1H), 2.29 (s, 3H), 2.52 (m, 1H), 2.41 (d, 1H), 1.39 (s, 9H).

tert-butyl ((2R*,3S*)-2-(4-chlorophenyl)-5-oxopyrrolidin-3-yl)carbamate (51): white solid (67% yield, mp: 195°C ; ^{1}H NMR (400MHz, $CDCl_3$) ppm 8.10 (s broad, 1H), 7.53 (d, 1H), 7.36-7.34 (m, 4H), 7.05 (d, 1H), 6.50 (s, 1H), 5.32 (s, 1H), 5.19 (s, 1H), 4.11-4.08 (m, 1H), 3.59 (s, 3H), 3.10-3.06 (dd, 1H), 2.47 (d, 2H), 2.37 (s, 3H), 1.46 (s, 9H).

2.6.1.12. Synthesis of 7-(3-amino-5-oxo-2-phenylpyrrolidin-1-yl)-1,4-dimethylquinolin-2(1H)-one (52)

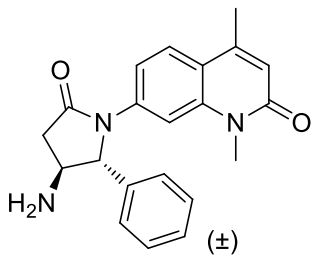

HCl/Dioxane (10 mL, 0.15M) was added to **49** (654 mg, 1.32 mmol) and the reaction was stirred at ambient temperature for 16 hours. The solvent was removed under vacuum, then EtOAc was added and the solvent was again removed. The material was acidified with 1M HCl and the aqueous phase was washed with DCM. The aqueous phase was then basified with Na_2CO_3 and extracted with DCM. The combined organic extractions were dried over Na_2SO_4, filtered and concentrated under reduced pressure to yield **51** (502 mg, 96%) as a white amorphous solid.

7-((2R*,3S*)-3-amino-5-oxo-2-phenylpyrrolidin-1-yl)-1,4-dimethylquinolin-2(1H)-one (51): white solid (96% yield,, mp: 193°C ; ^{1}HNMR (400MHz, $CDCl_3$) ppm: 7.70 (s, 1H), 7.50 (d, 1H), 7.35-7.26 (m, 5H), 7.23-7.21 (dd, 1H), 6.47 (s, 1H), 4.95 (d, 1H), 3.59 (m, 1H), 3.54 (s, 3H), 3.07-3.03 (dd, 1H), 2.49-2.41 (dd, 1H), 2.35 (s, 3H) ^{13}C-NMR (100MHz, $CDCl_3$): δppm 173.4, 162.3, 149.5, 140.15, 140.1, 138.4, 129.4, 125.9, 125.5, 120.2, 118.2, 115.1, 107.2, 73.5, 54.5, 40.8, 29.7, 29.2, 18.8.

2.6.1.13. Synthesis of isobutyl (1-(1,4-dimethyl-2-oxo-1,2-dihydroquinolin-7-yl)-5-oxo-2-phenylpyrrolidin-3-yl) carbamate (53)

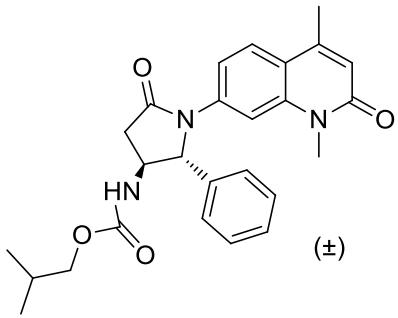

TEA (20 μL, 0.14 mmol) was added to a mixture of **52** (20 mg, 0.05 mmol) in DCM (0.22 mL, 0.25 M), then *i*-butyl chloroformate (0.14 mmol) was added dropwise and the reaction was allowed to stir for six hours at room temperature. Water was added and the organic phase was separated and was extracted with DCM three times. The organic phases were combined, washed with brine, dried over Na_2SO_4 and concentrated under reduced pressure. The crude mixture was purified by FCC (DCM/MeOH 1% v/v) and by preparative TLC (EtOAc) yielding compound **53**.

isobutyl ((2R*,3S*)-1-(1,4-dimethyl-2-oxo-1,2-dihydroquinolin-7-yl)-5-oxo-2-phenylpyrrolidin-3-yl)carbamate (53): white solid 23% yield, mp: 147°C ; ^{1}H NMR (400MHz, $CDCl_3$) ppm: 7.97 (s, 1H), 7.43-7.40 (d, 1H), 7.31-7.29 (m, 4H), 7.29-7.27 (m, 1H), 7.06 (dd, 1H), 6.40 (s, 1H), 5.62 (s, 1H), 5.30 (s, 1H), 4.14-4.12 (t, 1H), 3.91-3.87 (m, 1H), 3.83 (d, 1H), 3.46 (s, 3H), 3.09-3.03 (dd, 1H), 2.45 (d, 1H), 2.27 (s, 3H), 1.89-1.85 (m, 1H), 0.87 (d, 6H).

2.6.2.14. General procedure for the preparation of the 1-(1-(1,4-dimethyl-2-oxo-1,2-dihydroquinolin-7-yl)-5-oxo-2-phenylpyrrolidin-3-yl)ureas (54-55)

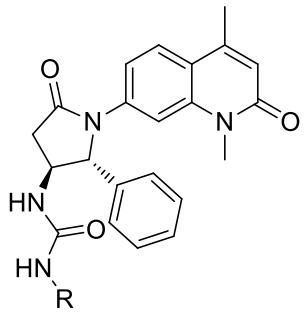

The suitable isocyanate (0.14 mmol) was added dropwise to a solution of **52** (1 eq) in DCM (0.25M). The reaction was stirred at ambient temperature for fifteen hours before the solvent was removed under reduced pressure. The resulting crude material was purified through FCC (DCM/MeOH 3% v/v) and preparative TLC (EtOAc) giving the desired products **54** and **55**.

1-(tert-butyl)-3-((2R*,3S*)-1-(1,4-dimethyl-2-oxo-1,2-dihydroquinolin-7-yl)-5-oxo-2-phenylpyrrolidin-3-yl)urea (54): amorphous solid 24% yield; ^{1}HNMR (400MHz, $CDCl_3$) δ ppm: 8.49 (s, 1H), 7.25 (d, 4H), 7.17 (s, 1H), 6.64-6.61 (dd, 1H), 6.46-6.44 (dd, 1H), 6.32 (s, 1H), 5.20 (s, 1H), 5.07, (s, 1H), 4.23 (t, 1H), 3.39 (s, 3H), 2.97-2.91 (dd,1H), 2.37 (d, 1H), 2.20 (s, 3H), 1.34 (s, 9H). ^{13}C-NMR (100MHz, $CDCl_3$): δ ppm174.3, 162.67, 157.3, 140.8,139.8, 129.2,128.1, 125.7,125.1, 118.8,104.5, 77.0, 71.3, 50.5, 37.9, 29.7, 29.4.

1-((2R*,3S*)-1-(1,4-dimethyl-2-oxo-1,2-dihydroquinolin-7-yl)-5-oxo-2-phenylpyrrolidin-3-yl)-3-phenylurea (55):white solid 34% yield; mp: 214 °C; ^{1}HNMR (400MHz, $CDCl_3$)ppm: 8.49, s, 1H), 7.77 (s, 1H), 7.42 (d, 2H), 7.26-7.20 (m, 6H), 7.15 (m, 2H), 6.98-6.94 (m, 1H), 6.55-6.53 (dd, 1H), 6.31, (s, 1H), 5.26 (s, 1H), 4.40 (t, 1H), 3.40 (s, 3H), 3.03-2.97 (dd, 1H), 2.45 (d, 1H), 2.18 (s, 3H).

2.6.2.15. General procedure for the preparation of the 1-(1-(1,4-dimethyl-2-oxo-1,2-dihydroquinolin-7-yl)-5-oxo-2-phenylpyrrolidin-3-yl)sulphonamides (56-57)

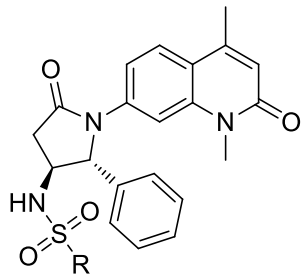

52 (20 mg, 0.05 mmol) was dissolved in DCM (0.22 mL, 0.25M) and TEA (20 μL, 0.14 mmol) was added. The appropriate sulphonyl chloride was added dropwise and the reaction was stirred at ambient temperature for six hours. Water was added and the organic phase was separated. The aqueous phase was then extracted with DCM three times. The organic phases were combined, dried over Na_2SO_4 and concentrated under reduced pressure. The resulting crude material was purified through FCC (DCM/MeOH 2% v/v) and preparative TLC (EtOAc) to yield the title compound.

N-((2R*,3S*)-1-(1,4-dimethyl-2-oxo-1,2-dihydroquinolin-7-yl)-5-oxo-2-phenylpyrrolidin-3-yl)-2-methylpropane-1-sulfonamide (56): amorphous solid, 27% yield; ^{1}HNMR (400MHz, $CDCl_3$) ppm: 8.48 (s, 1H), 7.90 (s broad , 1H), 7.34-7.28 (m, 4H), 7.18 (d, 1H), 6.63 (s, 1H), 6.61 (d, 1H), 5.47 (s, 1H), 4.02 (t, 1H), 3.57 (s, 3H), 3.15-3.10 (dd, 1H), 3.02 (d, 2H), 2.64 (d, 1H), 2.35-2.33 (m, 1H), 2.25 (s, 3H), 1.13 (s, 6H).
N-((2R*,3S*)-1-(1,4-dimethyl-2-oxo-1,2-dihydroquinolin-7-yl)-5-oxo-2-phenylpyrrolidin-3-yl)benzenesulfonamide (57): white solid, (23% yield), mp 121 °C; ^{1}HNMR (400MHz, $CDCl_3$) ppm: 8.43 (s broad, 1H), 8.25 (s, 1H), 7.94 (d, 2H), 7.61-7.45 (m, 4H), 7.38-7.35 (dd, 1H), 7.25-7.21 (m, 2H), 7.15 (d, 1H), 7.07 (d, 2H), 6.56-6.54 (dd, 1H), 6.50 (s, 1H), 5.37 (s, 1H), 3.80 (s broad 1H), 3.34 (s, 3H), 2.90-2.83 (dd, 1H), 2.40 (d, 1H), 2.20 (s, 3H); ^{13}C-NMR (100MHz, $CDCl_3$): δppm 198.6, 172.0, 161.7, 145.4, 140.0, 139.1, 136.2, 131.7, 128.4, 128.2, 126.0, 124.4, 123.9, 118.1, 116.4, 112.0, 103.6, 100.2, 70.0, 53.7, 37.0, 37.0, 28.5, 17.6.

2.6.2.16. General procedure for the preparation of the 1-(1-(1,4-dimethyl-2-oxo-1,2-dihydroquinolin-7-yl)-5-oxo-2-phenylpyrrolidin-3-yl) amides (58-59)

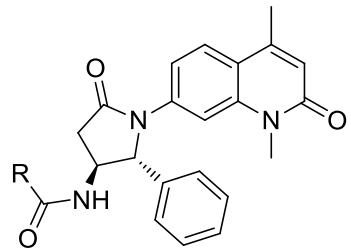

TEA (20 μL, 0.14 mmol) was added to a solution of **52** (20 mg, 0.05 mmol) in DCM (0.22 mL, 0.25M), then the suitable chloride(0.05 mmol) was added dropwise and the reaction was stirred at room temperature. After six hours water was added and the organic phase was separated. The aqueous phase was then extracted with DCM three times. The organic phases were combined, dried over sodium sulphate and concentrated under vacuum. The resulting crude material was purified through FCC (DCM/MeOH 2% v/v) and preparative TLC (EtOAc) to yield the title compound.

N-((2R*,3S*)-1-(1,4-dimethyl-2-oxo-1,2-dihydroquinolin-7-yl)-5-oxo-2-phenylpyrrolidin-3-yl)benzamide (58): amorphous solid, (19% yield); ^{1}HNMR (400MHz, $CDCl_3$)ppm:8.15 (s, 1H), 7.96-7.92 (m, 3H), 7.48-7.46 (m, 1H), 7.42-7.40 (m, 4H), 7.34-7.32 (m, 2H), 7.26-7.24 (m, 2H), 6.84-6.81 (dd, 2H), 6.23 (s, 1H), 5.41 (s, 1H), 4.59 (t, 1H), 3.34 (s, 3H), 3.20-3.13 (dd, 1H), 2.64 (d, 1H), 2.17 (s, 3H).

N-((2R*,3S*)-1-(1,4-dimethyl-2-oxo-1,2-dihydroquinolin-7-yl)-5-oxo-2-phenylpyrrolidin-3-yl)-2-phenylacetamide (59): amorphous solid, (21% yield); ^{1}HNMR (400MHz, $CDCl_3$)ppm: 8.15 (s, 1H), 7.55 (d, 1H), 7.37-7.26 (m, 11H), 6.87-6.85 (dd, 1H),6.31 (s, 1H), 5.30 (s, 1H), 4.40 (t, 1H), 3.69 (s, 2H), 3.39 (s, 3H), 3.09-3.03 (d, 1H), 2.48 (d, 2H), 2.27 (s, 3H).

2.6.2. Biology

2.6.2.1. Differential Scanning Fluorimetry (DSF)

Thermal melting experiments were carried out using an Mx3005p Real Time PCR machine (Stratagene). Proteins were buffered in 10 mM HEPES pH 7.5, 500 mM NaCl and assayed in a 96-well plate at a final concentration of 2 μM in 20 μL volume. Compounds were added at a final concentration of 10 μM. SYPRO Orange (Molecular Probes) was used as a fluorescence probe at a dilution of 1:1000. Excitation and emission filters for the SYPRO-Orange dye were set to 465 nm and 590 nm, respectively. The temperature was raised with a step of 3 °C per minute from 25 °C to 96 °C and fluorescence readings were taken at each interval.

2.6.2.2. Isothermal Titration Calorimetry (ITC)

Experiments were carried out on a VP-ITC microcalorimeter (MicroCal™). All experiments were performed at 15 °C in 20 mM HEPES pH 7.5, 150 mM NaCl, 0.5 mM TCEP. BRD9 protein solution was buffer exchanged by gel filtration or dialysis into the ITC buffer. The titrations were conducted using an initial injection of 2 μl followed by 34 identical injections of 8 μl. The dilution heats were measured on separate experiments and were subtracted from the titration data. Thermodynamic parameters were calculated using $\Delta G = \Delta H - T\Delta S = -RT\ln K_B$, where ΔG, ΔH and ΔS are the changes in free energy, enthalpy and entropy of binding respectively. In all cases a single binding site model was employed.

References

1. Bannister, A. J. & Kouzarides, T. Regulation of chromatin by histone modifications. *Cell Res.* **21,** 381-395 (2011).

2. Josling, G. A. *et al.* The Role of Bromodomain Proteins in Regulating Gene Expression. *Genes* **3,** 320-343 (2012).

3. Prinjha, R. K. *et al.* Place your BETs: the therapeutic potential of bromodomains. *Trends Pharmacol. Sci.* **33,** 146-153 (2012).

4. Filippakopoulos, P. *et al.* Histone Recognition and Large-Scale Structural Analysis of the Human Bromodomain Family. *Cell* **149,** 214-231 (2012).

5. Filippakopoulos, P. & Knapp, S. Targeting bromodomains: epigenetic readers of lysine acetylation. *Nat. Rev. Drug Discov.***13,** 337-356 (2014).

6. Mujtaba, S. *et al.* Structure and acetyl-lysine recognition of the bromodomain. *Oncogene* **26,** 5521–5527 (2007).

7. Owen, D. J. The structural basis for the recognition of acetylated histone H4 by the bromodomain of histone acetyltransferase Gcn5p. *EMBO J.* **19,** 6141-6149 (2000).

8. Papavassiliou, K. A. & Papavassiliou, A. G. Bromodomains: pockets with therapeutic potential. *Trends Mol. Med.* **20,** 477-478 (2014).

9. Workman, P. & Collins, I. Probing the Probes: Fitness Factors For Small Molecule Tools. *Chem. Biol.* **17,** 561-577 (2010).

10. Gallenkamp, D. *et al.* Bromodomains and Their Pharmacological Inhibitors. *ChemMedChem* **9,** 438-464 (2014).

11. Sanchez, R. *et al.* The bromodomain: From epigenome reader to druggable target. *Biochim. Biophys. Acta* **1839,** 676-685 (2014).

12. Hewings, D. S. *et al.* Progress in the Development and Application of Small Molecule Inhibitors of Bromodomain–Acetyl-lysine Interactions. *J. Med. Chem.* **55,** 9393-9413 (2012).

13. Fedorov, O. *et al.* [1,2,4]Triazolo[4,3- *a*]phthalazines: Inhibitors of Diverse Bromodomains. *J. Med. Chem.* **57,** 462-476 (2014).

14. Maiti, A. *et al.* Synthesis of Casimiroin and Optimization of Its Quinone Reductase 2 and Aromatase Inhibitory Activities. *J. Med. Chem.* **52,** 1873-1884 (2009).

15. Larsson, E. A. *et al.* Fragment-Based Ligand Design of Novel

Potent Inhibitors of Tankyrases. *J. Med. Chem.* **56,** 4497-4508 (2013).

16. Pelletier, S. M.-C., Ray, P. C. & Dixon, D. J. Diastereoselective Synthesis of 1,3,5-Trisubstituted 4-Nitropyrrolidin-2-ones via a Nitro-Mannich/Lactamization Cascade. *Org. Lett.* **13,** 6406-6409 (2011).

17. Pelletier, S. M.-C. *et al.*Nitro-Mannich/Lactamization Cascades for the Direct Stereoselective Synthesis of Pyrrolidin-2-ones. *Org. Lett.* **11,** 4512-4515 (2009).

18. Verkade, J. M. M. *et al.* Mild and efficient deprotection of the amine protecting p-methoxyphenyl (PMP) group. *Tetrahedron Lett.* **47,** 8109-8113 (2006).

19. Klapars, A. *et al.* General and Efficient Copper Catalyst for the Amidation of Aryl Halides and the *N* -Arylation of Nitrogen Heterocycles. *J. Am. Chem. Soc.* **123,** 7727-7729 (2001).

20. Niesen, F. H. *et al.* The use of differential scanning fluorimetry to detect ligand interactions that promote protein stability. *Nat. Protoc.* **2,** 2212-2221 (2007).

Il Comitato editoriale assicura una valutazione trasparente e indipendente delle opere sottoponendole in forma anonima a due valutatori, anch'essi anonimi. Per ulteriori dettagli si rinvia al sito: www.editricesapienza.it

Collana Studi e Ricerche

Per informazioni sui precedenti volumi in collana, consultare il sito:
www.editricesapienza.it

80. «Pendono interrotte le opere»
Antichi monumenti incompiuti nel mondo greco
Massimiliano Papini

81. La disabilità tra riabilitazione e abilitazione sociale
Il caso dei Gudat Akal a Mekelle e Wukro
Virginia De Silva

82. I Consoli del Mare di Firenze nel Quattrocento
Eleonora Plebani

83. Le categorie flessive nella didattica del tedesco
Un confronto tra grammatiche Deutsch als Fremdsprache internazionali e per italofoni
Claudio Di Meola e Daniela Puato

84. Il corpo degli altri
a cura di Anna Belozorovitch, Tommaso Gennaro, Barbara Ronchetti, Francesca Zaccone

85. El largo viaje de los mitos
Mitos clásicos y mitos prehispánicos en las literaturas latinoamericanas
edición de Stefano Tedeschi

86. Analysis and Design of Antennas and Algorithms for Near-Field Sensing
Davide Comite

87. Synthesis and biological evaluation of 1,5-diphenylpyrrole derivatives as COX-2 selective inhibitors and NO-releasing agents and development of a novel BRD9 chemical probe
Sara Consalvi

88. New Techniques for Adaptive Program Optimization
Daniele Cono D'Elia

89. La spiegazione delle disuguaglianze attraverso modelli generativi
Un contributo alla comprensione della mobilità sociale nella prospettiva della sociologia analitica
Pasquale di Padova

90. La dinamica degli opposti
Ricerca letteraria, cultura mediatica e media in Georges Perec
Loredana Fiorletta

91. Seismic Performance of Masonry Cross Vaults
Learning from historical developments and experimental testing
Angelo Gaetani
92. What's behind neuropathic pain?
Neurophysiological diagnostic tests investigating mechanisms underlying neuropathic pain
Caterina Maria Leone
93. Getting ready to act
Neurocognitive aspects of action preparation
Rinaldo Livio Perri
94. Trust e Impresa in Crisi
Elena Signori

This PhD thesis consists of three projects: the first and the second ones, carried out at Sapienza University of Rome, deal with the design and synthesis of novel COX-2 selective inhibitors and dual COX-2 inhibitors/NO-releasing agents, respectively. The third project concerns the development of a novel BRD9 chemical probe and was realized at the University of Oxford (Department of Chemistry).

Sara Consalvi earned her PhD in Pharmaceutical Sciences in 2015 and is currently a research fellow at Department of Chemistry and Technology of Drugs. Her research focus is on drug discovery, in the field of anti-inflammatory and antimycobacterial agents.

ISBN 978-88-9377-137-5

Winner of the Competition "Prize for PhD Thesis 2016" arranged by Sapienza University Press.

www.editricesapienza.it